OFF-GRID SOLAR-POWERED NANOFILTRATION PILOT STUDY RELEVANT TO THE NAVAJO NATION

by

Ailyn Brizo

A Thesis Submitted to the Faculty of the

DEPARTMENT OF CHEMICAL & ENVIRONMENTAL ENGINEERING

In Partial Fulfillment of the Requirements

For the Degree of

MASTER OF SCIENCE

WITH A MAJOR IN ENVIRONMENTAL ENGINEERING

In the Graduate College

THE UNIVERSITY OF ARIZONA

2022

THE UNIVERSITY OF ARIZONA
GRADUATE COLLEGE

As members of the Master's Committee, we certify that we have read the thesis prepared by Ailyn Brizo, titled *Off-Grid Solar-Powered Nanofiltration Pilot Study Relevant to the Navajo Nation* and recommend that it be accepted as fulfilling the dissertation requirement for the Master's Degree.

Vasiliki Karanikola Date: Aug 18, 2022

Andrea Achilli Date: Aug 18, 2022

Kerri Hickenbottom Date: Aug 18, 2022

Final approval and acceptance of this thesis is contingent upon the candidate's submission of the final copies of the thesis to the Graduate College.

I hereby certify that I have read this thesis prepared under my direction and recommend that it be accepted as fulfilling the Master's requirement.

Vasiliki Karanikola Date: Aug 18, 2022
Master's Thesis Committee Chair
Department of Chemical and Environmental Engineering

ACKNOWLEDGEMENTS

This thesis would not have been possible without the help and support of so many people and I am immensely greatly to all of them. First and foremost, thank you Dr. Vasiliki "Vicky" Karanikola for all of your guidance and patience. Your encouragement has helped me grow as a researcher.

Thank you to everyone in the KORES research group. A huge thank you to Mackenzie Bonny, who was instrumental in so much of this work. Your work in the lab, on the TOC, and on the ICP-MS was of course so important, but just as important was having someone to complain to, bounce ideas off of, and laugh with in the lab. Thank you to Elizabeth Provencio, Arianna Tariqi, Lynn Carroll, Jack Welchert, and Christopher Yazzie, who all helped with some aspect of this thesis, whether that was ArcGIS, SEM, or answering instrument questions.

Thank you to the whole Indige-FEWSS team! I'm so grateful that I have been able to work on projects that I've found meaningful during my time at the University of Arizona and it is largely because of the Indige-FEWSS program. Thank you to the previous trainees, staff, and faculty who built the SNF unit and laid the groundwork for the work I've done. In particular, thank you to Dr. Karletta Chief for your leadership and thank you to Cara for your gentle reminders to do things.

Thank you Dr. Armando Durazo for your help using analytical equipment and answering all my questions. Thank you to Dana Clashin for motiving me and commiserating in the thesis writing process. Thank you to Dr. Kerri Hickenbottom and Dr. Andrea Achilli for being a part of my thesis committee.

Thank you to Tariq Samji for being endless supportive, especially when it became crunch time, and cheering me up when I got frustrated. Finally, thank you to my mom, Lani Brizo, for your support and making me the person I am today.

LAND ACKNOWLEDGEMENT

We respectfully acknowledge the University of Arizona is on the land and territories of Indigenous peoples. Today, Arizona is home to 22 federally recognized tribes, with Tucson being home to the O'odham and the Yaqui. Committed to diversity and inclusion, the University strives to build sustainable relationships with sovereign Native Nations and Indigenous communities through education offerings, partnerships, and community service.

Table of Contents

List of Figures

List of Tables

Abstract

Rural communities that are not connected to the electric or water grid often face challenges with access to affordable and safe potable water. Photovoltaic-powered membrane processes are being explored as an option to meet this need for cost-effective, safe drinking water in rural communities. In particular, the lower power requirements and palatable product water make nanofiltration an attractive option. The suitability of nanofiltration depends on many factors such as water quality, operating conditions, and maintenance. Commercially produced nanofiltration membranes are generally assumed to be operated near-continuously, but the nature of the solar power means that photovoltaic water filtration systems are operated intermittently, which may increase fouling and increase likelihood of microbial growth.

Water quality analyses was conducted on at 17 sites on the Navajo Nation to determine the need for water treatment and the suitability of nanofiltration. Exceedances of water quality standards for arsenic and/or uranium were found at five sites and exceedances for total dissolved solids were found at 12 water sources, indicating the need for water treatment. Intermittent operation was tested on a pilot-scale nanofiltration prototype for two months with a salt solution with a total dissolved solids concentration of 1350 mg/L containing Mg^{2+}, SO_4^{2+}, Cl^-, and Ca^{2+}. There was little to no change in performance over the two months. Operation with a solution including ferric sulfate caused membrane fouling within 3 days. The system was also tested with a solution containing humic acid alone and a solution containing humic acid and Mg^{2+}, SO_4^{2+}, Cl^-, and Ca^{2+} with a TDS of 1350 mg/L. The addition of salts decreased flux by about 30% when pH was maintained above 7.5 and about 12% when pH was not controlled. Finally, the membrane fouled by ferric iron was subjected to an autopsy. The results suggest the foulant layer consists primarily of amorphous, colloidal iron.

Chapter 1: Introduction

1.1. Food-Energy-Water Nexus

In the past decade, the academic and international community has increasingly recognized the interconnected nature of food, energy, and water (Simpson and Jewitt, 2019). The "food-energy-water nexus" encourages policymakers, academics, and scientists to consider how changes in food production may impact energy and water demand and vice versa. This interconnected nature is particularly relevant in indigenous communities. Indigenous communities in the United States are more likely to face water and food insecurity than non-Indigenous communities (Cozzetto et al., 2013). Certain tribes such as the Navajo Nation also have significant portions of the population not connected to the electrical grid (Begay, 2018). Historical, socio-economic, and cultural factors also impact the dynamics of the food-energy-water nexus in Native American communities in the United States. Tribal communities may have less access to water and less agriculturally favorable soil than the land that tribes originally occupied (Cozzetto et al., 2013). Culturally-important sources of food are threatened by climate change in some tribal communities, which may exacerbate food insecurity within Native American populations (Martin et al., 2020). Finally, Western scientists have a history of discounting Indigenous and Native American knowledge and conducting research in Indigenous communities not always for benefit of the communities, leading to a mistrust of scientists (Mello and Wolf, 2010; Necefer et al., 2015). Technologies and policies that aim to address the food-energy-water nexus in Indigenous and Native American communities must conduct research that is respectful of their culture to regain that trust.

1.2. Water Resources on the Navajo Nation

The interconnected nature of food, energy, and water security can be seen on the Navajo Nation, where an estimated 32% of the population are without electricity (Begay, 2018) and an estimated 15% are not connected to public utilities (US EPA, 2022).. The large distances between houses make energy access costly and have also hindered efforts to provide public water utilities to all Diné people, which is what the Navajo People refer to themselves as. These households must either haul water from regulated water points, which may be distant and costly, or use unregulated water sources, which may have unsafe levels of pathogens or heavy metals. Studies have found unsafe levels of arsenic, uranium, and other contaminants in unregulated water sources on the Navajo Nation (Credo et al., 2019; Hoover et al., 2017; Jones et al., 2020).

1.3. Off-Grid Water Purification Options

Water purification processes that can remove contaminants of interest, such as arsenic and uranium and can operate in remote and off-grid locations is necessary to ensure sustainable safe water access within remote communities. Ideal candidate processes must be economically sustainable, maintain environmental health, and allow for self-reliance by the users. Solar-powered water purification can be economically sustainable because the significant solar potential availability on the Navajo Nation allows energy production without miles of costly electrical wiring (Sneezer, 2020). The majority of the Navajo Nation has the potential for a solar photovoltaic resource of 6.1 $kW/m^2/day$ and the average household consumption is about 30 kW/m2/day, so household needs could be met with about 5 m^2. Some water purification technologies such as membrane distillation (MD) can be used in conjunction with solar power but are not sustainable in terms of the ability to be operated and maintained by a typical user. MD is a novel technology and while some vendors offer MD products, they are not typically available as “off-the-shelf” products (Hussain et al., 2022). Components for nanofiltration such as membrane elements, on the

other hand, are available online and can purchased by anyone. The lower power requirements also make it an attractive choice for off-grid water purification applications, as opposed to reverse osmosis (Cai et al., 2019).

1.4. Nanofiltration: Opportunities and Limitations

Nanofiltration is a pressure-driven membrane technology that can be used to separate compounds based on mass, typically capable of removing compounds with masses on the order of 200 to 100 Da, and based on electrostatic repulsion, typically removing divalent ions better than monovalent ions (Mariën et al., 2004). Size exclusion or electrostatic (Donnan) exclusion is affected by factors affecting compound size and charge such as pH, valence state, and ionic strength will affect rejection (Mariën et al., 2004). Rejection of arsenic by nanofiltration membranes is being studied and has been found to depend on pH and valence state (Boussouga et al., 2021a). Studies have also found that rejection of uranium depends on pH, speciation, and operating conditions such as pressure (Richards et al., 2011; Schulte-Herbrüggen et al., 2016). The results from these studies indicate the importance of understanding water quality parameters where nanofiltration is used as water purification.

Solar-powered nanofiltration (SNF) has advantages over some other water purification technologies because of its availability and lower costs, but it also has some limitations. Like other membrane driven processes, SNF is subject to fouling, which is the decline in permeate water production caused by deposition of material on the membrane surface or changes to the membrane surface (Schäfer et al., 2004). Fouling is also dependent on water quality characteristics, which also emphasizes the need for water quality information. Another factor that may impact fouling, is intermittent operation which is caused by the intermittent nature of solar energy and water

demand. Intermittent operation has not been the topic of many studies and is still not well understood (Freire-Gormaly and Bilton, 2019b).

1.5. Goals of the Study

The need for better understanding of the water treatment needs of the Navajo Nation and the limitations of the SNF systems were the motivation for this study. In particular, we aimed to understand the performance of a pilot-scale SNF system that was constructed by University of Arizona faculty and students. This study aimed to understand factors that will affect the performance of the SNF unit on the Navajo Nation. Water quality was tested at unregulated water sources where the unit could potentially be deployed. Performance with solutions of different water quality (divalent ions, heavy metals and organic compounds, and divalent ions and organic compounds) was quantified and monitored over weeks, or months. Different operating conditions, specifically rinsing after operation and no rinsing after operation, were tested as well. Finally, a membrane irreversibly fouled in the SNF system was autopsied and subjected analyses that would provide insight into the nature of the foulant.

Chapter 2: Water Quality Analysis of Unregulated Wells on the Navajo Nation

2.1. Introduction

The Navajo Nation covers about 25,000 square miles and is home to about 160, 000 people according to data from the 2020 census (U.S. Census Bureau, 2021). Due to the geology of the Navajo Nation, certain elements are naturally abundant, such as uranium, vanadium, and copper (Chenoweth and Malan 1973). One study that summarized water quality results from unregulated water sources in every agency in the Navajo Nation found that 12.5% of water sources exceeded the EPA Maximum Contaminant Level (MCL) for uranium, 30 μg/L, and 15% of sources exceeded the MCL for arsenic, 10 μg/L(Environmental Protection Agency n.d.; Hoover et al. 2017). While arsenic and uranium have been the focal point of several studies and regulatory guidelines, other elemental ions and heavy metals found in unregulated water sources on the Navajo Nation may be of concern as well. A study by Credo et al. that collected 296 samples from sources on the Western Navajo Nation looked at a wide variety of elemental contaminants and found that vanadium, calcium, arsenic, manganese, lithium, uranium, aluminum, molybdenum, strontium, and iron were the 10 elements that most commonly exceeded a health guideline (Credo et al., 2019). Of the guidelines used, only EPA MCLs are enforceable, but even those contaminants not subjected to an MCL may be of particular importance to human and livestock health. For example, molybdenum has been associated with developmental effects in infants (Nozadi et al., 2022) and high levels of aluminum, molybdenum, and vanadium may be toxic for lifestock (Meehan et al., 2021).

The natural abundance of dangerous elements in groundwater may be exacerbated by the history of mining on the Navajo Nation. Mining activities, especially uranium mining, took place

from the 1950s through the 1980s and left a complicated legacy of negative health effects and environmental impacts (Brugge and Goble, 2002). Many mines throughout the Western area of the United States, including the Navajo Nation, were abandoned without proper cleanup procedures and have degraded the environment (Government Accountability Office 2011). Several studies have found elevated levels of compounds such as uranium, arsenic and vanadium in groundwater in the vicinity of abandoned mines on the Navajo Nation (Blake et al. 2015; Hoover et al. 2017; Credo et al. 2019).

The presence of the aforementioned contaminants in the Navajo Nation groundwater is especially important because of the limited access to public water utilities on the Navajo Nation. While efforts to improve access to treated drinking water on the Navajo Nation has been made by federal entities, the most recent data from the EPA estimates that 15% of households still lack access to public water service (US EPA 2016). Those who lack access to piped water must haul water from regulated or unregulated water sources. The Navajo Nation Environmental Protection Agency has issued a health advisory against the use of unregulated sources because of the possibility of exposure to contaminants or pathogens (Navajo Nation Environmental Protection Agency n.d.), but for sparsely populated areas far from regulated sources, unregulated wells are still an important source of water both for human and livestock consumption.

Understanding the distribution of these contaminants is of great importance because of the potential effect on health from drinking contaminated water. Arsenic has been linked with cancers of the bladder, lungs, skin, kidney, nasal passage, liver, and prostate as well as other non-cancer cardiovascular, pulmonary, immunological, neurological, and endocrine effects (Environmental Protection Agency 2001a). The effects of uranium in drinking water include kidney toxicity as well as increased cancer risk (Environmental Protection Agency 2001b). Health disparities

including lower life expectancy and increased occurrence of birth defects between Native Americans, especially those living near abandoned uranium mines, and other populations in the United States have been documented that may be related to these groundwater issues (Lewis et al., 2017). Exposure to other heavy metals have been correlated with other adverse effects, such as deficits in an infant development screener associated with lead, arsenic, antimony, barium, copper, and molybdenum (Nozadi et al., 2022).

To address the need for groundwater treatment in areas with limited access to public infrastructure, off-grid pressure-driven membrane systems have been developed (Bouhadjar et al., 2019; García-Vaquero et al., 2014). Faculty and students at the University of Arizona developed a pilot-scale solar-powered nanofiltration (SNF) system and a solar-powered ultraviolet (SUV) system to meet water purification needs. The SNF system was designed to remove salinity and dissolved contaminants, while the SUV system can remove larger particles such as sediments and disinfect water. The suitability of these systems depends on the water quality, since nanofiltration may be unnecessary where only pathogens are present or may be insufficient if contaminants resistant to nanofiltration are present. The rejection of some of contaminants, such as uranium and arsenic of nanofiltration has been studied, but the results suggest that performance varies with other water quality characteristics such as pH and the presence of organic matter (Boussouga et al., 2021a; Schulte-Herbrüggen et al., 2016; Tanne et al., 2019). For those reasons, more information is needed to understand the nature of the contaminants and to understand factors that may impact the effectiveness of nanofiltration, especially at sites where a nanofiltration system may be deployed.

In this study, natural water samples were collected from a total of 17 sites from around the Navajo Nation. These samples were subjected to Inductively Coupled Plasma Mass Spectrometry

(ICP-MS) to quantify elemental contaminants including uranium, arsenic, iron, manganese, vanadium, and molybdenum and cation and anion chromatography (IC) to quantify the concentration of major ionic species including fluoride, nitrate, and nitrite which can also have health effects. Conductivity was measured, which can be used to estimate total dissolved solids (TDS). Total organic carbon (TOC) and pH were measured at 10 and 4 sites respectively. MCL exceedances for arsenic and/or uranium were found at five water sources, all in the Dilkon Chapter. SMCL exceedances for TDS were found at 12 water sources and SMCL exceedances for manganese and/or iron were also found at six water sources.

2.2. Materials and Methods

The selection of water sampling sites was based on areas where field work had previously been conducted by faculty, students, and staff from University of Arizona and local collaborators Sixth World Solutions, Dig Deep, and the Dilkon Chapter House and where future fieldwork was anticipated. Additionally, many sites were sampled at the request of community members who were present at a community meeting at the Dilkon Chapter House. Samples were collected during three sampling events that occurred in July 2021, October 2021, and March 2022. Each sampling event consisted of a different team of individuals, which may account for some variability in results and sampling procedure.

Methods for the analysis of water samples were based on US EPA Methods 200.8 for analysis of trace metals with ICP-MS and 415.3 for TOC analysis. Statistical analysis was conducted in Excel and ArcGIS was used to create maps demonstrating spatial distribution of results. Field measurements of conductivity, pH, and temperature were taken when possible, however due to the limited availability of equipment, field measurements of pH were only taken during the third sampling event and only for some sites. Sampling instructions for ICP-MS and

TOC are included in Appendix B, as well as instructions for the collection of water samples from a SNF unit. The SNF unit instructions were not used during collection of the samples included in this study, but are recommended for future sampling events.

2.2.1. Site Selection

Permission to sample groundwater was granted through chapter resolutions from the Dilkon Chapter and permission from homeowners. Funding for sampling was provided in part from the Agnese Nelms Haury Program in Environmental and Social Justice and in part from the Arizona Institute for Resilient Environments and Societies. The first sampling event collected water samples from Sand Springs, Oljato UT in July 2021. The second sampling event occurred in October 2021 and collected water from Black Falls AZ, Oljato UT, San Juan NM, and Lupton AZ. This sampling event collected water samples from water sources as well as treated water from a solar-powered nanofiltration unit (SNF) and a solar-powered UV (SUV) unit. A third sampling event took place March 2022 and took samples from 15 water sources, including 14 groundwater sources and one rainwater catchment source. Additionally, samples were taken of the treated water from the same SUV unit tested during the second sampling event. The majority of the groundwater sources were located in the Dilkon Chapter, Fort Defiance Agency. The rest of the samples were from the same sources as the second sampling event, namely Black Falls Drinking, Lupton Well, Lupton Rain, and Lupton Permeate. The results from those sites sampled twice can provide some indication of seasonal variation of water quality. Private water sources are referred to by the chapter they are located in to protect the privacy of their owners and publicly known water sources are referred to by the name that community members know them as.

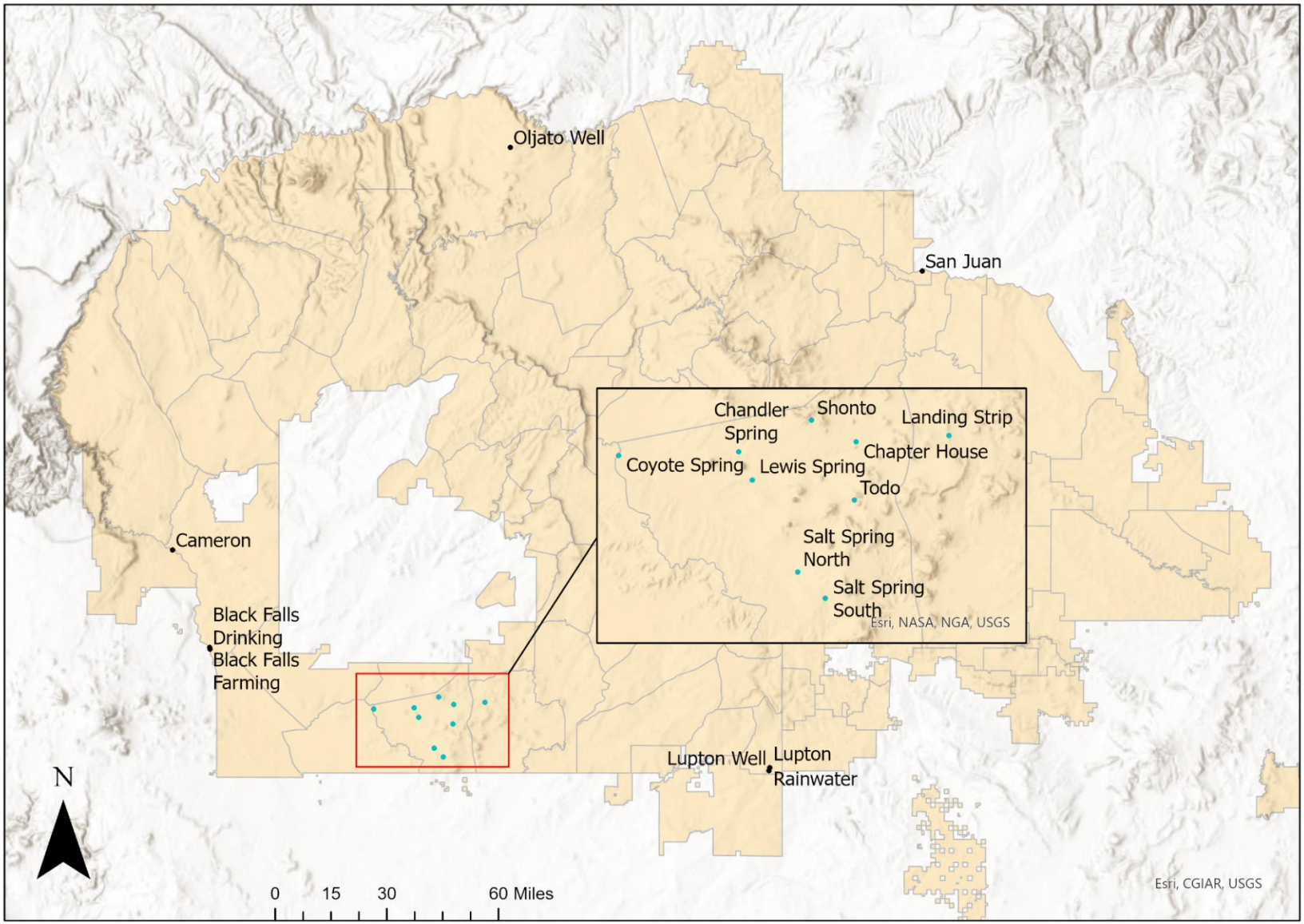

Figure 2.2.1 Map of the Navajo Nation with sampling locations and inset map of Dilkon Chapter sampling locations

2.2.2. Field Sampling Methods and Sample Preparation

The GPS coordinates of each sample were recorded and used to create a map demonstrating the spatial distribution of the samples collected, Figure 2.2.1. Photos were also taken at each location as well as notes of relevant geographic and constructed features in the vicinity of the water source. An Oakton PC650 conductivity meter was used to collect conductivity measurements for all sampling events and was calibrated before each sampling event. The conductivity was used to estimate the concentration of total dissolved solids (TDS) and was calibrated before each sampling event. For the third sampling event in March 2022, a YSI ProPlus was used to collect pH and temperature information. The samples for TOC analysis were collected in 40 mL amber glass vials and acidified to less than pH 2 with 1 M hydrochloric acid immediately after collection. Samples were not filtered and the values for TOC presented include suspended particulate matter, organic colloids, and dissolved organic matter. Samples intended for ICP-MS analysis were collected in plastic 50 mL polypropylene conical vials and acidified to less than pH 2 with 67% trace metal grade nitric acid. Samples for IC analysis were collected in 50 mL polypropylene conical vials and left at the natural pH. All samples were immediately stored at less than 6°C in a temperature-controlled container and then a refrigerator at 4°C until analysis. The complete water source list can be found in Table 2.1.

Table 1 Water Source List and Analyses Conducted.

Site Name	**Longitude**	**Latitude**	**Date(s) of sample collection**	**Field Measurements Taken**	**Analyses Conducted**
Sand Spring			Sept 2021	Conductivity	TOC, IC, ICP-MS

Black Falls Drinking	-111.26944	35.56829	October 27th 2021, March 7th 2022	pH, Conductivity	TOC, IC, ICP-MS (Oct-ALEC)
Black Falls Farming	-111.26862	35.56284	March 7th 2022	pH, Conductivity	TOC, IC, ICP-MS
Oljato	-110.10137	37.132896	October 28th 2021	Conductivity	TOC, IC, ICP-MS (ALEC)
San Juan	-108.50205	36.74911	October 28th 2021	Conductivity	TOC, IC, ICP-MS (ALEC)
Lupton Rainwater	-109.09684	35.17786	October 29th 2021, March 8th 2022	pH, Conductivity, Temperature	TOC, IC, ICP-MS (Oct-ALEC)
Lupton Well	-109.09497	35.18629	October 29th 2021, March 8th 2022	pH, Conductivity, Temperature	TOC, IC, ICP-MS (Oct-ALEC)
Lupton UV-Treated Rainwater	-109.09684	35.17786	March 8th 2022	pH, Conductivity, Temperature	TOC, IC, ICP-MS
Lupton UV-Treated Well Water	-109.09497	35.18629	October 29th 2021	Conductivity, Temperature	TOC, ICP-MS (ALEC)
Chandler Spring	-110.47560	35.37740	March 8th 2022	Conductivity, Temperature	IC, ICP-MS
Coyote Spring	-110.63233	35.37315	March 8th 2022	Conductivity, Temperature	IC, ICP-MS
Dilkon Chapter House	-110.32287	35.38815	March 7th 2022	Conductivity	IC, ICP-MS
Landing Strip	-110.201357	35.39464	March 7th 2022	Conductivity	IC, ICP-MS
Shonto	-110.38069	35.41112	March 7th 2022	Conductivity	IC, ICP-MS
Lewis Spring	-110.45800	35.34700	March 7th 2022	Conductivity, Temperature	IC, ICP-MS
Salt Spring North	-110.39878	35.24922	March 8th 2022	Conductivity	IC, ICP-MS
Salt Spring South	-110.36275	35.22116	March 8th 2022	Conductivity	IC, ICP-MS
Todo	-110.32510	35.32582	March 7th 2022	Conductivity	IC, ICP-MS

2.2.3. Laboratory Analyses and Interpretation of Results

A Dionex ICS-5000 cation ion chromatography was used to test for K^+, Na^+, Ca^{2+}, Mg^{2+} and anion ion chromatography was used to test for Fl^-, Cl^-, NO_2^-, SO_4^{2-}, Br^-, NO_3^- and PO_4^{3-}. The Dionex Six Cation-I Standard was used to construct the calibration curve for each cation analyte and the Dionex Seven Anion Standard II was used to construct the calibration curve data for each anion analyte. Samples were diluted as needed to so that concentrations of ions were within the limits of the instrument.

TOC analysis with a Shimadzu TOC-L was used to quantify non-purgeable organic carbon present in samples. Calibration standards were created using potassium hydrogen phthalate (KHP) at a concentration of 25 mg C/L. An Agilent 7800 ICP-MS was used to quantify the following elements: Li 7, Be 9, Na 23, Mg 24, Al 27, K 39, V 51, Cr 52, Mn 55, Fe 56, Co 59, Ni 60, Cu 63, Zn 66, As 75, Se 78, Sr 88, Mo 95, Ag 107, Cd 111,Sn 118, Sb 121, Ba 137, Tl 205, Pb 208, U 238. The Agilent Pharma Internal Standard 1, which contains Bi, Ge, and In was used as the internal standard to monitor instrument drift. Samples were diluted with a 2% nitric acid solution.

After unexpected results were found from the October 2021 sampling trip (see Table 4), the Arizona Laboratory for Emerging Contaminants (ALEC) at the University of Arizona was used to conduct ICP-MS re-analysis for those samples. They measured a slightly different list of analytes: Li 7, Be 9, Na 23, Mg 24, Al 27, K 39, Ca 40, V 51, Cr 52, Mn 55, Fe 56, Co 59, Ni 60, Cu 63,Zn 66, Ga 69, As 75, Se 78, Rb 85, Sr 88, Mo 95, Ag 107, Cd 111, In 155,Sn 118, Sb 121, Cs 133, Ba 137, Tl 205, Pb 208, Bi 209, U 238.

All of the water quality results from this study were organized in an Excel spreadsheet along with the GPS coordinates, site names, and sampling date. The results for sites that were sampled both in October 2021 and March 2022 (Black Falls Drinking and Lupton) were compared. Results were also compared to previous testing results if available on Navajo WaterGIS, which is a project by researchers from University of New Mexico, University of Arizona, and Northern Arizona University and the Southwest Research and Information Center. It is a database that compiles water quality data for certain Navajo Nation water sources that have been sampled by USGS, EPA, US Army Corps of Engineers, or other researchers. The sites that could be found were compared to the averages for arsenic, selenium, lead, and uranium that were presented in the Navajo Water GIS project.

2.3. Results

The results from field measurement, IC analysis, ICP-MS analysis and TOC analysis that are most relevant to human health or SNF operation are presented in Table 2. The results included are conductivity, pH, and TOC (when possible), anions with MCLs (nitrite, nitrate, and fluoride), and 10 elemental contaminants that a study of Western Navajo Nation groundwater found most commonly: vanadium, calcium, arsenic, manganese, lithium, uranium, aluminum, molybdenum, strontium, and iron (Credo et al., 2019). Additionally, the conductivity can be used to estimate total dissolved solids (TDS) by multiplying it by an empirically derived factor. This factor has been found to range from 0.54 to 0.96 and the American Water Works Assoc. (AWWA) recommends the use of 0.5 (Geddes, Kunihiro, and Turner 2004; Singh and Kalra 1975). A factor of 0.65 was used in this study to be more conservative than the AWWA recommendation. The data

were compared to US EPA MCLs, as well as relevant guidelines, including EPA Secondary Maximum Contaminant Levels (SMCLs) (US EPA, 2015b), EPA Drinking Water Standards and Health Advisory (DWSHA) (Office of Water Environmental Protection Agency, 2018), EPA Regional Screening Level (Environmental Protection Agency, 2021) and EPA Unregulated Contaminant Monitoring Rule (UCMR) reference level (US EPA, 2015a). The guidelines that were used to evaluate water quality results are presented in Table 2 along with the possible health effects and other concerns cited in the applicable guideline. Values that exceed the guidelines are highlighted in red in Table 3. The results for all analytes can be found in the Appendix. Further analyses of these results are broken down by location: Dilkon Chapter, Oljato Chapter, Coalmine Mesa Chapter (Black Falls), and Lupton Chapter.

Table 2 Guidelines applicable to analytes tested for in this study and potential health and aesthetic effects.

Contaminant	**Guideline**	**Guideline Source**	**Potential Health Effects**	**Other Concerns**
pH	6.5-8.5	EPA SMCL, not enforceable		At low pH: bitter taste, corrosion. At high pH: slippery feel, deposits.
TDS	500 mg/L	EPA SMCL, not enforceable		Hardness, colored water, staining, salty
Fluorine	4.0 mg/L (MCL) 2.0 mg/L (SMCL)	EPA MCL, enforceable EPA SMCL, not enforceable	Skeletal fluorosis – disorder causing extreme density and hardness and fragility of the bones	Tooth discoloration and/or pitting of teeth in children
Nitrate/nitrite	44 mg/L (nitrate) 3.28 mg/L (nitrite)	EPA MCL, enforceable	Blue-baby syndrome in infants under 6 months old, which can be	

			serious. Long-term exposure can cause increased urine production and bleeding of the spleen.	
Lithium	40 µg/L	EPA RSL, not enforceable	Impaired thyroid and kidney function	
Aluminum	50-200 µg/L	EPA SMCL, not enforceable		Colored water
Vanadium	21 µg/L	EPA UCMR Reference Level, not enforceable	Nausea, mild diarrhea, stomach cramps	
Manganese	50 µg/L	EPA SMCL, not enforceable	Neurological effects	Black/brown color, black staining, metallic taste
Iron	300 µg/L	EPA SMCL, not enforceable		Rusty color, sediment, staining, metallic taste
Arsenic	10 µg/L	EPA MCL, enforceable	Cancerous effects on the skin, bladder, lung, kidney, nasal passages, and prostate Cardiovascular, pulmonary, immunological, neurological and endocrine effects	
Molybdenum	80 µg/L	EPA DWSHA, not enforceable	Essential nutrient, but high levels can affect kidneys and liver	
Strontium	4 mg/L	EPA DWSHA, not enforceable	Musculoskeletal effects	
Uranium	30 µg/L	EPA MCL, enforceable	Increased risk of cancer Kidney toxicity	

Table 3 Selected results from field measurements, TOC analysis, IC analysis, and ICP-MS analysis.

Site Name	**pH**	**Conduct-ivity (µS/cm)**	**TDS (mg/L)**	**TOC (mg/L)**	**Fl^- (mg/L)**	**NO_2^- (mg/L)**	**NO_3^- (mg/L)**	**Ca^{2+} (mg/L)**	**Li (µg/L)**	**Al (µg/L)**	**V (µg/L)**	**Mn (µg/L)**	**Fe (µg/L)**	**As (µg/L)**	**Sr (µg/L)**	**Mo (µg/L)**	**U (µg/L)**
Guideline	6.5-8.5		500		4	3.29	44		40	50-200	21.0	50	300	10	4000	80	30
Sand Spring		570.30	370.70	0.58				110.99	20.01	1.68	8.30	0.03	0.89	2.05	341.75	1.45	4.02
Cameron		1737.00	1129.05	3.71	1.32	0.01	0.27	45.56	59.19	3.94	1.70	146.65	316.79	5.95	1694.81	7.54	3.64
Oct 2021 Black Falls Drinking		1354.00	880.10	2.50	1.17	0.19	0.27	64.56	16.54	27.02	8.77	46.55	266.46	2.27	1231.79	19.27	10.75
Oljato Feed		841.40	546.91	2.22	0.74	0.27	2.95	25.62	15.93	44.82	5.98	0.25	69.25	0.93	294.86	0.85	2.61
Oljato Permeate		313.00	203.45	2.54	1.02	0.26	1.50	34.36	12.85	45.88	1.47	11.69	82.51	0.69	209.55	0.34	0.03
Oljato Brine		1340.00	871.00	5.15	1.03	0.51	2.59	48.21	29.41	56.29	8.02	20.50	146.24	1.61	552.74	1.59	4.42
San Juan		812.60	528.19	2.60	0.93	1.21	0.12	356.63	31.89	42.83	2.19	88.54	198.01	1.34	1061.97	2.07	3.00
Oct 2021 Lupton Rain		98.24	63.86	5.09	0.34	0.35	0.92	3.57	1.38	191.04	2.15	8.95	782.65	0.47	52.08	0.12	0.05
Oct 2021 Lupton Feed		297.20	193.18		0.61	0.39	6.95	39.73									
Oct 2021 Lupton UV-Treated Well		262.00	170.30	0.79					10.74	54.55	2.40	1.88	0.12	0.87	227.98	0.28	0.52
Oct 2021-Lupton Well		297.60	193.44		0.51	0.64	6.77	39.61	8.92	54.20	7.85	4.50	1049.95	2.55	259.21	0.37	0.99
Landing Strip		1802.00	1171.30		3.08	0.07	ND	10.47	33.83	22.80	0.09	3.66	291.20	6.79	2411.11	156.49	0.45

Mar 2022 Black Falls Drinking	7.63	1313.00	853.45		0.71	0.03	0.01	62.53	17.26	96.60	8.02	51.09	85.57	1.75	1230.43	24.16	10.96
Black Falls Farming	7.75	1540.00	1001.00		0.66	0.14	1.14	55.92	22.58	84.64	12.83	0.50	7.84	2.42	848.10	10.31	12.08
Chandler Spring		568.10	369.27		0.40	0.03	1.22	32.25	24.16	105.72	35.69	1.85	21.62	8.19	970.98	16.19	4.19
Coyote Creek		1600.00	1040.00		3.34	0.03	9.49	16.34	63.60	106.19	134.89	3.25	219.29	39.87	704.38	29.01	31.79
Dilkon Chapter House		757.00	492.05		1.07	0.17	0.09	49.89	79.55	6.62	0.11	29.88	126.94	2.29	1288.02	8.54	0.06
Shonto		466.00	302.90		0.17	0.08	0.79	9.81	8.30	106.54	14.93	0.62	15.46	2.80	126.44	2.73	2.84
Lewis Spring		1028.00	668.20		1.50	0.01	24.99	10.96	26.87	100.78	76.20	0.37	11.24	32.62	429.17	20.11	8.62
Salt Spring North		2464.00	1601.60		3.48	0.20	2.59	7.35	145.34	145.42	235.18	8.26	498.02	95.74	397.79	12.97	131.99
Salt Spring South		12830.00	8339.50		1.14	0.17	0.39	18.75	144.96	96.10	43.29	1.01	71.86	21.49	834.65	6.32	56.83
Todo		683.10	444.02		0.81	0.05	2.07	1.56	8.58	132.58	85.57	0.57	25.60	54.42	57.38	44.42	7.77
Mar 2022 Lupton Rain	6.79	76.00	49.40	4.513	0.81	0.05	2.07	1.56	1.08	98.79	1.90	1.83	13.88	0.46	41.03	0.16	ND
Mar 2022 Lupton Well	7.14	313.20	203.58	0.688	0.12	0.07	8.77	37.84	9.22	82.99	4.45	8.44	ND	1.63	267.52	0.66	0.70
Mar 2022 UV-Treated Rain	6.35	96.80	62.92	4.184	0.03	0.08	3.99	12.68	4.13	89.75	1.94	1.58	9.53	0.67	129.98	0.47	0.11

ND indicates the analyte was not detected

2.3.1. Dilkon Chapter

Water sampling results from the Dilkon area indicated that five out of the nine groundwater sources tested exceeded an MCL for at least one contaminant. Arsenic was the most common contaminant present of the regulated species tested for, with five sampling sites exceeding the MCL and one site approaching the MCL, with a concentration of 8.2 μg/L. The uranium MCL was exceeded in three of the sources sampled, all of which were also in exceedance of the arsenic MCL. The results for arsenic and uranium concentrations were mapped in Figures 2.3.1 and 2.3.2 to demonstrate the spatial distribution. Conductivity is also mapped in Figure 2.3.3 and water sources estimated to exceed the SMCL of TDS of 500 mg/L using the conversion factor 0.65 are labelled in red. Five water sources are estimated to exceed the SMCL of TDS, which would cause unpleasantly salty water.

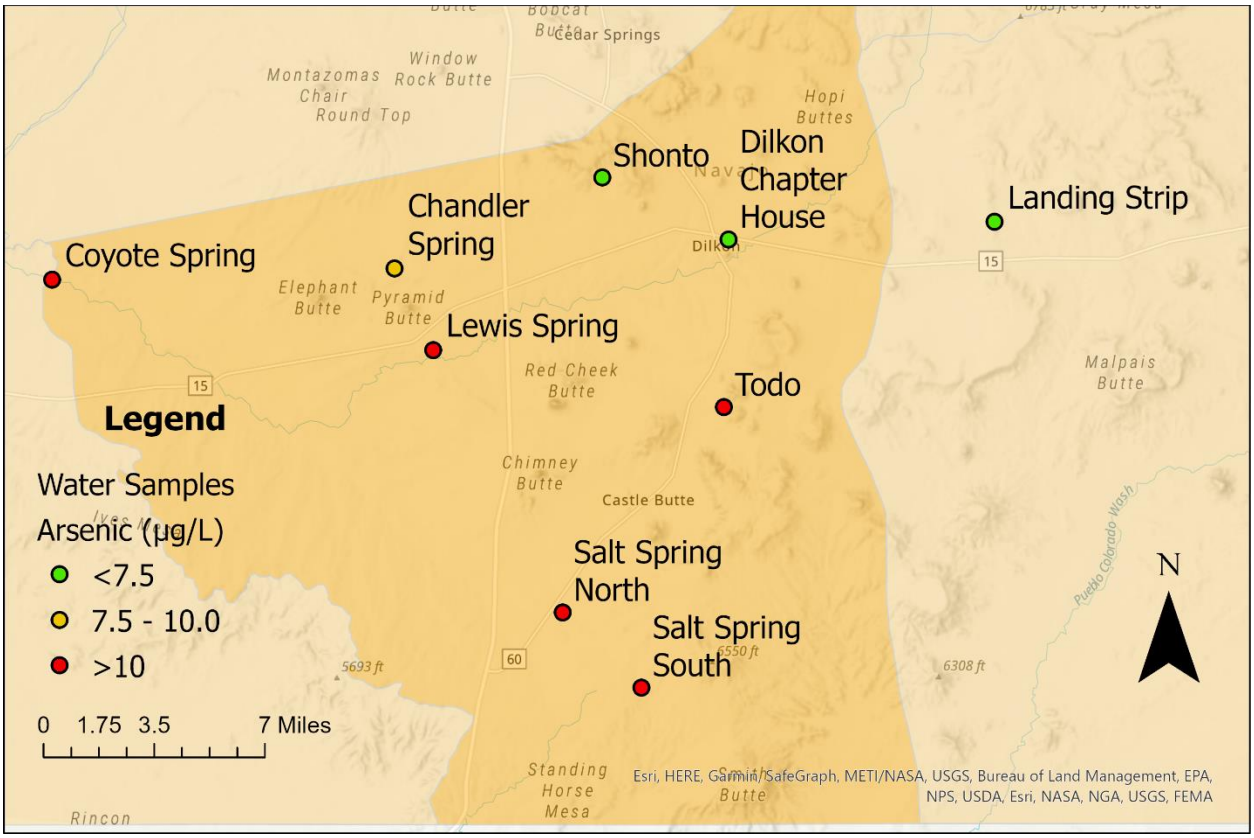

Figure 2.3.1 Map of arsenic concentrations in µg/L of groundwater samples from the Dilkon Chapter.

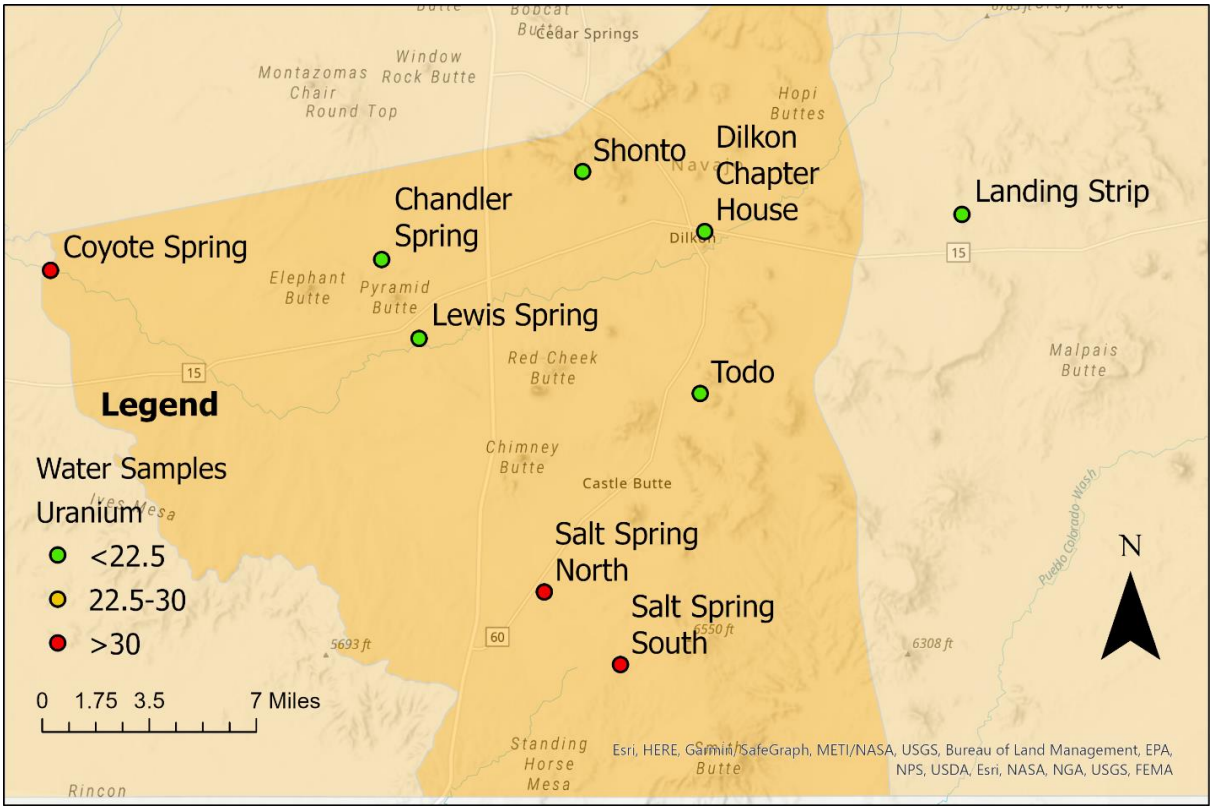

Figure 2.3.2 Map of uranium concentrations in µg/L of groundwater samples from the Dilkon Chapter.

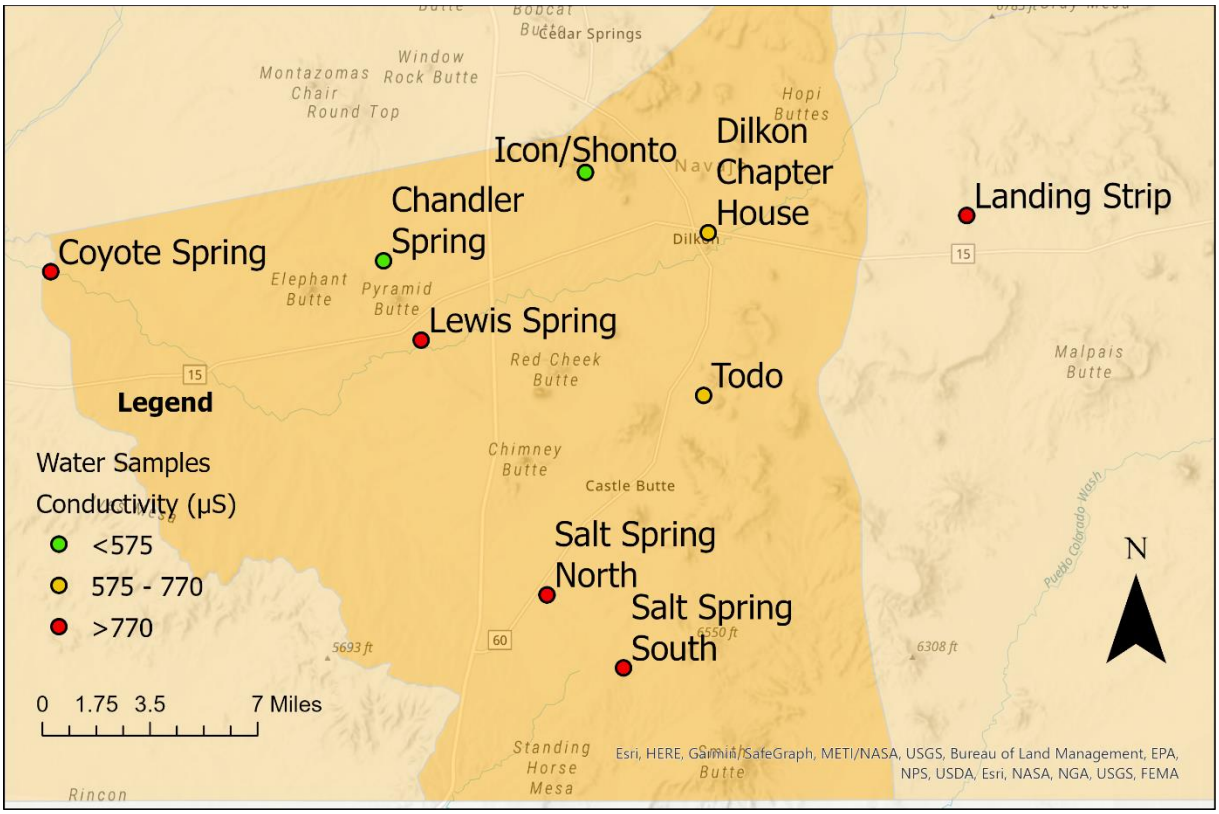

Figure 2.3.3 Map of conductivity in µS/cm of groundwater samples from the Dilkon Chapter.

The concentrations of anions and cations detected with ion chromatography and selected elemental contaminants are presented in Figure 2.3.4 and compared to the relevant guidelines. There were no exceedances of the MCLs for any ionic contaminant, although the SMCL of fluoride was exceeded at Landing Strip, Coyote Creek, and Salt Spring North. The EPA RSL for lithium was exceeded at four sites: Coyote Creek, Dilkon Chapter House, Salt Spring North, and Salt Spring South. All samples were within the SMCL range for aluminum (50 µg/L – 200 mg/L), except Landing Strip and Dilkon Chapter which were below the SMCL range. However, aluminum is only of concern because of aesthetic effects so these results are not concerning from a health perspective. Vanadium was another common contaminant and was presented above the guideline

of 21 μg/L at Chandler Spring, Coyote Creek, Lewis Spring, Salt Spring North, Salt Spring South, and Todo. Iron was only present above the SMCL in Salt Spring North. The DWSHA for molybdenum was only exceeded by the water sample from Landing Strip.

The water sampling results indicate that arsenic and uranium are the contaminants of greatest concern in the Dilkon area. Although exceedances of the vanadium guideline are also common, the guideline is not enforceable and the associated health effects are not as severe as those associated with uranium and arsenic. The removal of TDS is also necessary for five of the sources. These results can guide SNF design and maintenance for units deployed in the Dilkon area. For example, selection of the nanofiltration membrane may depend on the contaminants present and disposal of brine may require additional procedures if the brine contained high levels of uranium or arsenic.

(1a)

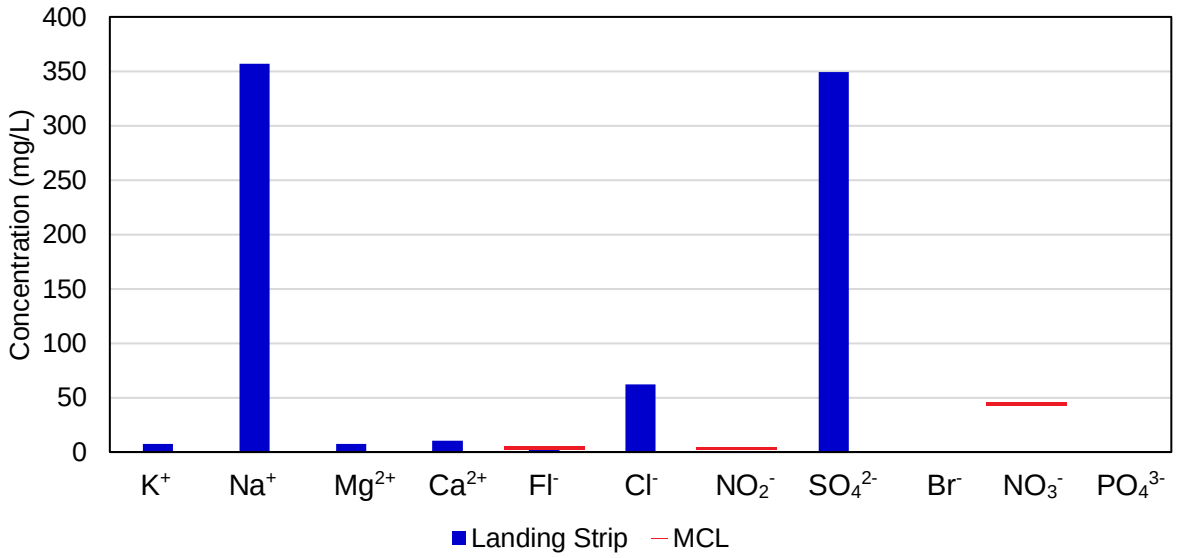
400
350
300
250
200
150
100
50
0
Concentration (mg/L)
K+
Na+
Mg2+
Ca2+
Fl-
Cl-
NO2-
SO42-
Br-
NO3-
PO43-
Landing Strip
MCL

(1b)

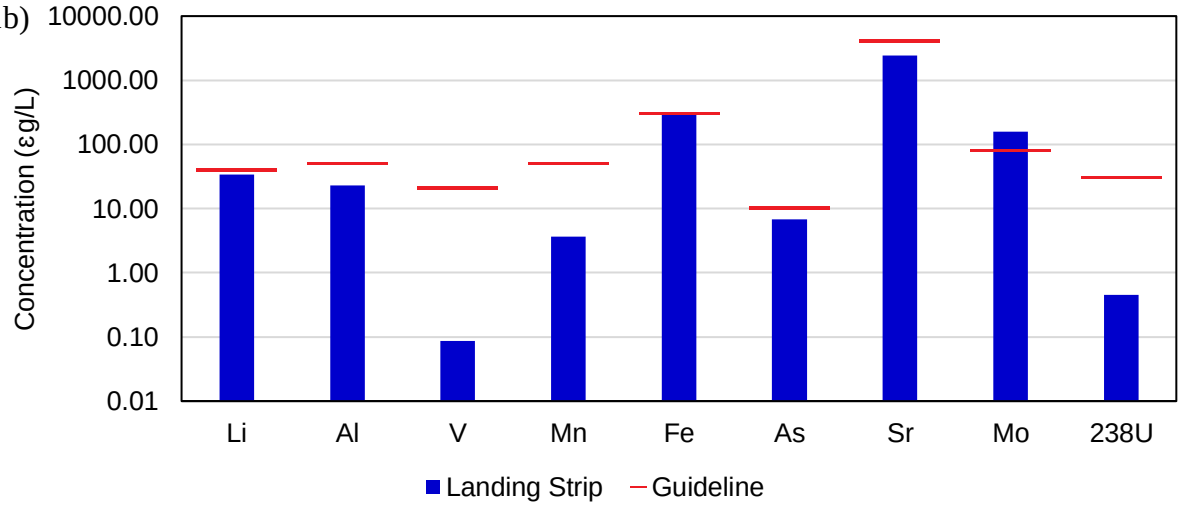
10000.00
1000.00
100.00
10.00
1.00
0.10
0.01
Concentration (εg/L)
Li
Al
V
Mn
Fe
As
Sr
Mo
238U
Landing Strip
Guideline

(2a)

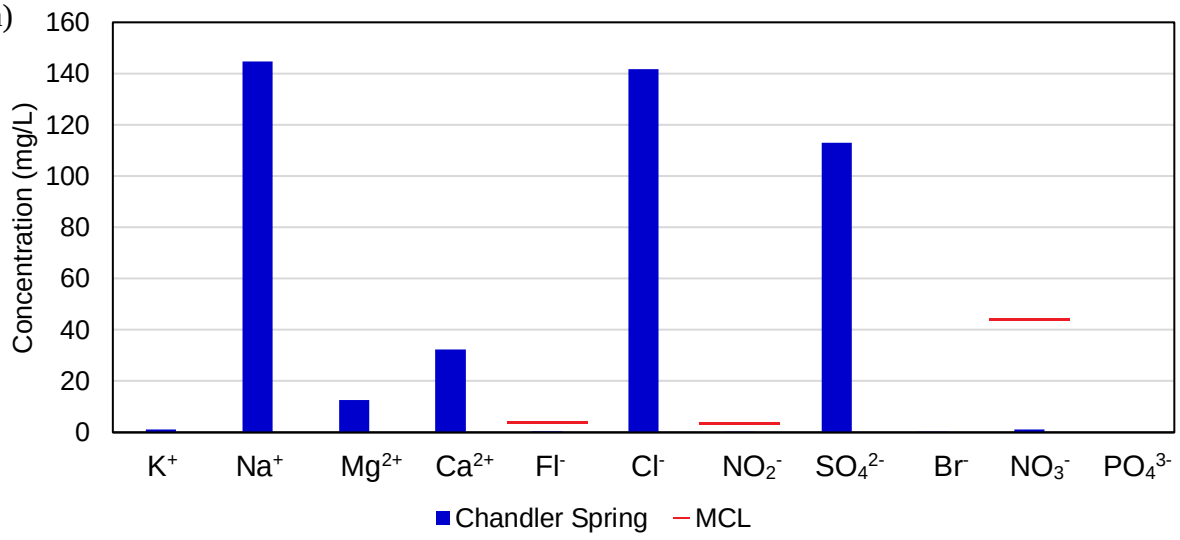
160
140
120
100
80
60
40
20
0
Concentration (mg/L)
K+
Na+
Mg2+
Ca2+
Fl-
Cl-
NO2-
SO42-
Br-
NO3-
PO43-
Chandler Spring
MCL

(2b)

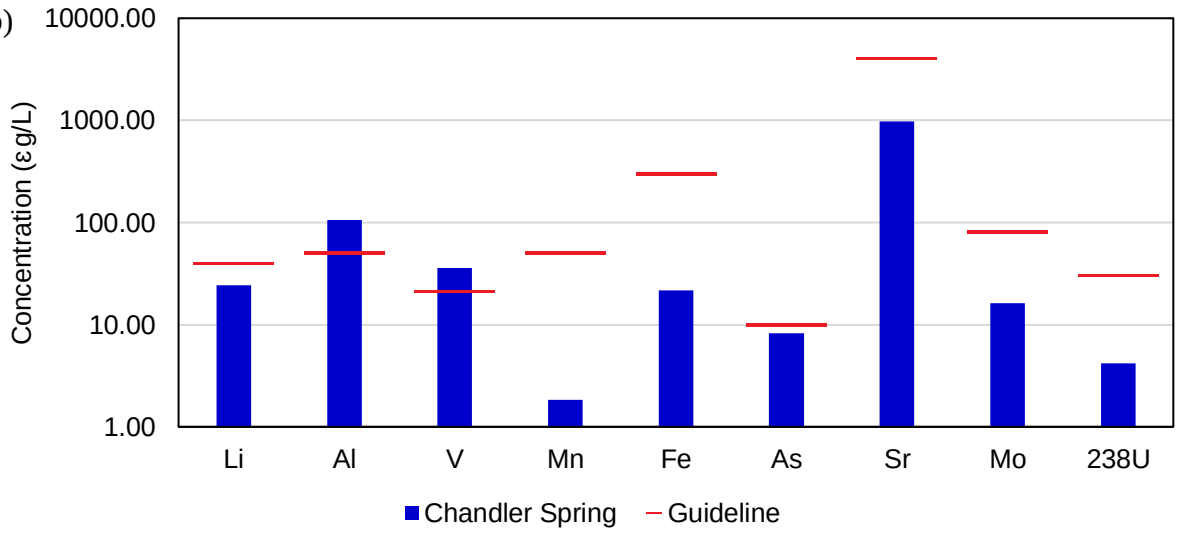
10000.00
1000.00
100.00
10.00
1.00
Concentration (ε g/L)
Li
Al
V
Mn
Fe
As
Sr
Mo
238U
Chandler Spring
Guideline

(3a)

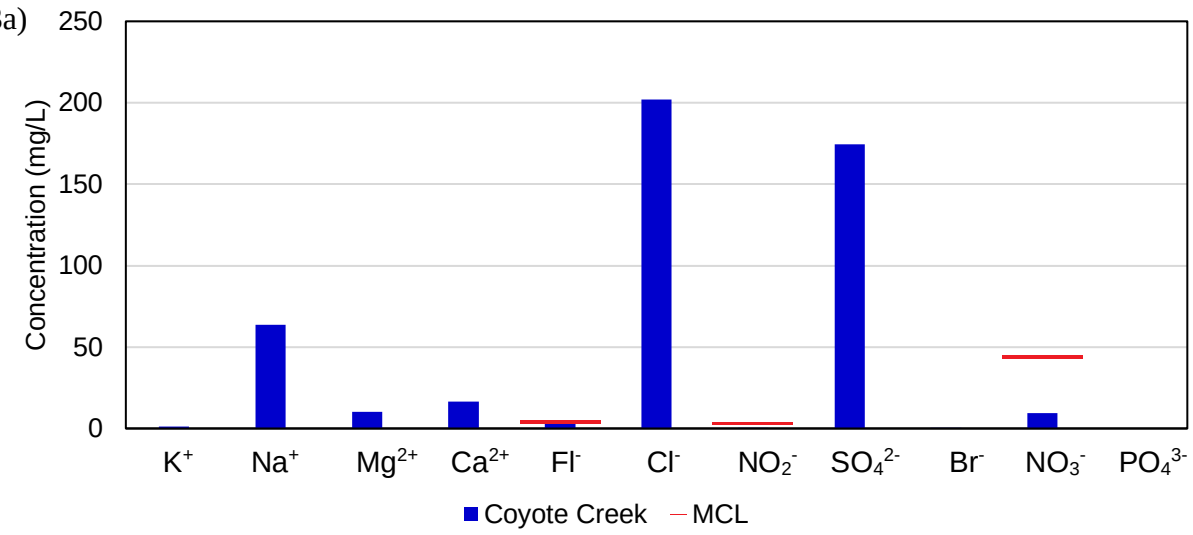
250
200
150
100
50
0
Concentration (mg/L)
K+
Na+
Mg2+
Ca2+
Fl-
Cl-
NO2-
SO42-
Br-
NO3-
PO43-
Coyote Creek
MCL

(3b)

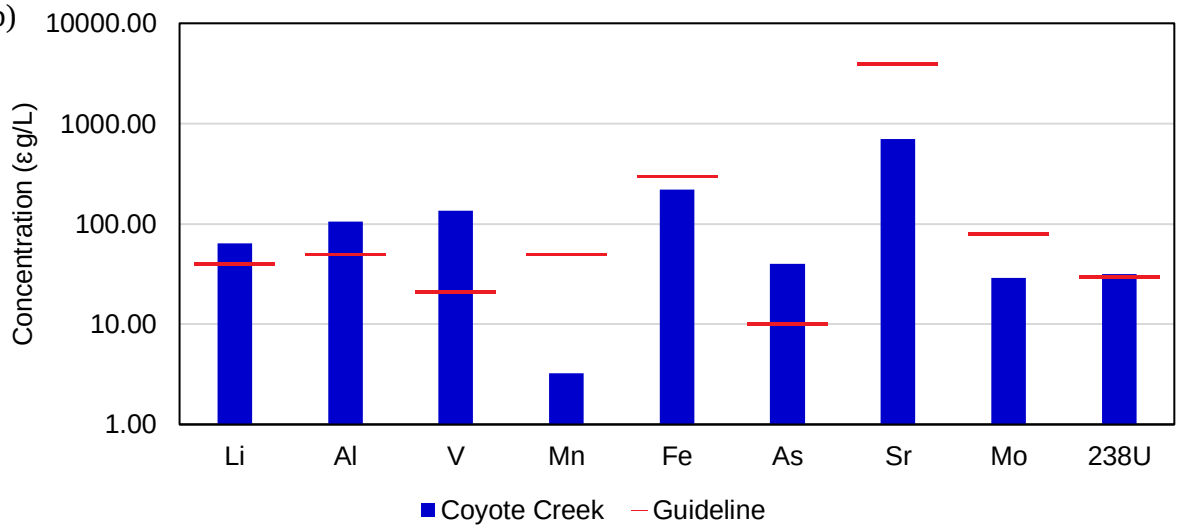
10000.00
1000.00
100.00
10.00
1.00
Concentration (εg/L)
Li
Al
V
Mn
Fe
As
Sr
Mo
238U
Coyote Creek
Guideline

(4a)

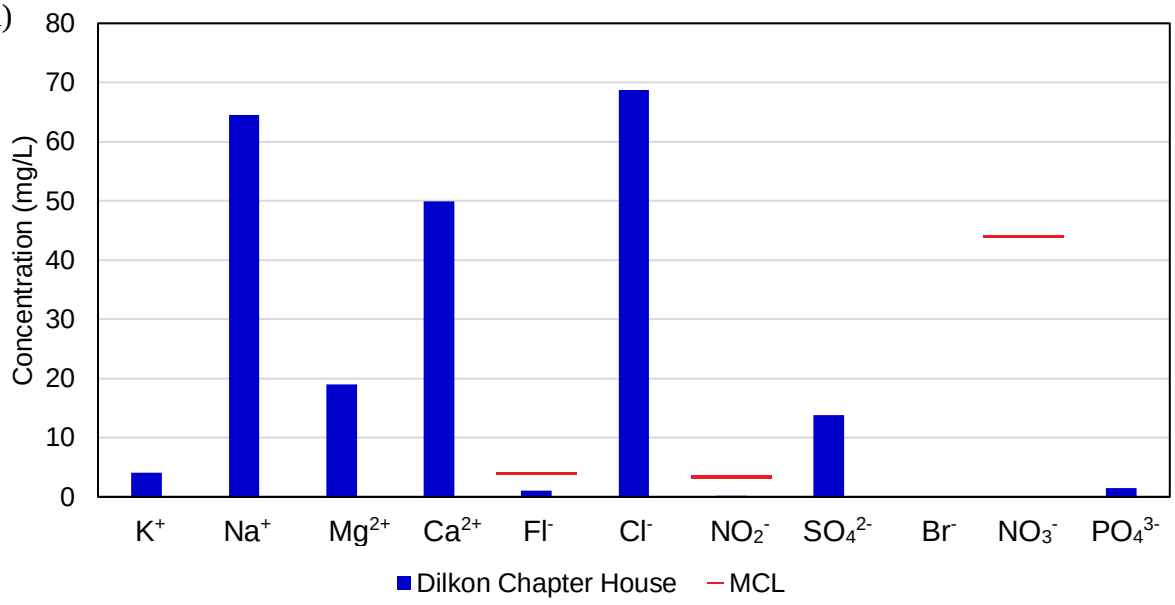
80
70
60
50
40
30
20
10
0
Concentration (mg/L)
K+
Na+
Mg2+
Ca2+
Fl-
Cl-
NO2-
SO42-
Br-
NO3-
PO43-
Dilkon Chapter House
MCL

(4b)

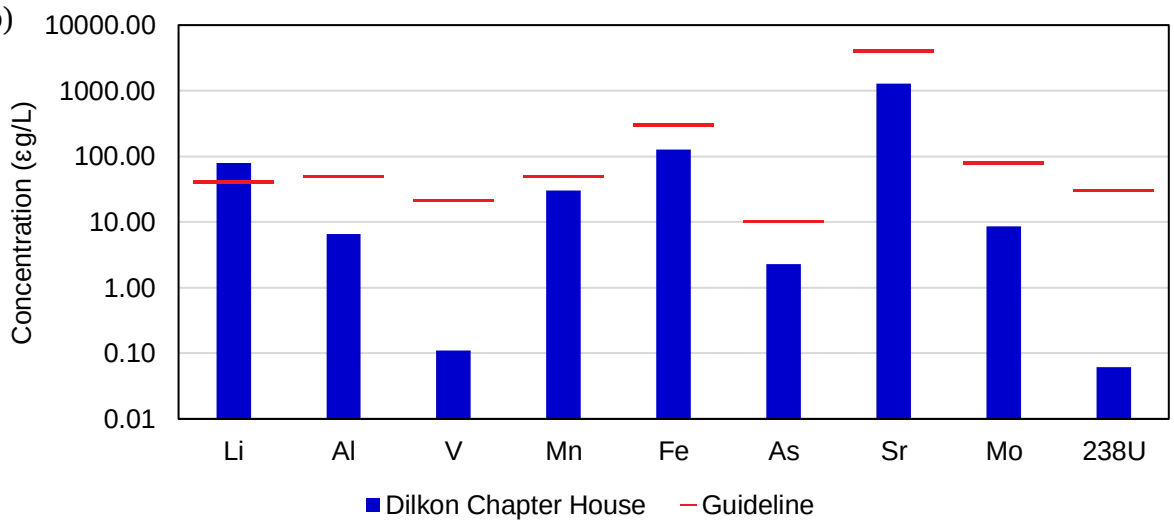
10000.00
1000.00
100.00
10.00
1.00
0.10
0.01
Concentration (εg/L)
Li
Al
V
Mn
Fe
As
Sr
Mo
238U
Dilkon Chapter House
Guideline

(5a)

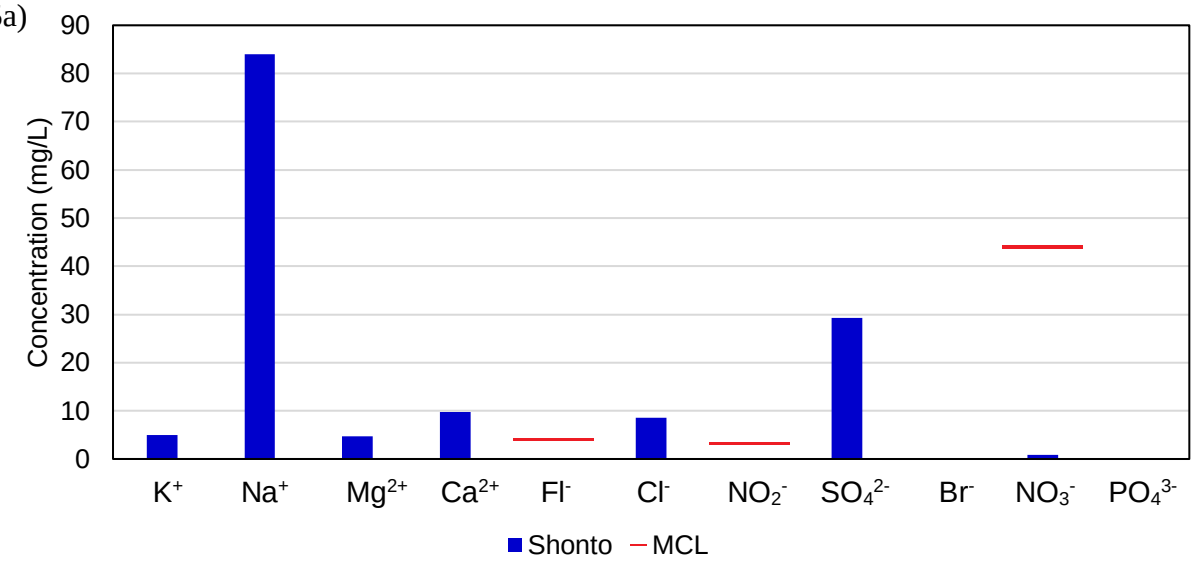
90
80
70
60
50
40
30
20
10
0
Concentration (mg/L)
K+
Na+
Mg2+
Ca2+
Fl-
Cl-
NO2-
SO42-
Br-
NO3-
PO43-
Shonto
MCL

(5b)

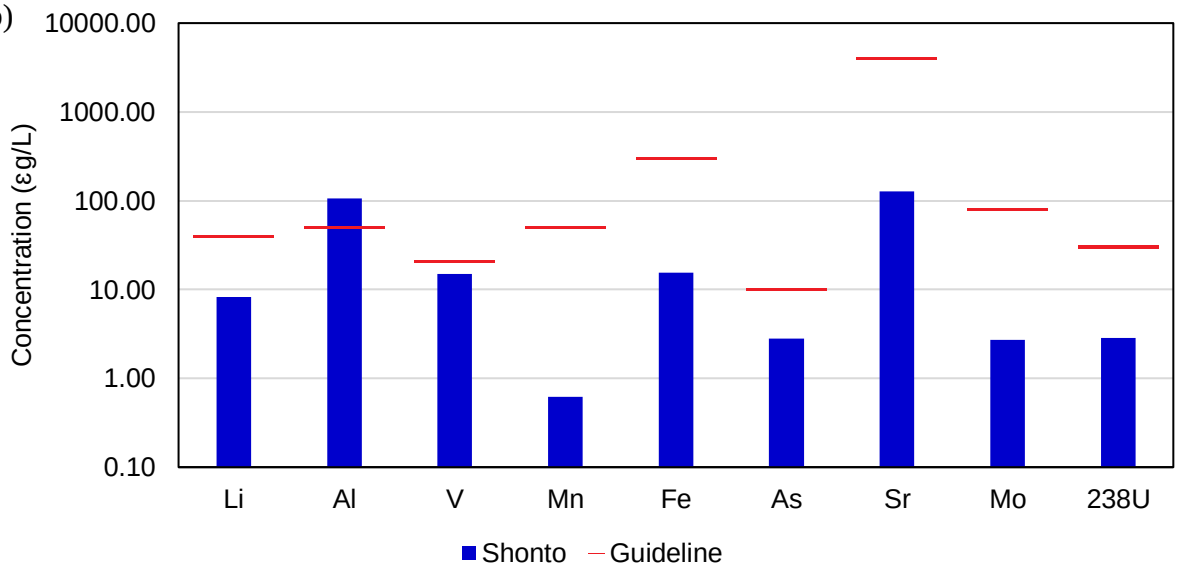
10000.00
1000.00
100.00
10.00
1.00
0.10
Concentration (εg/L)
Li
Al
V
Mn
Fe
As
Sr
Mo
238U
Shonto
Guideline

(6a)

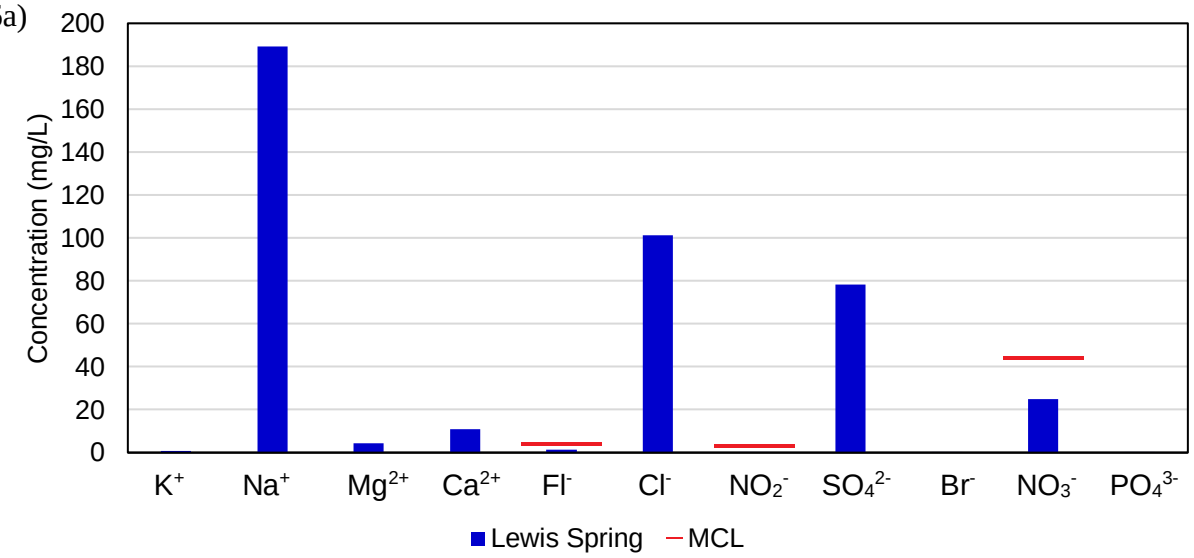
200
180
160
140
120
100
80
60
40
20
0
Concentration (mg/L)
K+
Na+
Mg2+
Ca2+
Fl-
Cl-
NO2-
SO42-
Br-
NO3-
PO43-
Lewis Spring
MCL

(6b)

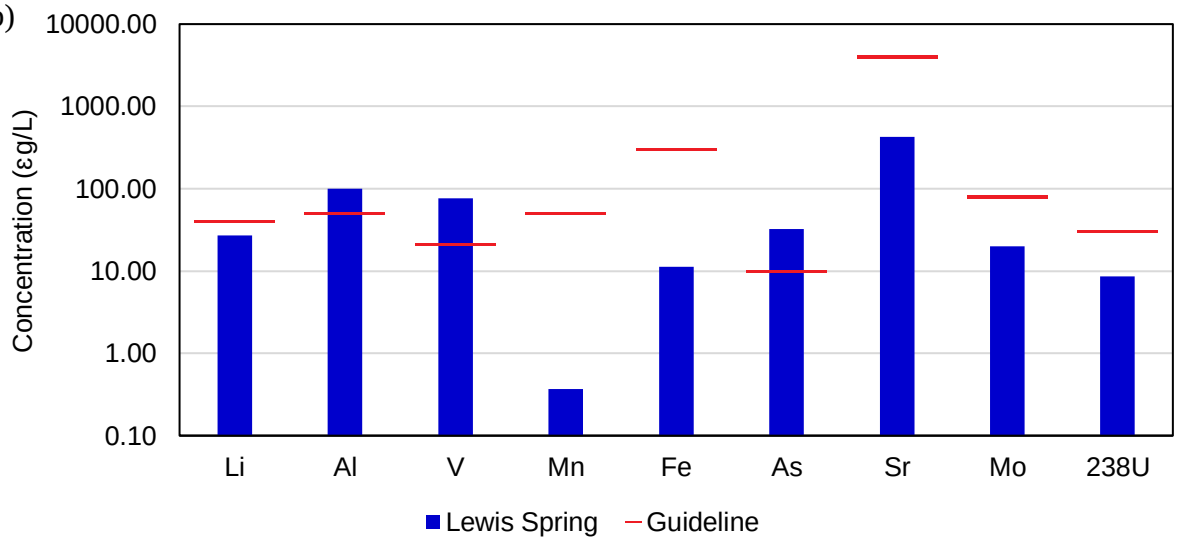
10000.00
1000.00
100.00
10.00
1.00
0.10
Concentration (εg/L)
Li
Al
V
Mn
Fe
As
Sr
Mo
238U
Lewis Spring
Guideline

(7a)

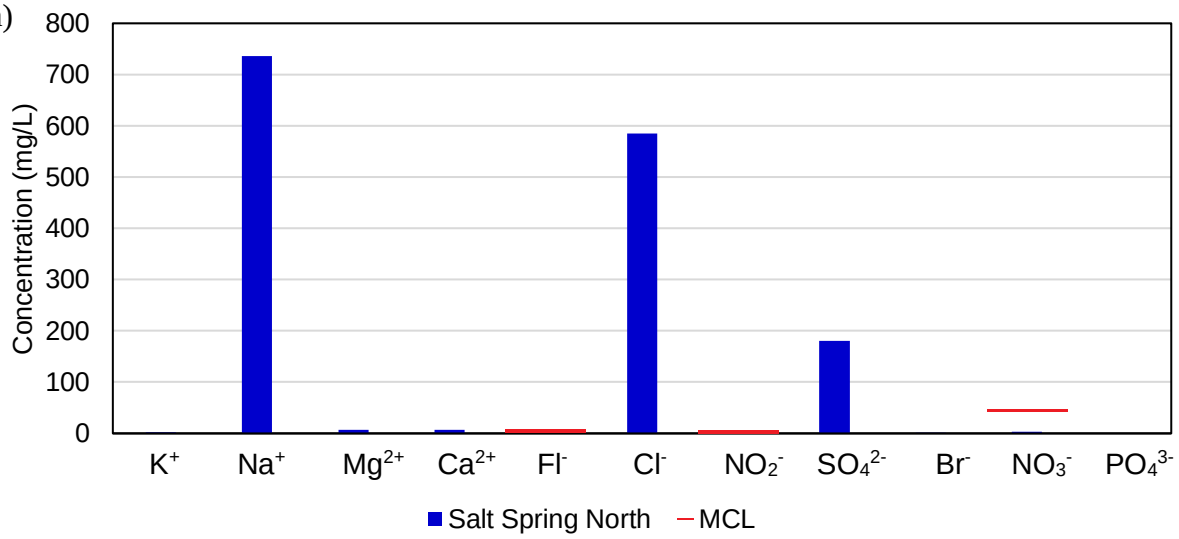
800
700
600
500
400
300
200
100
0
Concentration (mg/L)
K+
Na+
Mg2+
Ca2+
Fl-
Cl-
NO2-
SO42-
Br-
NO3-
PO43-
Salt Spring North
MCL

(7b)

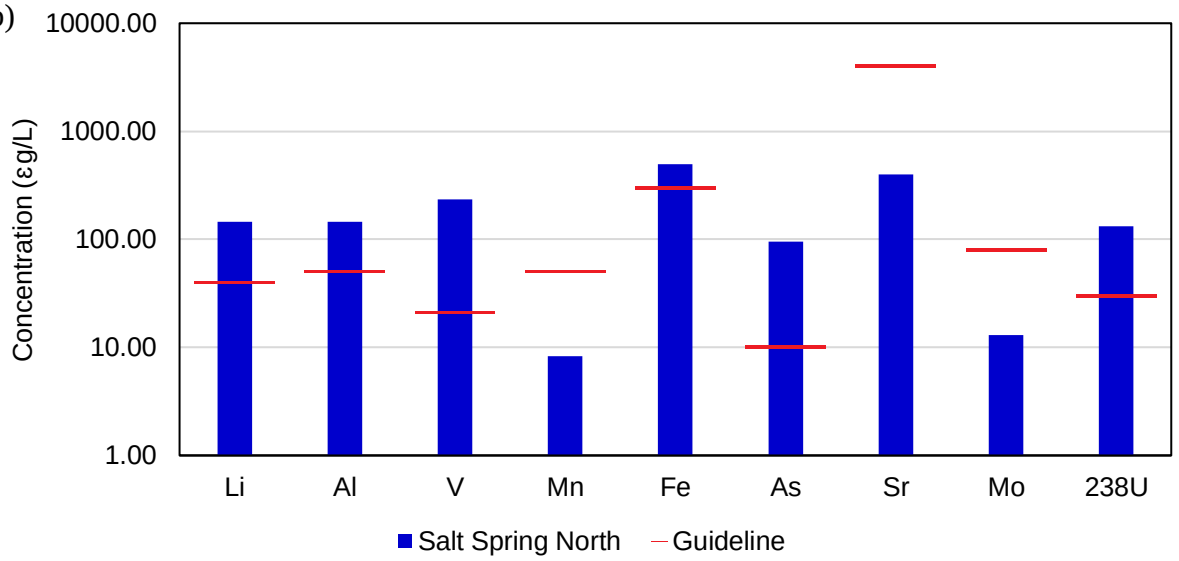
10000.00
1000.00
100.00
10.00
1.00
Concentration (εg/L)
Li
Al
V
Mn
Fe
As
Sr
Mo
238U
Salt Spring North
Guideline

(8a)

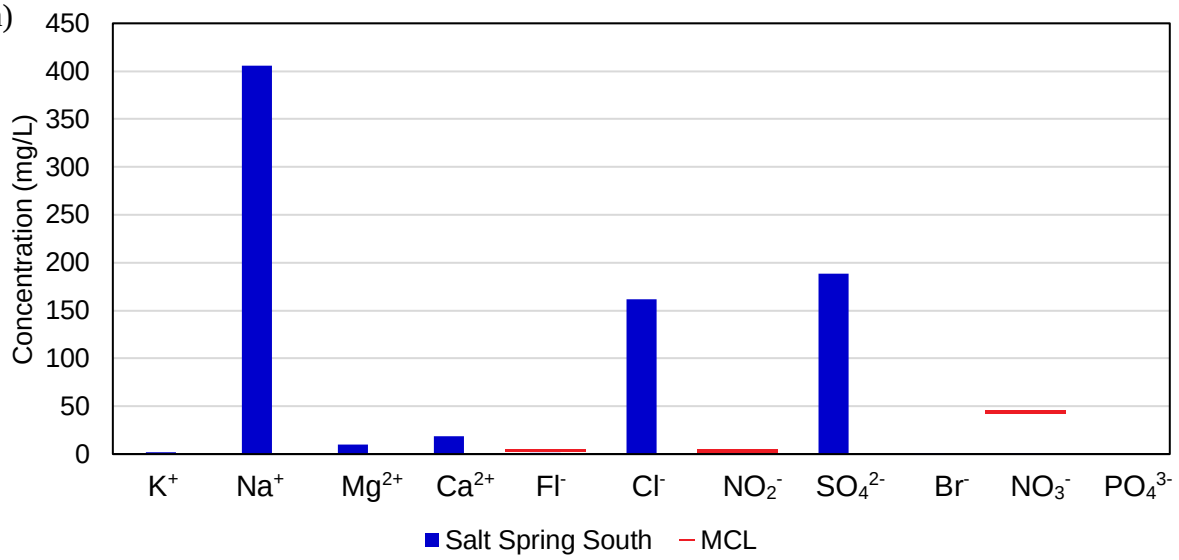
450
400
350
300
250
200
150
100
50
0
Concentration (mg/L)
K+
Na+
Mg2+
Ca2+
Fl-
Cl-
NO2-
SO42-
Br-
NO3-
PO43-
Salt Spring South
MCL

(8b)

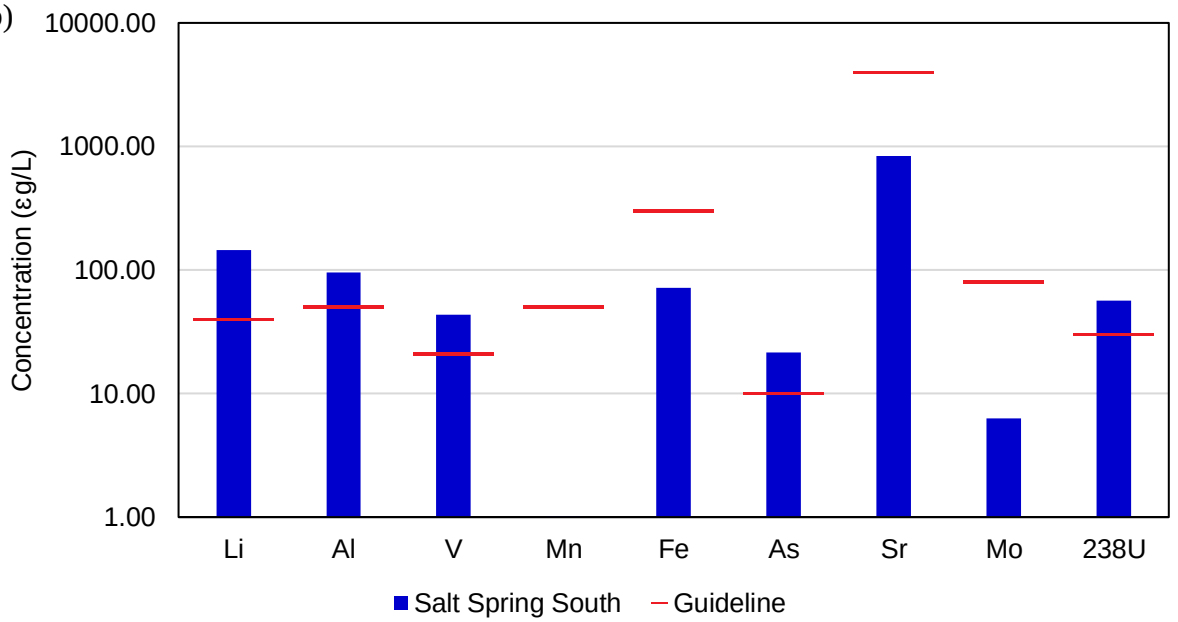
10000.00
1000.00
100.00
10.00
1.00
Concentration (εg/L)
Li
Al
V
Mn
Fe
As
Sr
Mo
238U
Salt Spring South
Guideline

(9a)

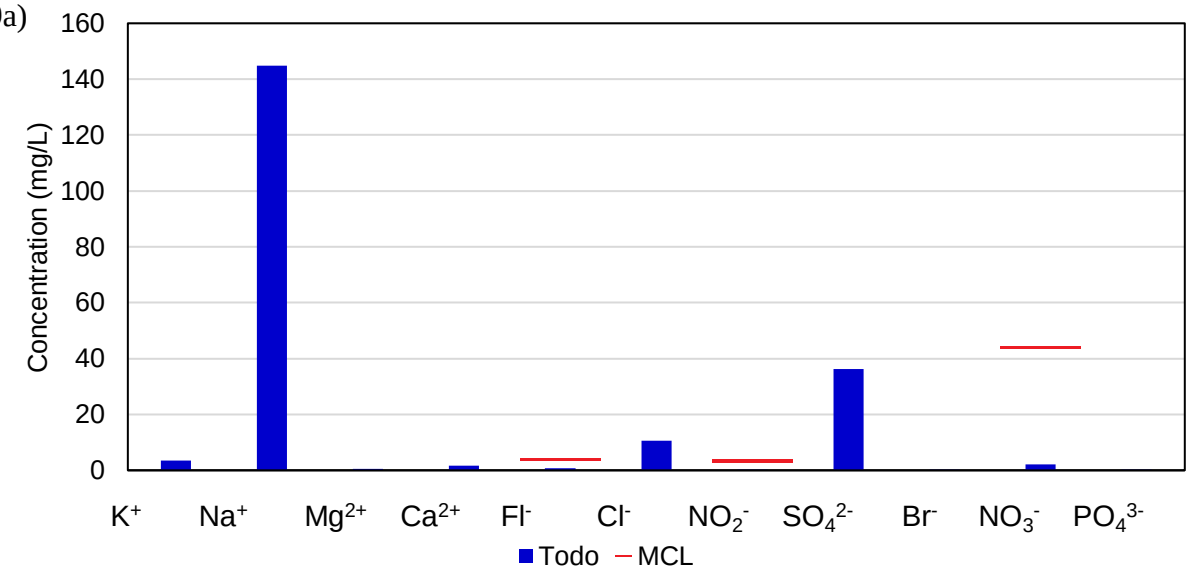

(9b)

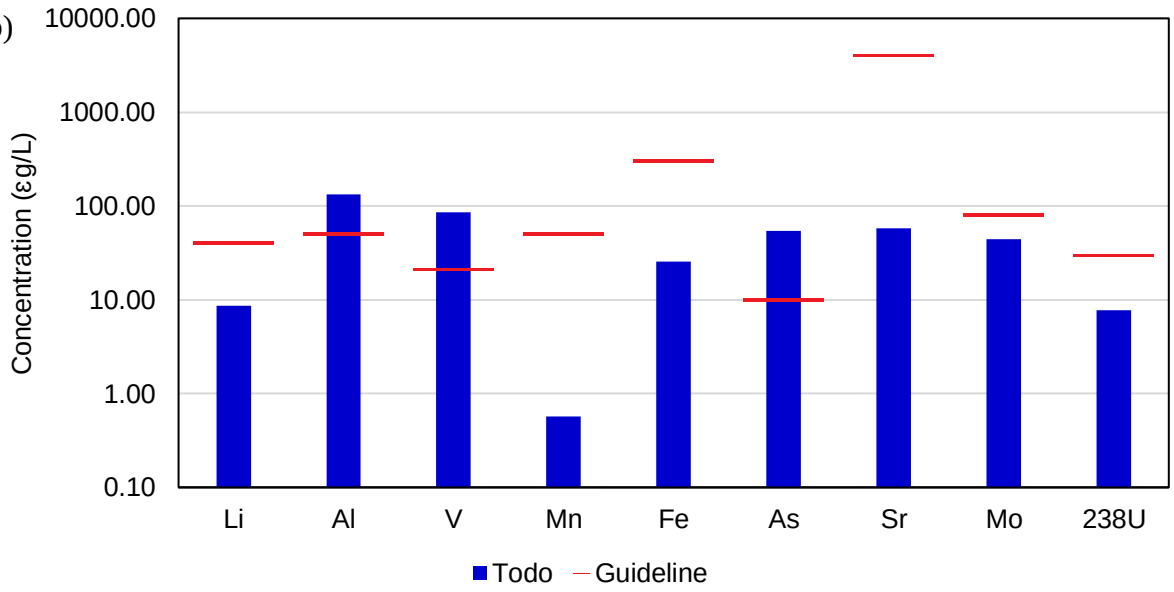

Figure 2.3.4 Concentrations of selected analytes by sampling site: Landing Strip (1a) ions, (1b) selected elemental contaminants; Chandler Spring (2a) ions, (2b) selected elemental contaminants; Coyote Creek (3a) ions, (3b) selected elemental contaminants; Dilkon Chapter House (4a) ions, (4b) selected elemental contaminants; Shonto (5a) ions, (5b) selected elemental contaminants; Lewis Spring (6a) ions, (6b) selected elemental contaminants; Salt Spring North (7a) ions, (7b) selected elemental contaminants; Salt Spring South (8a) ions, (8b) selected elemental contaminants; Todo (9a) ions, (9b) selected elemental contaminants.

Three sampling sites from the present study were also identified on the Navajo WaterGIS database: Dilkon Chapter House, Chandler Spring, and Shonto. The average values presented in the Navajo WaterGIS website for arsenic, selenium, lead, and uranium were compared to the results from the present study, as presented in Figure 2.3.5. The results from the present study do not indicate any exceedances for the presented analytes, but the WaterGIS data for Chandler Spring exceeds the MCL for arsenic. This may indicate that Chandler Spring varies over time and if an SNF were installed it should include a membrane capable of removing arsenic.

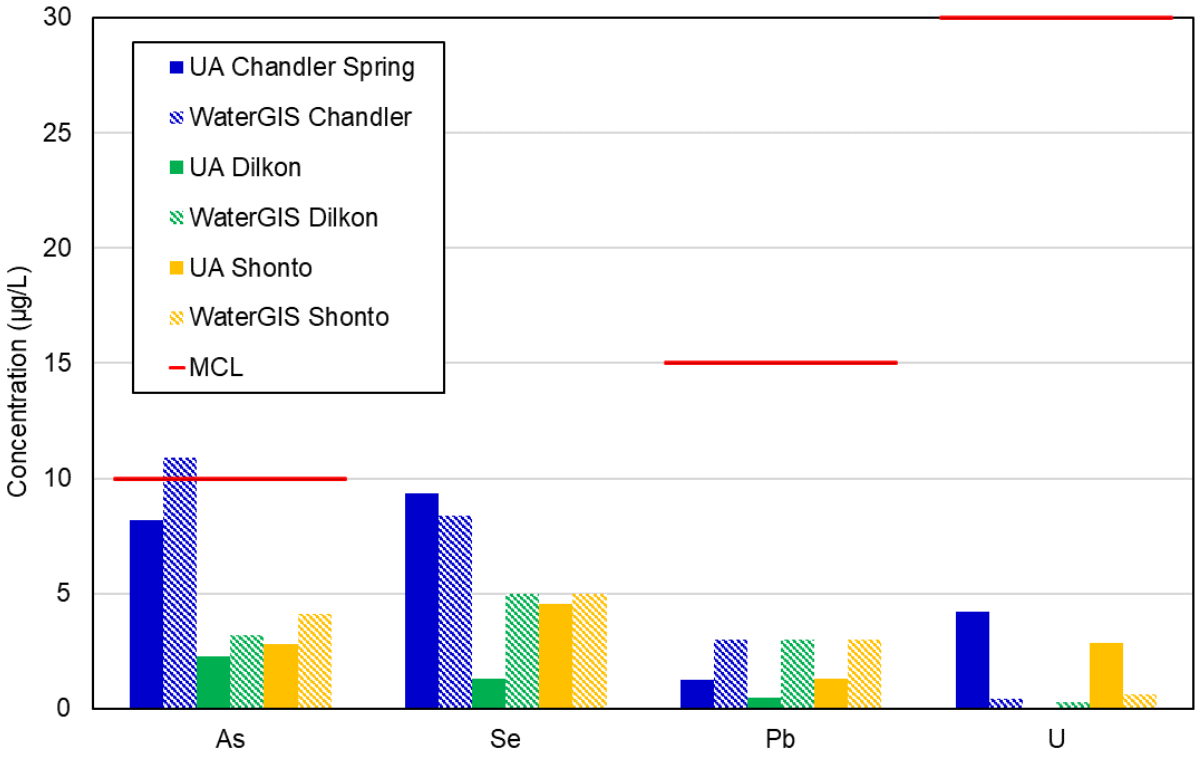

Figure 2.3.5 Comparison of results from the present study to Navajo WaterGIS data for arsenic, selenium, lead, uranium and EPA MCLs. The MCL for selenium (50 µg/L) is omitted for clarity.

2.3.2. Oljato Chapter

Water sources in Oljato Chapter were labelled as Sand Spring and Oljato and results are presented in Figure 2.3.6. The Oljato water source was used as feed water for a demonstration SNF unit, thus knowing the water quality can help understand if the SNF is a suitable treatment for the specific water source. There were no exceedances of MCLs for the samples taken in the Oljato area, although the estimated TDS is slightly above the SMCL at 546 mg/L. Nanofiltration would be sufficient to reduce the TDS concentration to below the SMCL.

(1a)

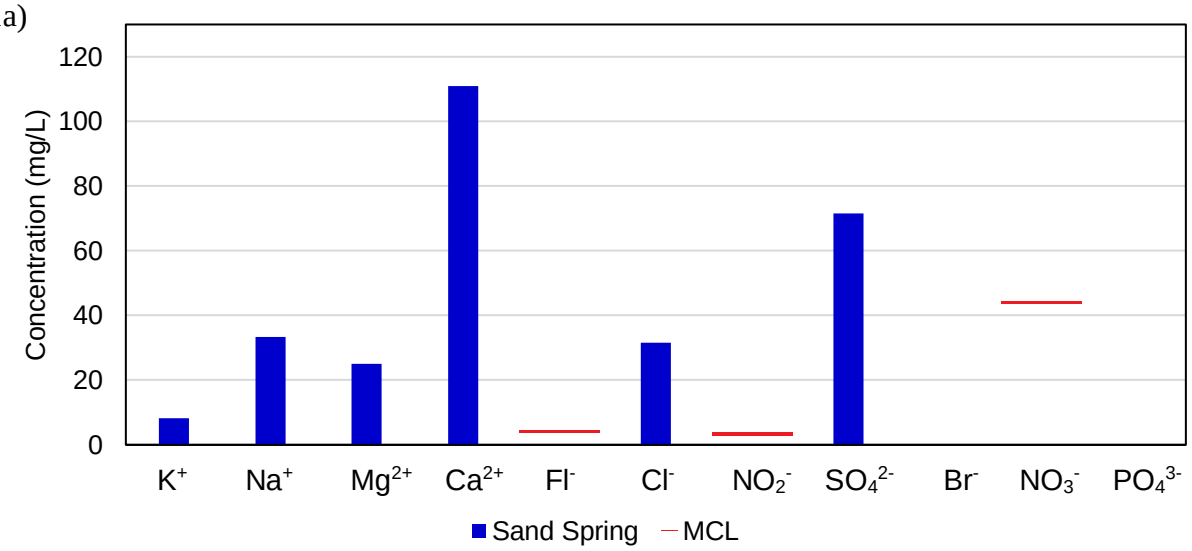

(1b)

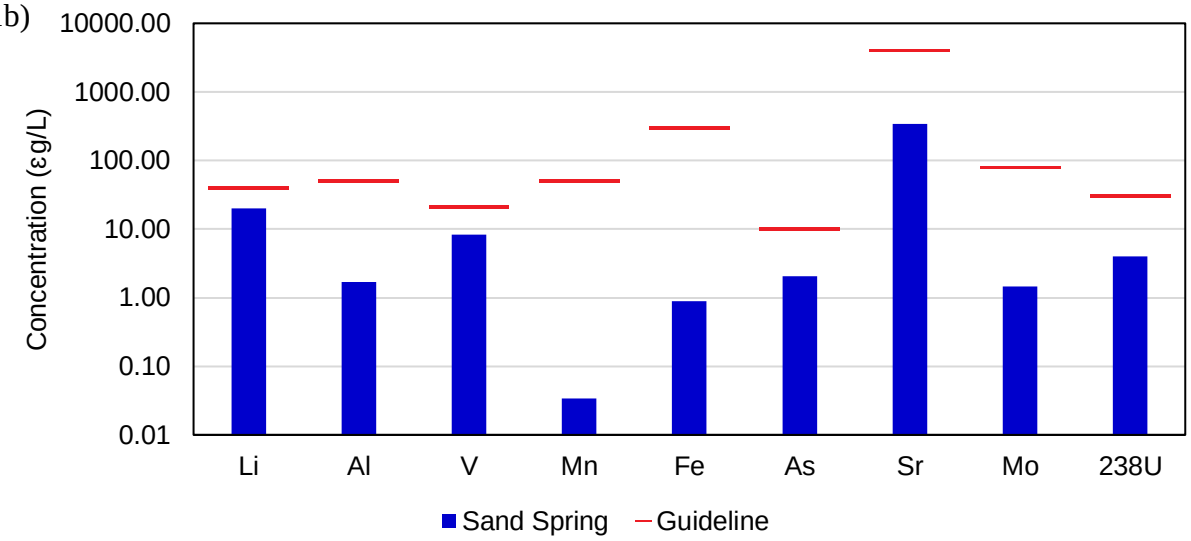
10000.00
1000.00
100.00
10.00
1.00
0.10
0.01
Concentration (εg/L)
Li
Al
V
Mn
Fe
As
Sr
Mo
238U
Sand Spring
Guideline

(2a)

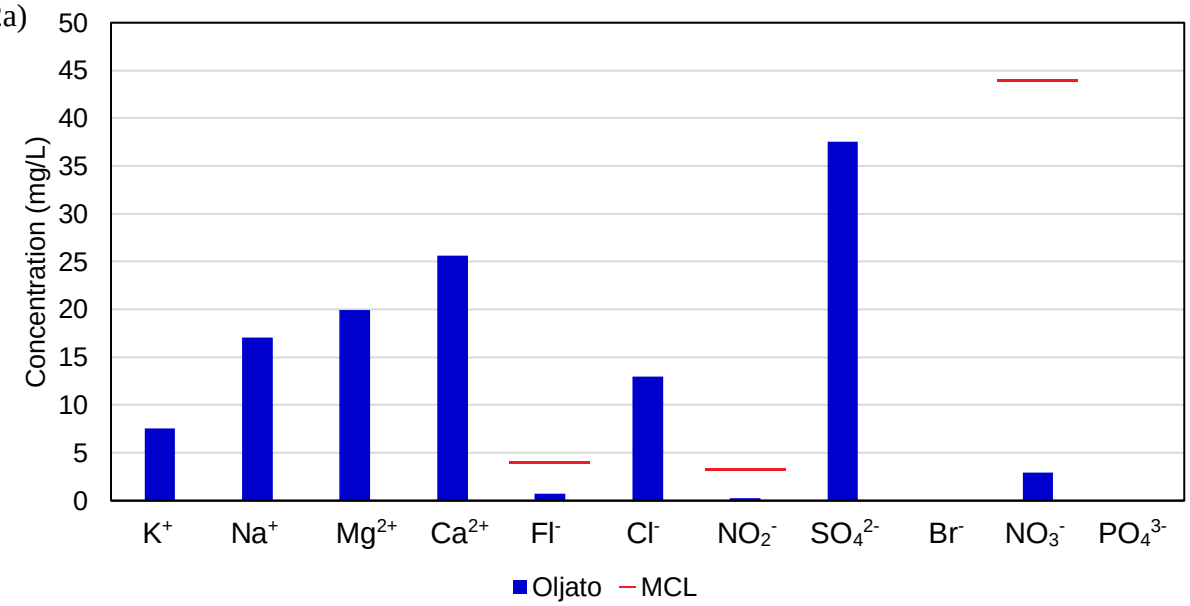
50
45
40
35
30
25
20
15
10
5
0
Concentration (mg/L)
K+
Na+
Mg2+
Ca2+
Fl-
Cl-
NO2-
SO42-
Br-
NO3-
PO43-
Oljato
MCL

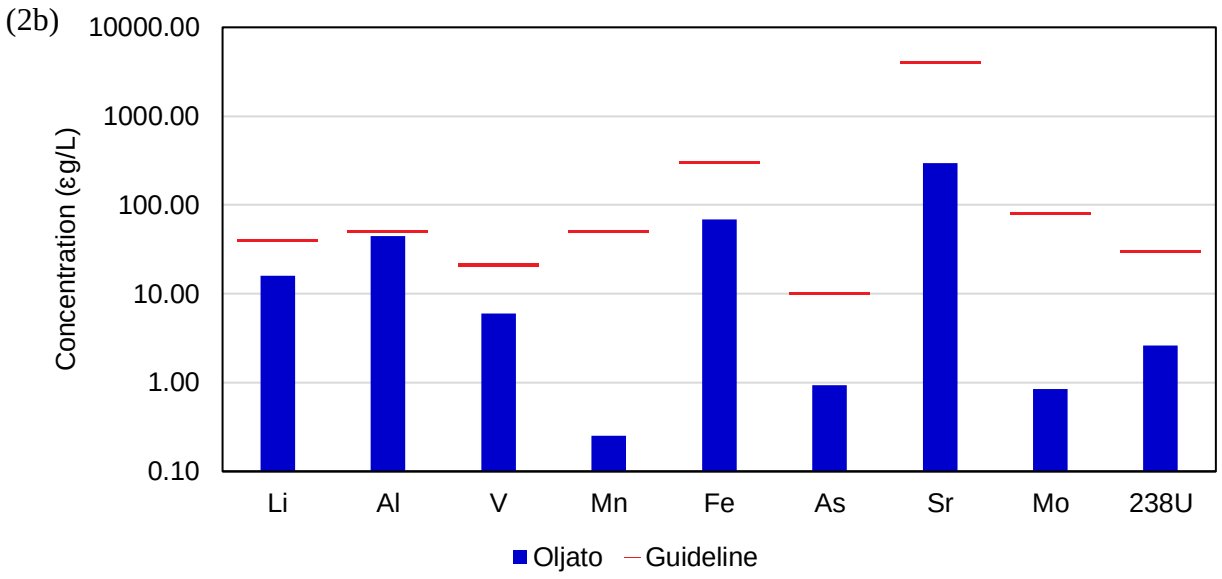

Figure 2.3.6 Concentrations of selected analytes by sampling site: Sand Spring (1a) ions, (1b) selected elemental contaminants; Oljato (2a) ions, (2b) selected elemental contaminants.

Additionally, the SNF unit deployed at Oljato was operated during the October 2021 sampling event with feed water from a well. The feed, permeate, and concentrate water was collected for sampling, and selected results are presented in Table 4 as "Oljato Feed," "Oljato Permeate," and "Oljato Brine" respectively. The results were unexpected because if the SNF is operated correctly, the permeate concentrations of each analyte should be lower than or equal to the feed concentration. However, certain analytes are present at higher concentrations in the permeate than in the feed water, such as iron and manganese. Sulfate, which is normally highly rejected by nanofiltration membranes, was measured as 169 mg/L in the permeate and 37.52 mg/L in the feed water. These discrepancies are likely caused by errors during the sample collection process as opposed to faulty SNF operation because other analytes show the expected distribution,

$C_{brine} > C_{feed} > C_{permeate}$, such as nitrate. ICP-MS analysis was conducted first by the KORES research group and was confirmed by analysis by the University of Arizona ALEC Laboratory. These discrepancies could not be further investigated through a mass balance because flow rates of the feed, brine, and permeate streams were not measured during operation of the SNF unit. Unfortunately, the performance of the SNF unit could not be evaluated due to the sampling error. Further water sampling should be conducted to monitor the performance of SNF unit. Instructions for future sampling of SNF units are included in Appendix B.

Table 4 Water quality results from operation of SNF unit in Oljato. Unexpected results are highlighted in red.

	Conduct-ivity (µS)	TOC (mg/L)	TDS (mg/L)	Cl (mg/L)	SO_4 (mg/L)	Al (µg/L)	Mn (µg/L)	Fe (µg/L)	As (µg/L)	U (µg/L)
Oljato Feed	841.40	2.22	546.91	11.63	37.52	44.82	0.25	69.25	0.93	2.61
Oljato Permeate	313.00	2.54	203.45	16.88	73.82	45.88	11.69	82.51	0.69	0.03
Oljato Brine	1340.00	5.15	871.00	26.12	104.34	56.29	20.50	146.24	1.61	4.42

2.3.3. Coalmine Canyon Chapter

The well used for drinking water in the Black Falls area was analyzed in October 2021 and March 2022. The results for cations and anions measured by IC are compared in Figure 2.3.8. It is difficult to definitively assess the scale of seasonal variability from two measurements. However, the data collected in this study do not suggest that the fall and spring water composition varies significantly. The same is indicated by a comparison of selected elemental contaminants presented in Figure 2.3.9.

The TDS is estimated to exceed the SMCL, with an estimated value of 880 mg/L in October and 853 mg/L in March. In October, aluminum and manganese exceeded the SMCLs. Aluminum

and manganese cause issues with color and staining, which could be prevented with an SNF unit. However, manganese can cause membrane fouling, thus maintenance such as regular rinsing of the unit would be important.

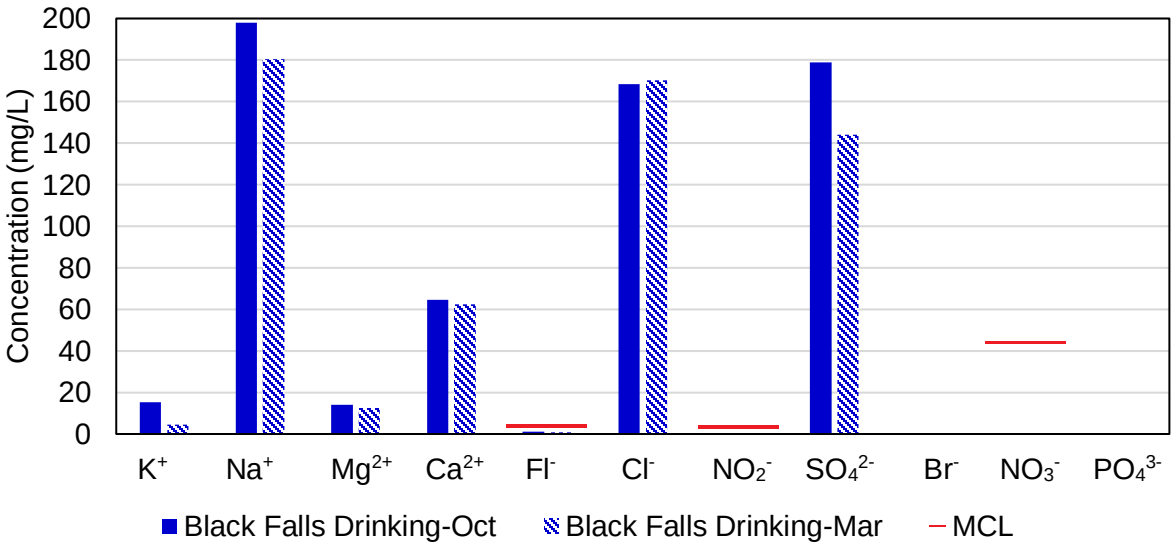

Figure 2.3.7 Seasonal variation in major cations and anions in groundwater sampled at Black Falls, AZ.

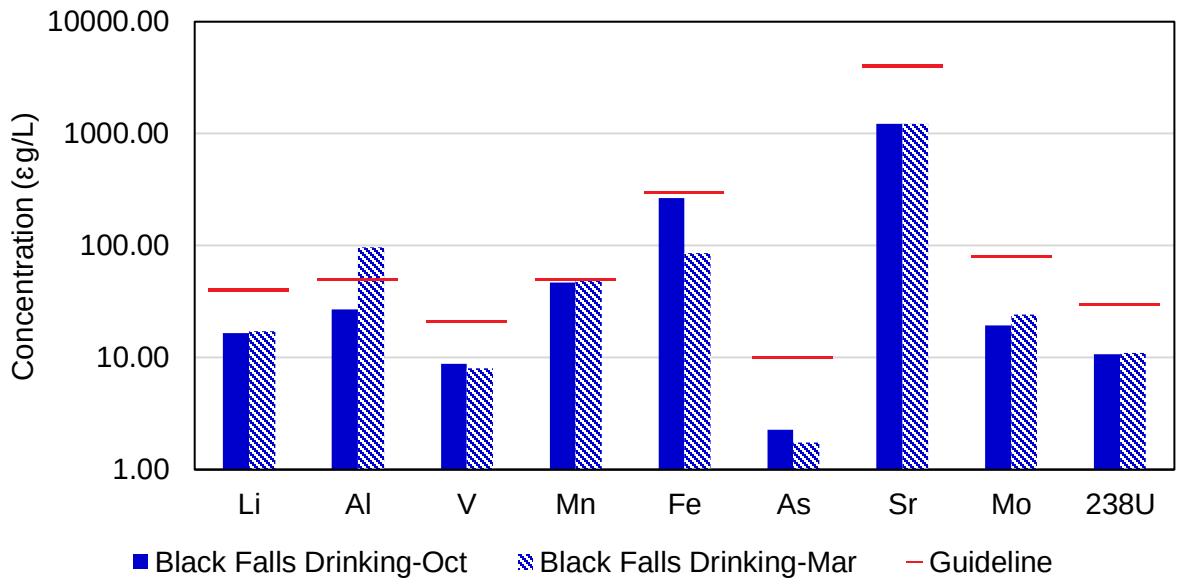

Figure 2.3.8 Seasonal variation in selected elemental contaminants in groundwater sampled at Black Falls, AZ.

2.3.4 Lupton Chapter

There were two water sources sampled in the Lupton area, a well and a rainwater catchment system. The rain water catchment system collected water from the roof and stored it in a tank for later use. The well water and the rainwater were sampled in the October 2021 and the March 2022 sampling events and are compared in Figure 2.3.10 and Figure 2.3.11. The difference between concentrations of analytes varies more for rainwater, which is plausible considering rainwater is more susceptible to variation in weather, atmospheric conditions, and contamination from dust or debris that can be present on the roof (Iavorivska et al., 2016). TDS was below the SMCL for all samples. All samples exceeded the SMCL of aluminum, and all samples except rainwater in March exceeded the SMCL of iron. Both of these contaminants cause aesthetic effects as opposed to health effects. There is currently a SUV unit deployed at the site, which would not remove

aluminum or iron. However, if the household has not experienced issues with staining or colored water, then there is no need for further treatment.

The SUV unit deployed at Lupton was operated with well water during the October sampling event and rainwater during the March sampling event and the treated water analyzed. The concentrations of the analytes in the treated water correspond to the concentrations in the source of the feed water (see Table 3), which is expected because the SUV does not remove dissolved species.

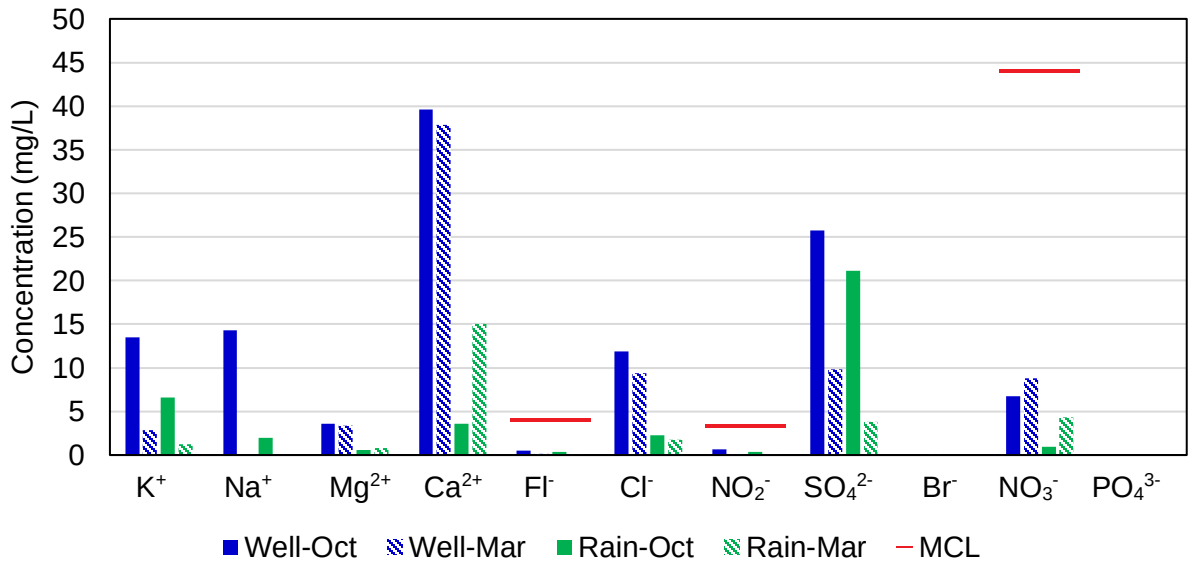

Figure 2.3.9 Seasonal variation in major cations and anions at Lupton, AZ for groundwater and water from a rainwater catchment system.

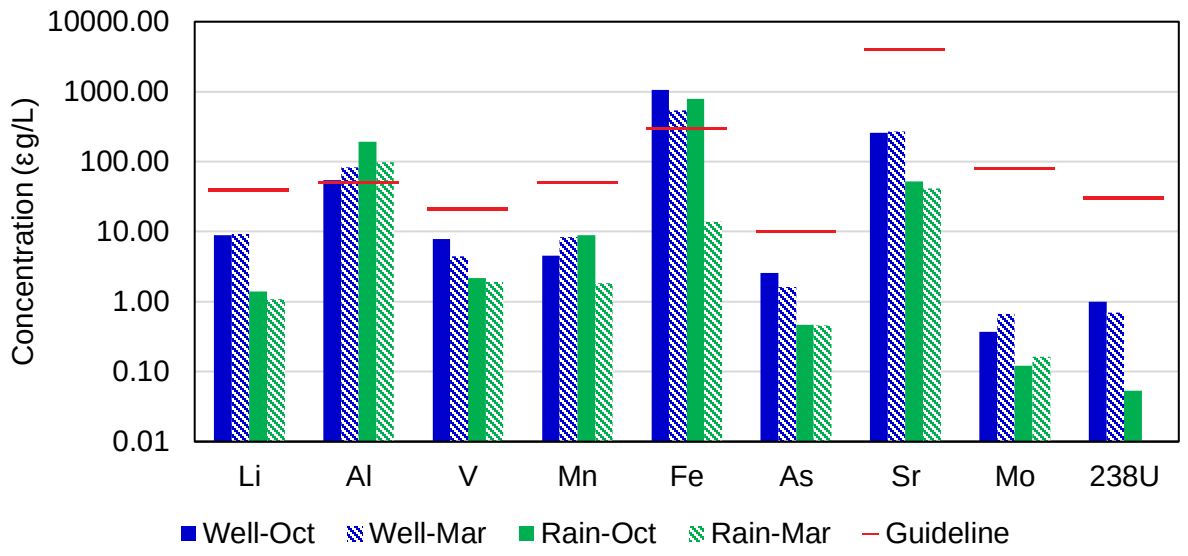

Figure 2.3.10 Seasonal variation in selected elemental contaminants at Lupton, AZ for groundwater and water from a rainwater catchment system.

2.4. Conclusions and Future Research

The results from this study have implications for both the health of the populations using the tested water sources as well as the feasibility of treatment with a solar-powered nanofiltration unit. The MCL exceedances of uranium and arsenic in certain Dilkon Chapter water sources pose a health risk for anyone who consumes water from those sources. A meeting at the Dilkon Chapter House informed the community of the five locations that had at least one MCL exceedance which allows community members to make more informed decisions about their usage of that water and emphasizes the need for water treatment or water hauling from regulated sources. TDS was the most common SMCL exceedance, with 12 sources expected to exceed 500 mg/L. Exceedances of the iron and/or manganese SMCLs also occurred at six sources.

The feasibility of the nanofiltration pilot system depends on the nature of the contaminants and other water quality factors. The sites in this study that exceeded the MCL for arsenic and/or uranium also had TDS concentrations higher than recommended for human consumption. More research is needed to understand if the nanofiltration is sufficient to address these quality issues. For some of the water sources tested, nanofiltration may not be sufficient. For example, nanofiltration could be effective at removing the arsenic and uranium presented in Salt Spring North, but it may not address the high concentrations of Na^+ and Cl^- that are also presented since nanofiltration is better suited for the removal of divalent ions (Schäfer 2004).

For those locations where SNF or SUV units are already present, this study can be used to comment on the suitability of the water treatment method. The water quality results in Lupton indicate that removal of TDS, uranium, or arsenic is not necessary. Therefore, UV disinfection may be sufficient. Collaborators at Northern Arizona University's Dr. Monroy's lab conducted heterotopic plate counting (HPC) analysis to evaluate presence of microbes, although further testing would be needed to evaluate disinfection effectiveness. Water quality data would also be useful to evaluate the performance of the SNF unit located at the Oljato sampling location. However, one or more of the samples were likely contaminated and therefore the water sampling results cannot be used to assess the SNF performance. Another water quality characteristic that is relevant to SNF operation is the presence of foulants, such as iron, manganese, or hardness. Knowing the concentrations of these foulants can guide recommendations for operation maintenance. Continue testing of the water sources that will be used with the SNF and SUV unit is recommended for further research.

Chapter 3: Long-Term Intermittent Operation of a Nanofiltration Pilot System

3.1. Introduction

Rural communities that are not on the electric or water grid often face issues with access to affordable and safe potable water. For example, on the Navajo Nation, the Environmental Protection Agency (EPA) estimated in 2021 that 15% of households are not connected to public utilities (US EPA, 2022). These households may instead use unregulated water sources which may have unsafe levels of pathogens or heavy metals. Uranium and arsenic are of particular concern on the Navajo Nation. A study by Hoover et al. examining 468 unregulated water sources found that 12.8% of sources exceeded the EPA maximum contaminant level (MCL) for uranium of 30 μg/L and 15.1% exceeded the arsenic MCL of 10 μg/L (Hoover et al., 2017). A water treatment option is needed that can address these issues as well as produce more palatable water that meets the secondary drinking water standards for total dissolved solids (TDS) of 500 mg/L (US EPA, 2015b).

Photovoltaic water filtration systems are being explored as an option to meet the need for cost-effective, safe drinking water in rural communities. Pilot studies of photovoltaic reverse osmosis systems have been conducted in various contexts and configurations (Abdelkareem et al., 2018; Freire-Gormaly and Bilton, 2019a, 2019b). However, the lower power requirements and greater water production of solar nanofiltration (SNF) systems may provide an attractive

alternative when it can achieve water quality standards (Cai et al., 2019). Research is being conducted on the removal of uranium and arsenic by nanofiltration under different conditions, but the preliminary results are promising (Richards et al., 2011; Schulte-Herbrüggen et al., 2016).

In addition to effectiveness, the operating costs and maintenance of such systems must be considered. NF and RO membranes are typically operated near-continuously in full-scale operation, but the nature of the power source and water demand means that photovoltaic water filtration systems would be operated intermittently which may impact performance. Some research on the effect of intermittent operation has been conducted for photovoltaic reverse osmosis (PVRO) operation and found that permeability during intermittent operation did not differ significantly from continuous operation (Freire-Gormaly and Bilton, 2019b, 2018). The researchers also found that scaling mitigation strategies such as rinsing with permeate water after operation and using antiscalants can slow the decline of membrane permeability for PVRO systems. A study using real-time imaging of PVRO membranes to examine $CaSO_4$ scaling behaviors actually found that intermittent operation resulted in less scaling than continuous operation (Sarker and Bilton, 2021). However, there have not been similar studies looking at the effect of intermittent operation on NF. If solar-powered nanofiltration (SNF) units are deployed on a household or community-wide scale, the training of operators and maintenance recommendations must take into account the potential impact by including effective fouling mitigation strategies.

In this study, the effect of intermittent operation on a pilot-scale solar-powered nanofiltration system was studied. Various feed water compositions were tested in order to

simulate water quality conditions that may be relevant to the Navajo Nation, including a solution composed of mostly divalent salts ($MgSO_4$ and $CaCl_2$), a solution with high levels of iron and manganese, a solution with humic acid alone, and a solution with humic acid and inorganic salts. The system was monitored for any decline in membrane performance, including water flux, salt flux, and salt rejection. Additionally, the effect of simple membrane maintenance such as rinsing the system after each day of operation was compared to not rinsing the system. The results from this study indicate that there was no significant decline in performance even over two months of operation for the solution containing $MgSO_4$ and $CaCl_2$ or the solution containing humic acid and inorganic salts, even without rinsing after operation. However, operation with a solution containing Fe^{3+} cause membrane failure after 3 days and the fouling could not be fully reversed with cleaning solutions containing NaOH, citric acid, EDTA, or SDS.

3.2. Materials and Methods

3.2.1. Nanofiltration System

All of the experiments were conducted using a pilot-scale solar-powered nanofiltration (SNF) system designed and built by students, faculty, and staff at the University of Arizona. The system was designed for use by households on the Navajo Nation and therefore prioritized cost effectiveness and simplicity of operation. A flow diagram of the pilot-scale SNF unit used in the experiments is shown in Figure 3.2.1 and picture of the system can be seen in Figure 3.2.2. The system includes a battery, which was designed to provide steady power during fluctuations in solar irradiance, but these experiments were operated with grid power through a power converter. The

system was designed to be modular, and the specific NF membrane should be chosen based on feed water characteristics. The FilmTec NF270-2540 (Dupont) was used for all experiments in this study. The system also includes pretreatment in the form of a ten-micron and a five-micron filter before the nanofiltration process. The recommended maximum pressure for the microfiltration cartridge filters was 50 psi, which was used as the maximum operational pressure for all experiments. To maintain the performance of the pump, it was operated at maximum pump speed for all experiments. The system was operated for five hours each day, five days a week, in every experiment unless otherwise noted.

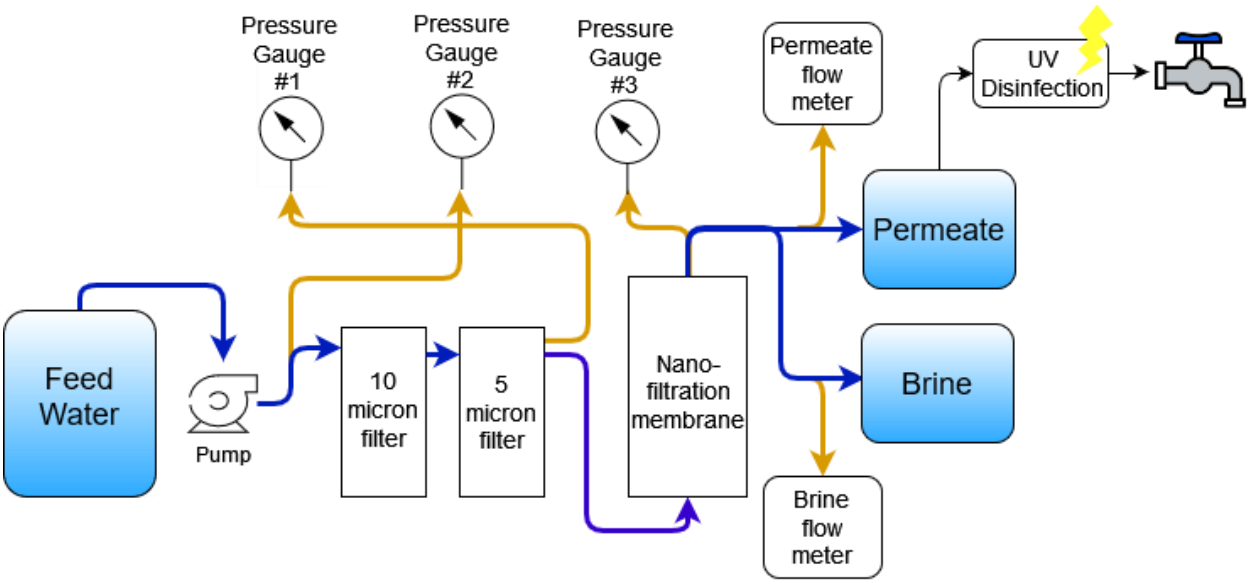

Figure 3.2.1 Flow diagram of the pilot-scale nanofiltration system.

For all experiments the system was run in recycle mode, meaning that the permeate and brine flows were returned to the feed water container. This was done to avoid the use of unreasonable amounts of water and chemicals. More than 200 gallons of would be needed per day if the experiments were conducted in batch mode. The modified water flow diagram corresponding

to the recycled mode of operation is shown in Figure 3.2.1. The figure also demonstrates the stages at which samples are collected.

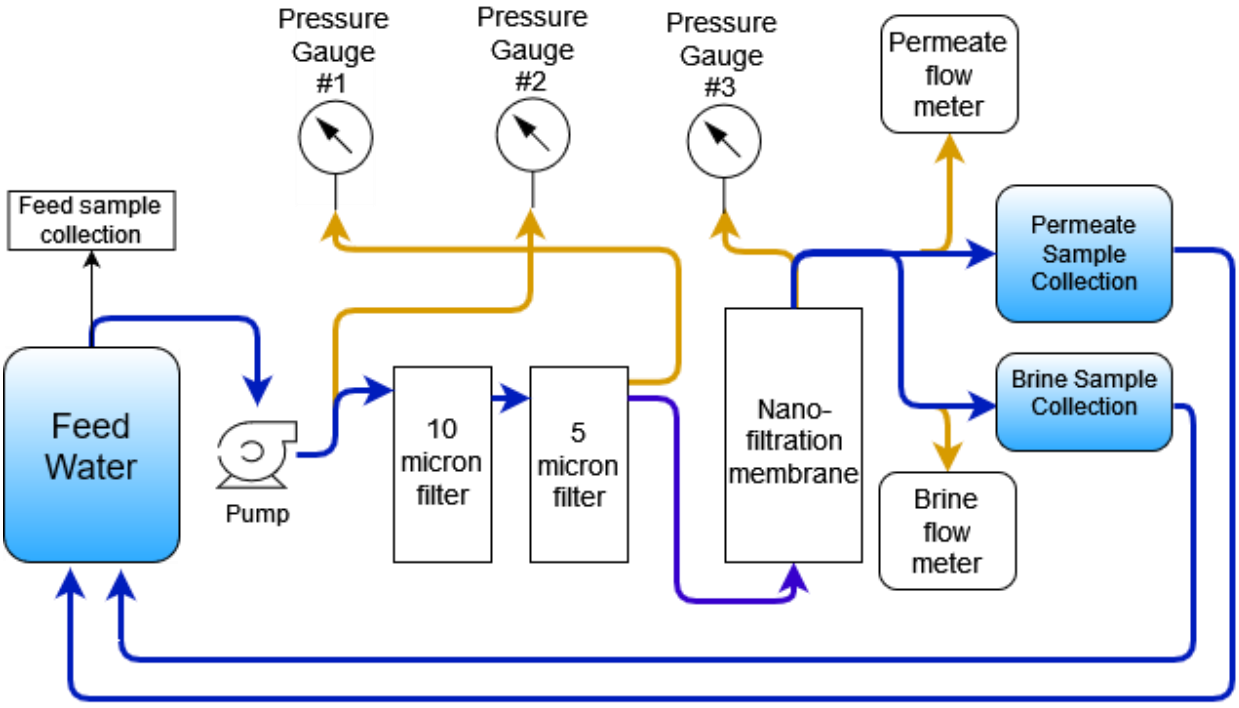

Figure 3.2.2 Modified flow diagram of the pilot-scale nanofiltration system with demonstration recycle mode and sampling locations.

The start-up procedure of the pilot-scale nanofiltration system was the same for all experiments. First, power was supplied through the power supply. The pump was turned on at maximum power with the brine flow valve, which can be noted in Figure 3.2.2.b, completely open to avoid suddenly applying pressure to the membrane which could damage it. The flow valve was then slowly closed until the pressure applied across the membrane reached 50 psi. If the system was already full of the test solution, as was the case if the system was not rinsed the day before, the experiment was ready to continue. If the system was full of a different solution, typically

distilled water from rinsing, at least 14 liters would be allowed to be flushed out to ensure the system contained only the solution being tested.

(a) 

(b) 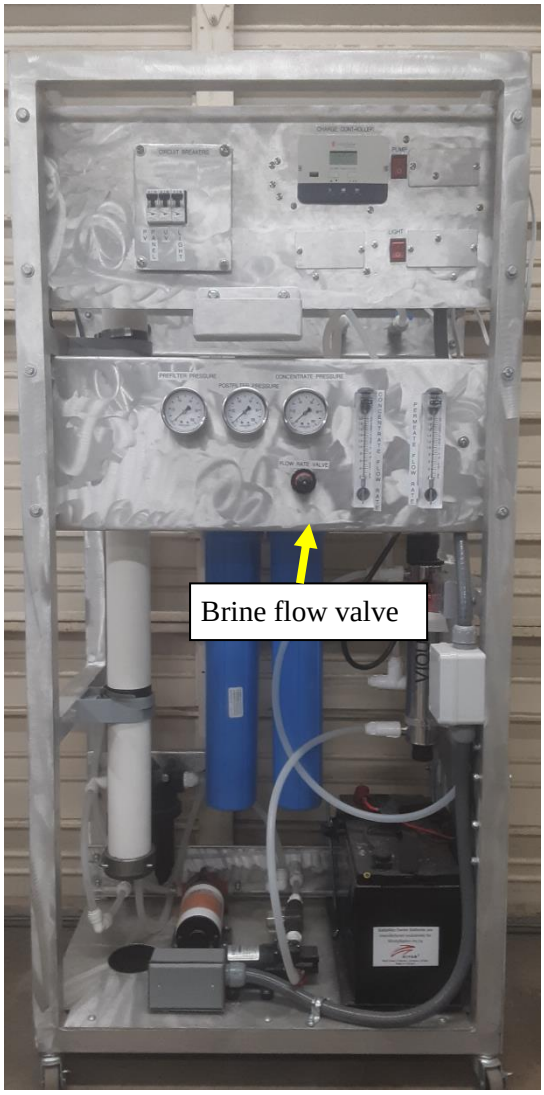

Figure 3.2.2 (a) Back view of pilot scale solar nanofiltration system (b) Front view of of pilot-scale nanofiltration system including the control panel.

For experiments in which the system was rinsed after each operation, the rinsing process was the same for each experiment. Distilled water was used to rinse the system when applicable

and at least 24 L of distilled water were used in each instance. During the rinsing process, the brine flow valve began fully open and the brine line was fully flushed out with distilled water. Once the brine line was flushed, the brine flow valve was slowly closed until the brine pressure reached 50 psi. About 10 L were allowed to rinse the permeate flow line. Once the permeate flow line was fully flushed, the brine flow valve was slowly opened and the rest of the distilled water allowed to flush out the system. The conductivity of the brine water was measured to ensure that the experimental solution was fully displaced.

The pH of the feed, brine, and permeate flows were measured hourly with Oakton pH 700 Benchtop Meter and the conductivity and temperature of the feed, brine, and permeate flows were measured with Oakton CON 550 Benchtop Conductivity Meter. The water flux was calculated using the estimated active area provided by the manufacturer ($2.6 m^2$) and adjusted for temperature differences with the following equation:

$$\text{illegible}$$

Solute flux was calculated with the following equation:

$$\text{illegible}$$

Where illegible is the solute flux, illegible is the water flux, and illegible is the solute concentration in the permeate.

Samples of the feed, brine, and permeate water were taken at the beginning and end of each day of operation and the concentrations of cationic and anionic solutes were measured with ion chromatography (Dionex ICS-5000). The Dionex Six-Cation-I Standard and the Dionex Seven Anion Standard used to create calibration curves for each cation and anion analyte respectively.

Total organic carbon in the feed, brine, and permeate was measured also measured at the beginning and end of each day with a Shimadzu TOC-L and using potassium hydrogen phthalate to construct the calibration curve.

3.2.2. Long-Term Operation with Inorganic Salts

In this experiment a solution was created that was intended to reflect a TDS concentration that could possibly occur on the Navajo Nation and examine the possibility of scaling due to the divalent ions. Ca^{2+}, Mg^{2+}, and SO_4^{2-}. While the geographical diversity and large size of the Navajo Nation results in a wide range of TDS concentrations in groundwater, studies have shown that some unregulated water sources used on the Navajo Nation exceed the SMCL of TDS of 500 mg/L. One study on the wells drawing from the N-aquifer in the Black Mesa Area in Northeastern Arizona found two of the ten wells sampled exceed the MCL of TDS, with a maximum of 649 mg/L (Macy and Unema, 2014). A different study focusing on wells in the Western part of the Navajo Nation used conductivity measurements to estimate that 23 of the 82 sources tested would exceed the SMCL of TDS (Jones et al., 2020). A TDS of 1350 mg/L was chosen for this experiment as it is significantly above the MCL, but still a realistic concentration for Navajo Nation groundwater. According to the same study focusing on Western Navajo Nation, only 7 out of the 82 conductivity measurements corresponded to a TDS greater than 1350 mg/L, which means the solution used in this study had a higher TDS than about 91% of the wells sampled in their study. Additionally, the mean TDS was estimated at 983 mg/L, which is below the TDS of the model

solution used in this study (Jones et al., 2020). This concentration was meant to provide a realistic view of the long-term performance of this system.

Table 5 Composition of $MgSO_4$ and $CaCl_2$ Solution.

Compound	Concentration (mg/L)
Mg^{2+}	151 mg/L Mg, S
SO_4^{2-}	598.6 mg/L
Ca^{2+}	216.7 mg/L
Cl^-	383.3 mg/L
TDS	1350

The composition of the solution tested in this experiment is shown in Table 5 and was made using Milli-Q® water deionized water, calcium chloride (Acros Organics, New Jersey, USA), and magnesium sulfate (Sigma-Aldrich, St. Louis, MO, USA). The TDS was meant to be a realistic representation of Navajo Nation groundwater, but the solutes chosen were not. Na^+ is frequently the dominant cation in Navajo Nation wells, but it was not included in this experiment because is not frequently a component of common inorganic foulants, as opposed to divalent cations like Ca^{2+} and Mg^{2+}. The solution has concentrations of both Ca^{2+}, Mg^{2+}, and SO_4^{2-} higher than typical Navajo Nation groundwater. For example, the water sampling results presented in Chapter 2 demonstrate that only one out of the 20 sources tested exceeded a Ca^{2+} concentration of 216.7 mg/L and none exceeded a Mg^{2+} concentration of 151 mg/L or a SO_4^{2+} concentration of 598.6 mg/L. Similarly, only one out of the 82 water sources tested in Western Navajo Nation

exceeded the Ca^{2+} concentration and none exceeded the Mg^{2+} or SO_4^{2+} concentrations used in this experiment (Jones, 2019).

This solution was used to operate the SNF unit for five days for five hours each day and rinsing with distilled water between each day of operation. The system was then run for another five days without rinsing between each day of operation and the water flux and solute rejection compared to the week of operation with rinsing. The solution was then used to operate the SNF system without rinsing for a total of 8 continuous weeks, or 39 days, to evaluate long-term performance.

3.2.3. Iron and Manganese Salts with Humic Acid and Cleaning Procedures

Iron and manganese were selected to be in the next solution tested because they are two common inorganic contaminants in Navajo Nation unregulated water sources (Credo et al., 2019). Additionally, humic acid (HA) was included to explore the interaction between metal contaminants and organics. HA is known to interact in complicated ways with other solutes that may have a significant impact on membrane performance and fouling (Li and Elimelech, 2004). Water sampling data for Navajo Nation indicates that TOC concentrations are relatively low. The sampling results presented in Chapter 2 of this thesis have a mean concentration of 1.5 mg/L TOC from the groundwater sources and the Western Navajo Nation sampling conducted by Jones found a mean concentration of 0.94 mg/L TOC from 82 sources (Jones, 2019). However, rainwater can also be used as feed water for SNF operation and often contains greater concentrations of organic compounds (Iavorivska et al., 2016).

Table 6 Composition of ferrous iron and manganese solution.

Solute	Concentration (mg/L)
Mg^{2+}	176.7
Mn^{2+}	261.4
Fe^{2+}	142.3
SO_4^{2-}	1400
Humic Acid	20
TDS	2000

Table 7 Composition of ferric iron and manganese solution.

Solute	Concentration (mg/L)
Mg^{2+}	176.7
Mn^{2+}	261.4
Fe^{3+}	108.1
SO_4^{2-}	1434.4
Humic Acid	20
TDS	2000

The solutions tested are presented in Tables 6 and 7 and were made using Milli-Q water, magnesium sulfate (Sigma-Aldrich, St. Louis, MO, USA), manganese(II) sulfate monohydrate (Sigma-Aldrich, St. Louis, MO, USA), iron(III) sulfate hydrate (Sigma-Aldrich, St. Louis, MO, USA), ferrous sulfate heptahydrate (Fisher Science Education, Hanover Park, Il, USA), and humic acid sodium salt (Sigma-Aldrich, St. Louis, MO, USA). Although iron, manganese, and humic acid are often present in Navajo Nation groundwater, the solution tested contained concentrations orders of magnitude greater than what is typically found. For example, a study which tested 121 unregulated water sources on Western Navajo Nation for Mn and Fe found median concentrations

of 3.44 μg/L and 23.1 μg/L, respectively (Credo et al., 2019). The higher concentrations of each solute were meant to accelerate fouling processes so that an understanding of their effect could be obtained without months of experimentation.

The solution containing ferrous iron was tested for five days, five hours each day, and the system was rinsed with distilled water between each day of operation. The solution containing ferric iron was tested for two days of operation, at which point the system could not maintain pressure. The system was then cleaned according to the manufacturer's recommendations with a 0.1% by weight NaOH solution. The cleaning procedure consisted of flushing the system with the NaOH solution followed by a one-hour soak three times and the following day flushing the system with the NaOH solution and soaking for one hour two times. The ferric iron solution was tested for one additional day and caused an immediate drop in permeate flux.

Further cleaning procedures were executed to attempt to restore permeate flux, based on a study focused on the removal of organic fouling (Li and Elimelech, 2004). The system was flushed with the 0.1% NaOH solution and soaked for five hours for two days. A 1 mM solution of ethylenediaminetetraacetate (EDTA), a chelating agent (adjusted to a pH of 12 with NaOH was flushed through the system followed by a soak with distilled water, followed by another flush with the EDTA solution and soak with distilled water. A 10 mM solution of sodium dodecyl sulfate (SDS), a surfactant (SDS info), adjusted to a pH of 12 with NaOH was used to complete the same cleaning procedure as the EDTA solution, consisting of flushing with the solution, soaking with distilled water, and repeating flush and soak process once more.

After these cleaning procedures a $MgSO_4$ and $CaCl_2$ solution with the same composition as in the previous section was run through the system and normalized with the average water flux from the last week of the two-month experiment. Because the normalized flux was still low, the system was cleaned with the EDTA solution again. The system was then run for five days with the $MgSO_4$ and $CaCl_2$ solution. A different cleaning procedure with a solution of 0.01% citric acid, diammonium salt (Acros Organics, New Jersey, USA) was attempted based on a study focused on cleaning membranes fouled with iron precipitation (Melliti et al., 2018). This solution was used to flush the system and soak for two hours. The system was operated with the MgSO4 and CaCl2 solution to compare the water flux to before the system was fouled with the ferric iron solution. A new FilmTec NF270-2540 (Dupont) membrane was installed after these cleaning procedures because the flux could not be restored. The ten-micron and five-micron cartridge filters were also replaced with new filters after these experiments.

3.2.4. Long-Term Operation with Humic Acid and Inorganic Salts

The fouling effect of natural organic matter (NOM), specifically humic acids, in conjunction with inorganic divalent salts was the focus of this set of experiments. Organic fouling of nanofiltration membranes is complex and can occur by numerous mechanisms including adsorption onto the membrane as precipitates, deposition of colloidal cake layer, and facilitation of biofouling. Humic acid was selected to be in the feed solution because it is a common component of NOM, has been observed to adsorb onto nanofiltration membranes, and interacts with common inorganic salts (Hong and Elimelech, 1997; Mänttäri et al., 2000; Mariën et al.,

2004). Divalent cations are known to interact with organic matter and therefore can have an effect on TOC rejection and membrane fouling.

The system was operated with a solution of only humic acid sodium salt (Aldrich, St. Louis, MO, USA) with a concentration of 5 mg/L for 10 days in order to be able to compare the effects of adding salts. NaOH was added to maintain the solution above pH 8, which was selected because humic acids are more soluble at high pH (Kipton et al., 1992). However, due to the difficultly in maintaining the solution above 8, the solution pH was sometimes as low as pH 7.1.

After operation with humic acid only, a feed solution including humic acid and inorganic salts was tested. The composition of the humic acid and inorganic salts solution is presented in Table 8 and was made using Milli-Q water, humic acid sodium salt (Aldrich, St. Louis, MO, USA), magnesium sulfate (Sigma-Aldrich, St. Louis, MO, USA), calcium chloride, and sodium chloride (EM Science, Gibbstown, NJ, USA). Concentrations of solutes were chosen based on Navajo Nation groundwater characteristics as well as the desire to avoid precipitation in the feed solution. The feed solution humic acid concentration of 5 mg/L was higher than the concentrations in any groundwater sample collected by us, but was similar to rainwater samples collected, as presented in Chapter 2. Previous studies have found that in the presence of NOM, calcium complexation with NOM increases until a critical Ca^{2+} concentration is reached (Hong and Elimelech, 1997). Above the critical Ca^{2+} concentration, NOM begins to precipitate out of the solution. This critical concentration has been found to be around 2.5×10^{-3} to 3×10^{-3} M at pH 8 (Amirbahman and Olson, 1995; Hong and Elimelech, 1997). The $CaCl_2$ concentration in this experiment was chosen to be

80 mg/L, which corresponds to a Ca^{2+} concentration of about 0.72 x 10^{-3} M, which was intended to avoid humic acid precipitation in the feed solution.

The pH solution was maintained above 7 with the addition of NaOH and used to operate the system for five days. The system was rinsed with distilled water after each day of operation. The same feed solution was left at natural pH (5.9-6.9) and run for two weeks and rinsed with distilled water after each day of operation. The humic acid and inorganic salts solution was then operated with the ten-micron and five-micron cartridge filters only in order to understand their effectiveness as pretreatment. Finally, the humic acid and inorganic salts solution was used to operate the NF system for 20 days without rinsing between each day of operation.

Table 8 Composition of humic acid and inorganic salts solution.

Solute	Concentration (mg/L)
Mg^{2+}	121.2
Ca^{2+}	28.9
Na^{+}	236.0
SO_4^{2-}	478.8
Cl^{-}	415.1
Humic Acid	5
TDS	1280

3.3. Results and Discussion

3.3.1. Long-Term Operation with Inorganic Salts

A comparison of the performance with rinsing between operation and without rinsing between each day of operation is presented in Figure 3.3.1. The results from one week of operation indicate little difference between operation with rinsing and without rinsing. TDS rejection for both modes of operation remained fairly consistent over the week. The week of operation with rinsing had an average rejection of 52.8% and the week of operation without rinsing had an average of 54.4%. The average temperature-corrected flux for operation with rinsing was 38.0 $L/m^2/hr$ while the average for operation without rinsing was 37.6 $L/m^2/hr$. While a week may not be enough for significant differences in performance to occur, the omission of rinsing did not cause a loss in performance over the short term.

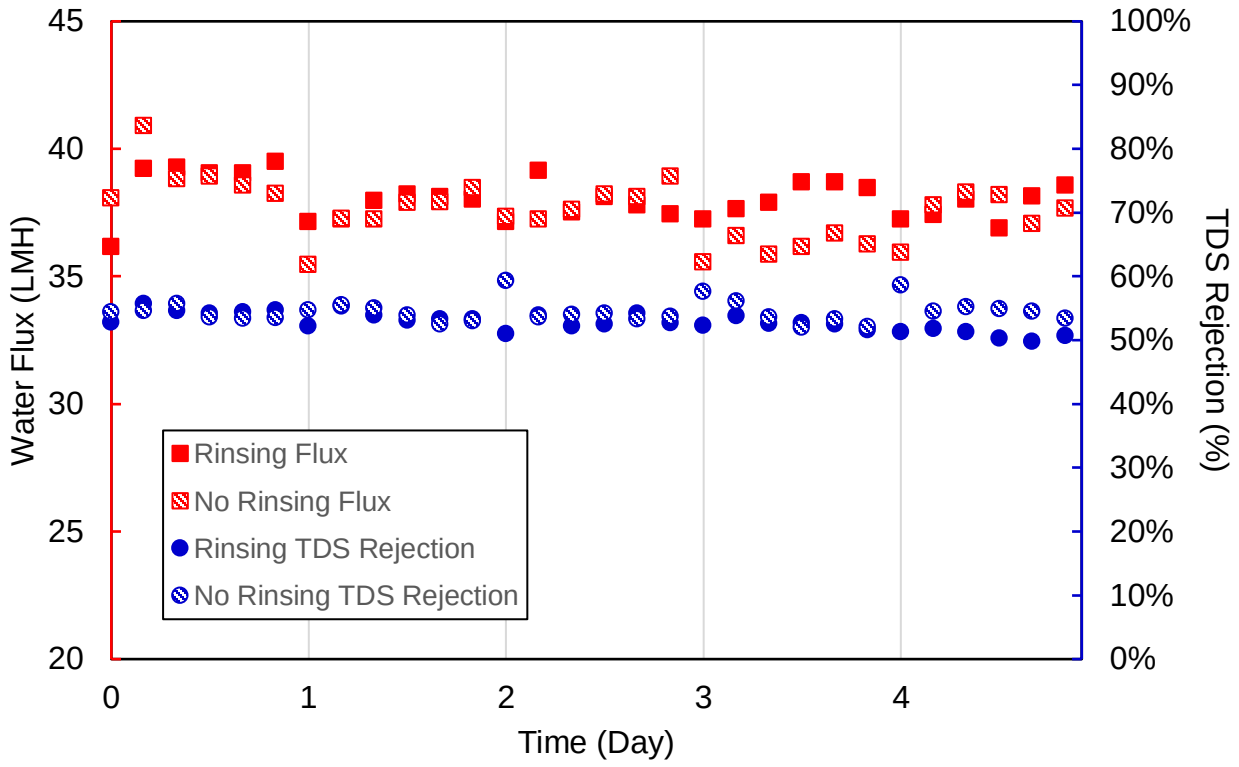

Figure 3.3.1 Comparison of TDS rejection and water flux for one week of operation with rinsing and without rinsing.

The results of two months (39 days) of SNF operation with the inorganic salt solution without rinsing may provide a better understanding of the effect of not rinsing. Temperature-corrected water flux and the rejection of each solute are presented in Figures 3.3.2 and 3.3.3. The temperature-corrected water flux, which would be expected to drop if significant scaling had occurred, did not decline significantly during the experiment. This indicates that despite having a high TDS and high concentrations of Ca^{2+}, Mg^{2+}, and SO_4^{2-}, the feed solution was not causing a decline in water production. Similarly, the rejection of the solutes does not drop significantly, although there is some fluctuation over the course of the experiment. The average TDS rejection

was about 52%, which would bring the permeate TDS concentration to about 650 mg/L. This is still above the SMCL for TDS of 500 mg/L, but that guideline is not enforceable and is based on aesthetic concerns, not health concerns. Two months of SNF operation with water simulating Navajo Nation groundwater with higher than average TDS showed consistent performance despite the lack of rinsing.

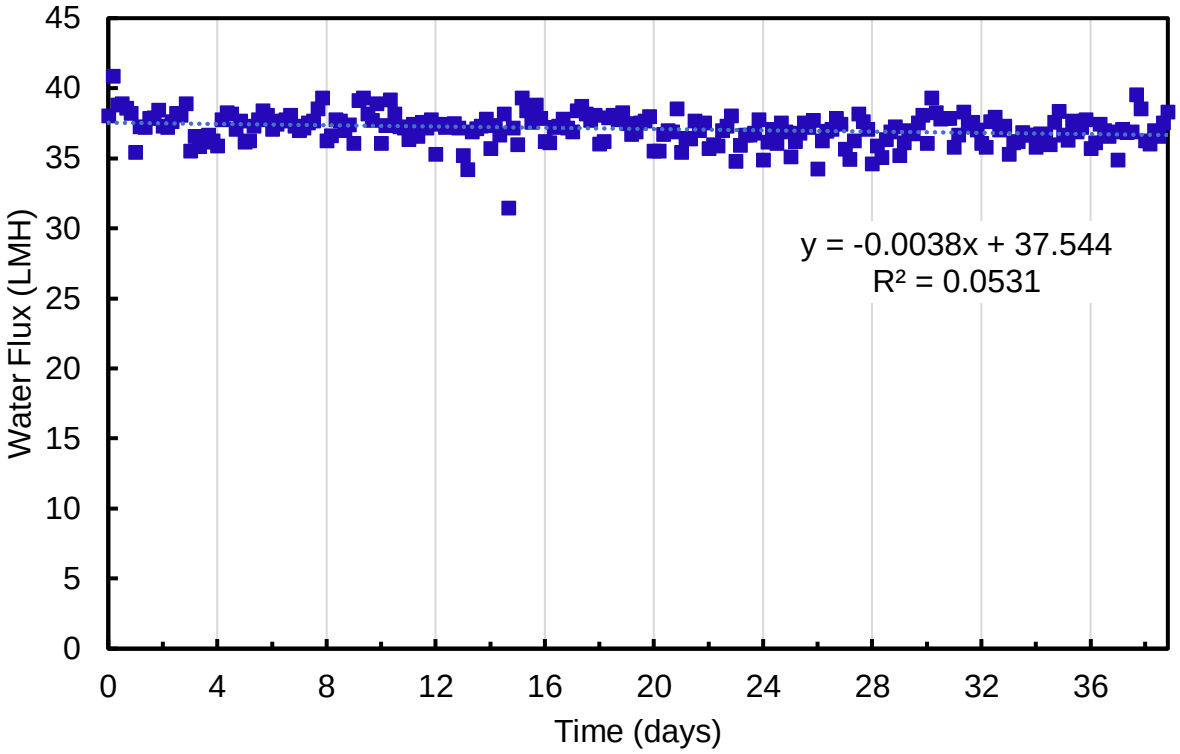

Figure 3.3.2 Temperature-corrected water flux over 8 weeks during operation with $MgSO_4$ and $CaCl_2$ and without rising between operation.

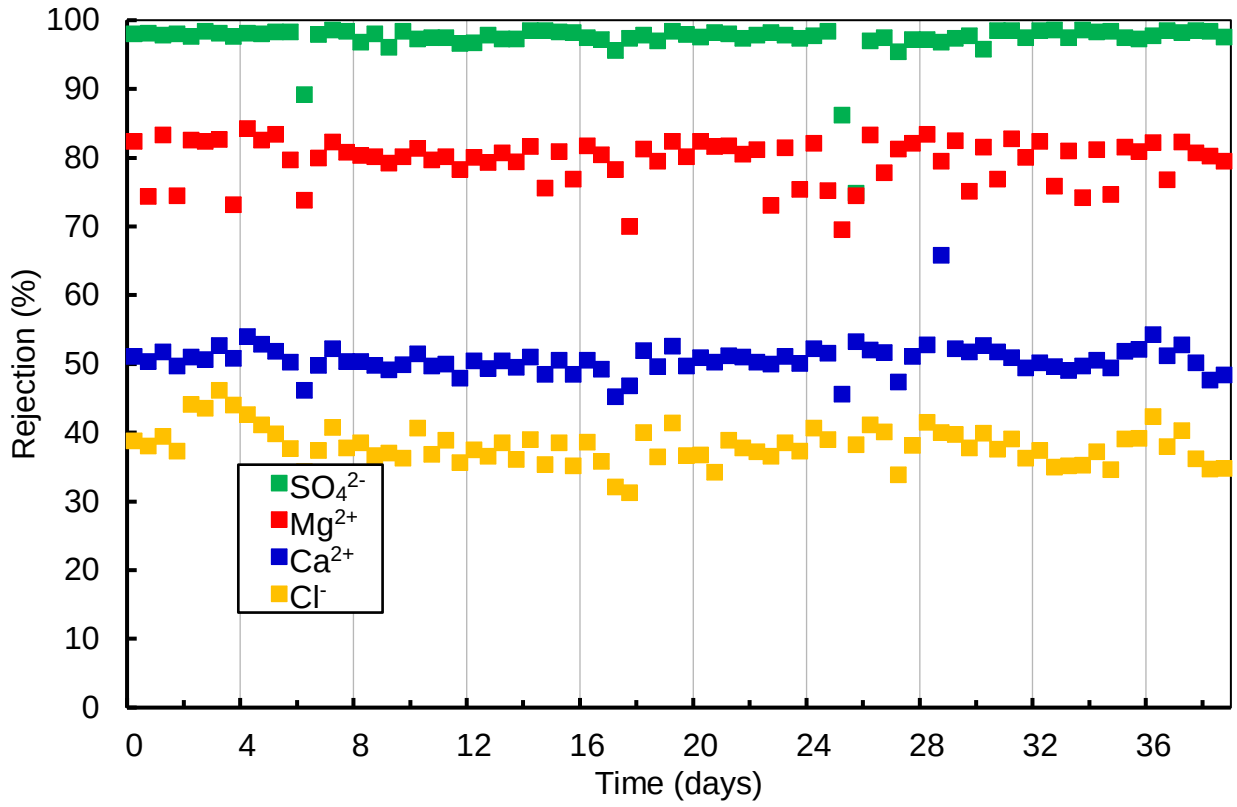

Figure 3.3.3 Ion rejection over 8 weeks during operation with $MgSO_4$ and $CaCl_2$ and without rising between operation.

3.3.2. Iron and Manganese Experiments and Cleaning Procedures

Unlike the $MgSO_4$ and $CaCl_2$ solution, which had above average but plausible concentrations, the solution containing iron and manganese were orders of magnitude higher than Navajo Nation groundwater. This made it much easier to identify that fouling had occurred. As shown in Figure 3.3.4, there was a very notable difference in the flux decline caused by ferrous iron, Fe^{2+}, and ferric iron, Fe^{3+}. Ferrous iron did not result in water flux decline over the test period and an increase is shown in the last day of operation. The increase in water flux during operation may have been related to the increase in humic acid rejection during that same time period.

Ferric iron, however, resulted in a steep and immediate decline in water flux to the point of system failure after less than two days. After two days of preliminary cleaning with a NaOH solution, the ferric iron solution was tested again and resulted in a steep decline in water flux. This is relevant to SNF operation on the Navajo Nation because iron is known as a contaminant.

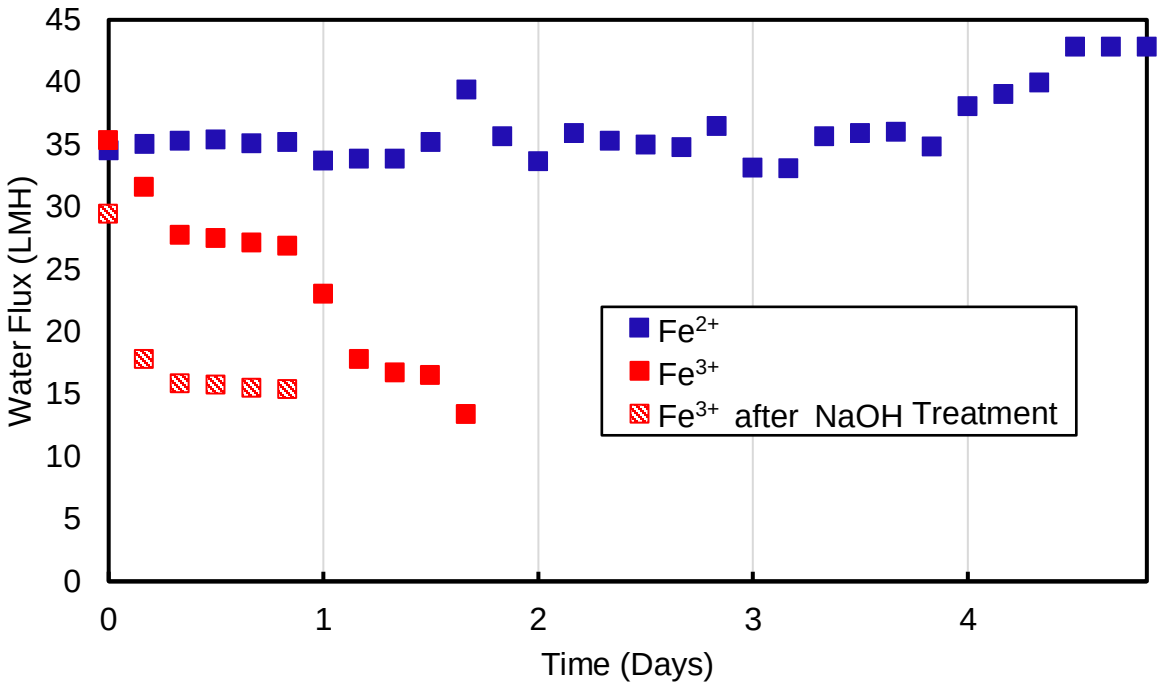

Figure 3.3.4 Comparison of operation with solution containing ferrous iron (Fe^{2+}) and ferric iron (Fe^{3+}). The solution containing ferric iron was run for one day after the membrane was treatment with NaOH.

The rejection data from operation with both solutions are presented in Figure 3.3.5. For both solutions, rejection of magnesium, iron, and manganese are high, with average rejections greater than 98%. This corresponded to concentrations of manganese and iron on the order of 1 mg/L. These concentrations are still above the SMCLs but permeate produced with more realistic Navajo Nation groundwater concentrations of iron and manganese is likely to meet SMCLs.

Sulfate rejection was high (greater than 96%) in the ferrous iron solution, but was significantly lower in the ferric iron solution, with an average of 85% over the two days of operation. Sulfate typically has high rejection due to its size and high magnitude of charge. Because the rejection of cations remained high, it was suspected that the rejection of sulfate decreased due to the deposition of positively charged Fe^{3+} precipitates onto the membrane surface which would decrease repulsion between the membrane and the sulfate ion. A study using Fe^{3+} as a coagulant pretreatment for nanofiltration found that the accumulation of Fe^{3+} had varying effects on rejection and that rejection of negatively charged acids increased with higher Fe^{3+} dose (Schäfer et al., 2001).

The TOC rejection also differed between the solutions. During operation with the ferrous iron solution, TOC rejection began low and increased over the week. The increase in TOC rejection may be related to the increase in water flux during that time period. One possible cause for the increase in TOC rejection over this time period could be fouling of the 10-micron and 5-micron prefilters, which decreases the effective pore size and changes rejection behavior (Chuang et al., 2008). An increase of TOC rejection the prefiltration stage would lower the humic acid concentration that reaches the nanofiltration membrane and impact water flux. Because the solution is not sampled in between the prefilters and the nanofiltration membrane (see Figure 3.2.2), it is difficult to determine what is the cause of the increase in TOC rejection. Future experiments should have a mechanism for separating the impact of the pretreatment and nanofiltration.

During operation with ferric iron the TOC rejection was even higher during the two days of operation. This may be because of the coagulation effects of Fe^{3+} allowing the prefilters to rejection more of the humic acid. A membrane autopsy was conducted to further understand this behavior and the results can be found in Chapter 4 of this thesis.

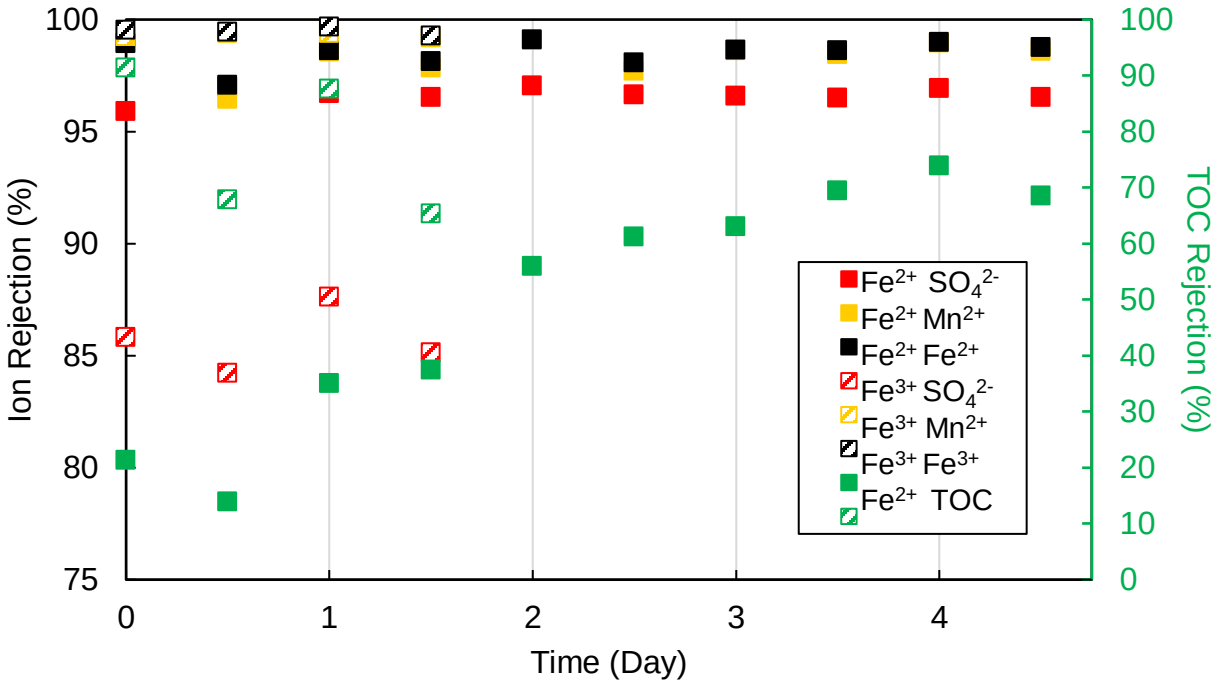

Figure 3.3.5 Ion rejection and TOC rejection for ferrous iron solution (solid markers) and ferric iron solution (patterned markers). Mg^{2+} rejection has been omitted for clarity.

The different fouling behaviors of ferric iron versus ferrous iron is related to the formation of sparingly soluble ferric oxides. Table 9 shows the saturation indices of ferric and ferrous oxides and hydroxides as predicted with Visual MINTEQ, a chemical equilibrium model. Supersaturated ferric oxides would tend to precipitate on the membrane surface or form colloids that deposit on the membrane. The actual solution is more complex because of the addition of humic acid, which

will complex with iron and manganese as well. However, the model indicates that there are numerous minerals that are supersaturated in the solution including ferric acid and will tend to precipitate. The formation of colloids from ferric complexes has been found to have varying effects on membrane fouling depending on conditions. For example, researchers have actually used ferric chloride as a pretreatment by coagulating organic matter prior to nanofiltration (Racar et al., 2017; Schäfer et al., 2001). These have successfully lowered the flux decline caused by organic matter. However, conditions were selected in these studies to reduce colloidal fouling by the iron itself by using lower Fe^{3+} doses, optimized pH, and sand filtration in one study. The Navajo Nation groundwater that may be used as feed water is unlikely to have these optimal conditions and ferric iron is more likely to negatively affect membrane performance.

Table 9 Saturation indices of ferrous iron and ferric iron solutions as predicted by Visual Minteq. Minerals with a saturation index greater than 0 are highlighted.

Fe^{2+} Mineral	Saturation Index	Fe^{3+} Mineral	Saturation Index
Brucite	-6.772	Brucite	-12.965
Epsomite	-2.801	Epsomite	-2.799
Fe(OH)2 (am)	-3.658	Fe2(SO4)3(s)	-13.187
Fe(OH)2 (c)	-3.058	Ferrihydrite	1.925
Melanterite	-3.215	Ferrihydrite (aged)	2.435
Mg(OH)2 (active)	-8.466	Goethite	4.634
MnSO4(s)	-7.686	Hematite	11.669
Periclase	-11.256	H-Jarosite	2.649
Pyrochroite	-5.045	Lepidocrocite	3.754
		Maghemite	3.865
		Magnesioferrite	-2.473
		Mg(OH)2 (active)	-14.659

		MnSO4(s)	-7.686
		Periclase	-17.448
		Pyrochroite	-11.240

After the system failed due to fouling, cleaning was attempted with several cleaning solutions. The cumulative effect of these cleaning procedures can be seen in Figure 3.3.6. where we compare the water flux results from last week out of the two months that the system was tested with $MgSO_4$ and $CaCl_2$ and a week operating with a solution of the same composition after fouling and cleaning. The water flux was about 28% lower than before the membrane was fouled with the ferric iron solution, which indicates irreversible fouling of the membrane. This is consistent with previous studies which have found that fouling due to iron is resistant to membrane cleaning procedures (Gwon et al., 2003). A flux decline of this magnitude could negatively impact the ability of SNF unit to meet the water needs of a household and may require replacement of the membrane. Further investigation of the nature of the membrane fouling and the effects of these cleaning procedures is presented in Chapter 4.

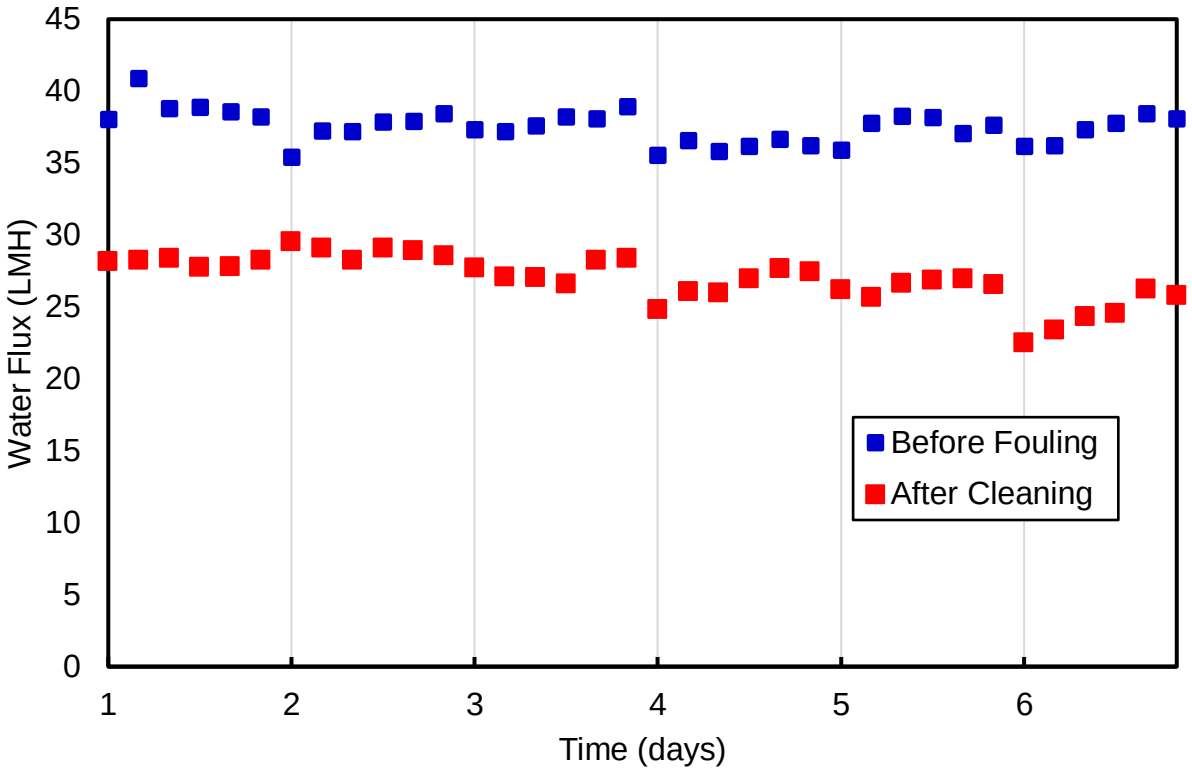

Figure 3.3.6 Comparison of water flux with $MgSO_4$ and $CaCl_2$ solution before fouling and water flux with $MgSO_4$ and $CaCl_2$ after cleaning with NaOH, EDTA, SDS, and citric acid.

3.3.3. Humic Acid without Inorganic Salts and with Inorganic Salts

The experiments with humic acid were meant to better understand the effect of organic matter in the fouling of the SNF system. A comparison of the water flux resulting from humic acid alone, humic acid plus inorganic salts above pH 7, and humic acid plus inorganic salts at natural pH of 6-7 is presented in Figure 3.3.7. Humic acid by itself had a higher average water flux than either solution that included salts. Humic acid plus inorganic salts at the natural pH of 6-7 had a higher average water flux than when that same solution was kept above pH 7. This could be attributed to changes in the humic acid configuration, which is smaller at lower pH and is therefore

less effected by size exclusion effects Additionally, the results for all three solutions do not exhibit a decline in water production over the test period. Rejection data from each test period is presented in Figure 3.3.7 and also demonstrates little to no change in performance over the test period.

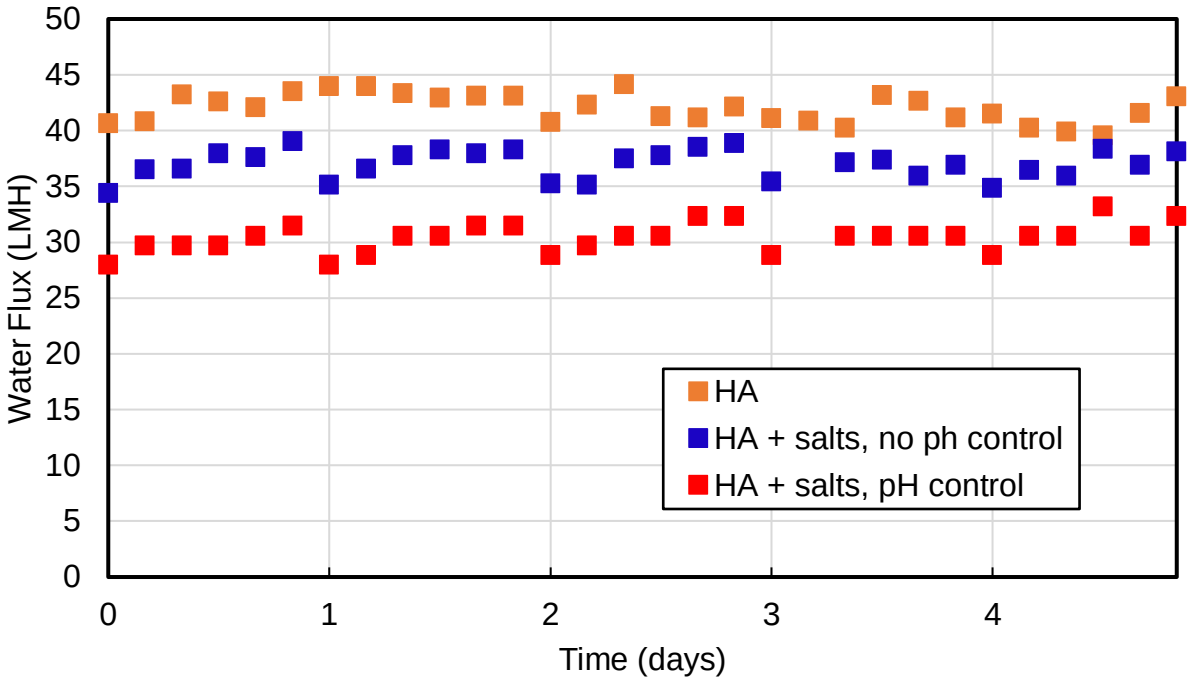

Figure 3.3.7 Comparison of solutions containing humic acid alone, humic acid MgSO4 and $CaCl_2$ at the natural pH, and humic acid $MgSO_4$ and $CaCl_2$ keeping the pH between 7 and 8.

Water flux results from five weeks of operation of the humic acid and inorganic salt solution without rinsing between operation are presented in Figure 3.3.8. A downward trend seems possible, but least squares regression analysis results in a very lower R^2 value which indicates that there is no significant trend. Little to no decline in membrane performance is an encouraging result because these operating conditions are likely to be more fouling than would occur in the field. Operation with high TOC and TDS concentration, without rinsing between operation, and with

feed water being left in the system overnight and over weekends can be thought of as a worst-case scenario for maintenance in the field. The lack of noticeable membrane decline in this time frame indicates the system may endure the varying levels of user maintenance that will likely occur in the field.

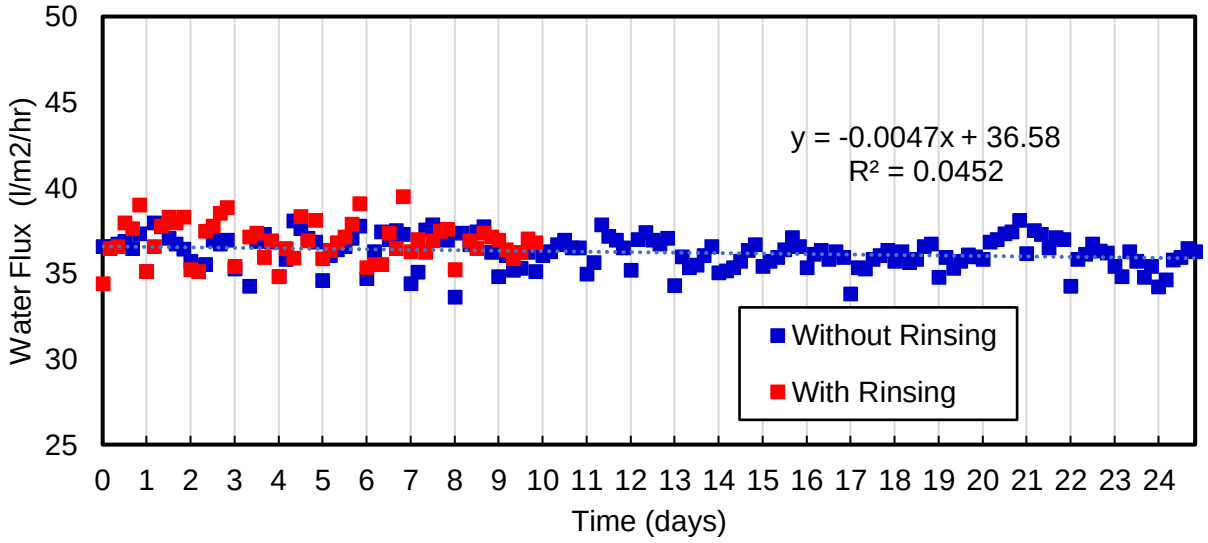

Figure 3.3.8 Long term operation of the SNF unit with a solution containing humic acid, $MgSO_4$, and $CaCl_2$ without rinsing between operation.

Rejection results for each solute are shown in Figure 3.3.9. Notable trends are the low rejections of Cl^- and Na^+ and decreasing rejection of humic acid. Rejection of humic acid It is expected that Cl^- and Na^+ will have low rejections because they are monovalent, but it is important for the SNF to remove enough to avoid the unpleasantly salty taste that Cl^- and Na^+ can cause. The decrease in TOC rejection may be attributed to decreased repulsion between the humic acid and the membrane surface, which could occur if the membrane has a lower surface charge due to deposition of foulants. The lack of change in other membrane performance parameters (ion

rejection or water flux) may could be explained if humic acid is the most sensitive to electrostatic exclusion effects. If this is the case, the lower rejection of humic acid may indicate that other aspects of membrane performance such as water flux will be affected it the fouling continues.

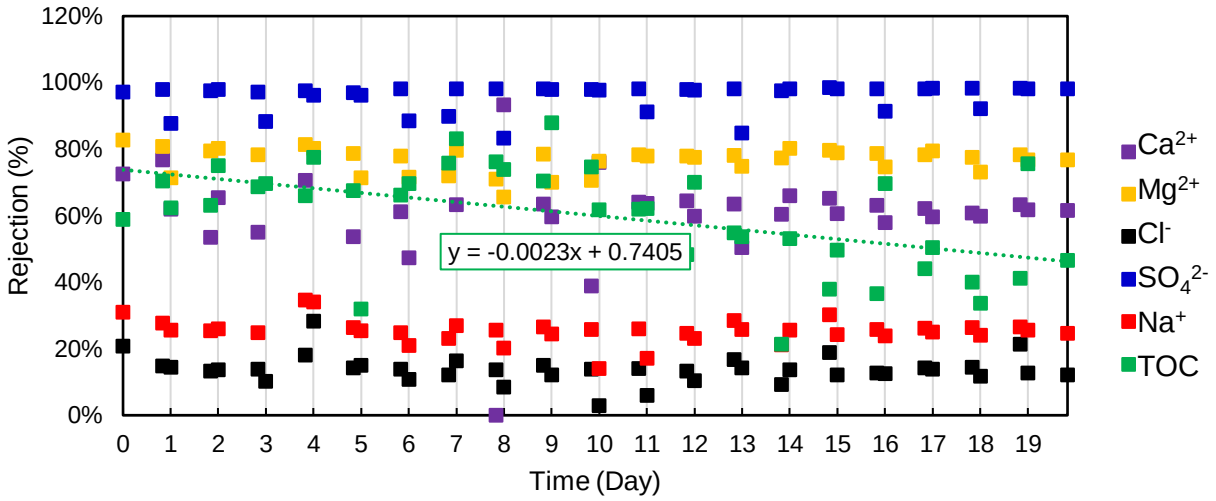

Figure 3.3.9 Solute rejection during four weeks of operation with humic acid solution without rinsing between operation.

3.4. Conclusions and Further Research

The results from these experiments are relevant to SNF operation on the Navajo Nation. The consistent performance after months of operation without rinsing and with relatively high concentrations of TDS indicate that the SNF may be a sustainable water treatment option on the Navajo Nation. Ferric iron has been identified as a potential foulant especially at high concentrations. The experiments conducted suggest that the cartridge filters may have a significant role in removal of TOC in the presence of ferric iron, however the system configuration did not allow the effects of the cartridge filters and the effects of the nanofiltration to be separated. Future experiments should include a mechanism to collect water samples after the cartridge filters, and

ideally between each cartridge filter as well. This will allow experiments to account for changes in water quality at the nanofiltration stage that may occur due to rejection at the cartridge filter stages.

Future work could further explore the role of ferric iron in fouling. For example, alternative pretreatment such as settling time or the use of a one-micron prefilter to remove ferric iron could be tested that would take advantage of its coagulant effect. Additionally, because ferric iron had such an immediate effect on fouling, it was difficult to determine if manganese and humic acid were causing additional fouling. Additional experimentation could compare the effect of iron by itself to iron with organics or manganese. Humic acid at realistic conditions did not have a significant effect on membrane fouling in the duration of these experiments. However, further research could accelerate fouling with higher concentrations of humic acid to examine the behavior under different operation conditions. Finally, for any of the water chemistry conditions tested, intermittent operation could be directly compared to continuous operation. This may require automation of the system to allow for operation and data collection without continuous supervision.

Another topic for future research is operation with real Navajo Nation groundwater. Navajo Nation groundwater varies significantly, as demonstrated in Chapter 2 of this thesis, so the groundwater should be chosen to represent high fouling potential. Additionally, further testing of groundwater at the sites where SNF units have already been deployed should be conducted to better understand the water treatment needs. The SNF units that have been deployed should also

be monitored. Although they may not be used consistently, it is still important to detect any trends or changes in performance.

Chapter 4: Membrane Autopsy

4.1. Introduction

Membrane fouling can have a large impact on membrane performance and lifetime, and thus it is critical to understand the mechanisms which cause fouling and the factors that affect the effectiveness of membrane cleaning processes (Guo et al., 2012; Mariën et al., 2004). Membrane autopsies can provide insight into these mechanisms by using analytical techniques to identify physical, chemical, and biological characteristics of membrane foulants (Pontié et al., 2005; Shon et al., 2013). These can involve identification of the specific compounds present in the fouling layer and detecting changes to the membrane surface. Especially for membranes that were used with natural waters it is important to understand the role of organic matter, both in terms of organic fouling but also in terms of microbial growth. Systems that treat water of unknown or variable quality such as those in wastewater treatment plants can use autopsies to determine which elements and compounds are present in the fouling layer. For example, researchers used scanning electron microscopy with an energy-dispersive X-ray (SEM-EDX) and X-ray diffractometer (XRD) to identify predominant foulants on nanofiltration (NF) membranes used in a demineralization plant in Morocco as calcium carbonate (El-ghzizel et al., 2019). Organic fouling can also be identified with other analytical techniques, such as high-performance size exclusion chromatography, Fourier transform infrared (FTIR), and UV spectrophotometry (Chon and Cho, 2016; Rahman et al., 2018). One study using membranes fouled by oil-field wastewater used the aforementioned techniques to identify the predominant foulants as crude oil and anionic polyacrylamide (APAM) (Zhao et al., 2019).

Autopsies can provide valuable information about membranes that are used to treat known water as well. XRD analysis can be used to identify the complexes that are responsible for fouling and the specific compounds that form on the membrane surface. A bench-scale study compared the fouling caused by a well-analyzed natural surface water on NF270 and NF90 membranes. NF90 are less permeable and more hydrophobic membranes than the NF270 membranes. They found that the NF270 was predominantly fouled by natural organic matter (NOM), while the tighter NF90 was fouled significantly by both NOM and $CaCO_3$ (Sari and Chellam, 2017).

Understanding fouling of nanofiltration membranes is especially important when membranes are used in off-grid applications as in most cases they are operated by users with limited training, and contrary to typical treatment trains that include membranes there are no opportunities for feed water pretreatment. Finally, in off-grid applications it is possible that the water source will have greater water quality variability which will lead to variable operating conditions and thus may be more prone to fouling (Boussouga et al., 2021b; Li et al., 2019). While off-grid nanofiltration systems may provide a useful alterative to piped water in rural areas, it is important for these systems to be as sustainable as possible by minimizing fouling and maximizing the lifetime of the nanofiltration membrane. With these goals in mind, students, faculty, and staff at the University of Arizona designed and built a solar-powered nanofiltration system that has been tested under different water quality and operating conditions to understand fouling behaviors. The system includes 10-micron and, 5-micron cartridge filters as pretreatment, followed by a nanofiltration membrane which can be selected to be more or less permeable based on the specific water treatment needs.

The solar-nanofiltration system was tested under water quality and operating conditions that are relevant to Navajo Nation water sources because there is an estimated 15% of households that lack access to public water utilities and the groundwater used often requires additional treatment before human consumption due to its brackish nature and regional contaminations (Credo et al., 2019; Hoover et al., 2017; US EPA, 2022). The system used an NF-270 membrane for two months running five hours a day, five days a week with a solution containing calcium chloride and magnesium sulfate and a total dissolved solids (TDS) concentration of 1350 mg/L to understand the impact of intermittent operation on fouling. This experiment resulted in minimal reduction of flux despite containing a significant amount of calcium which is a common foulant on nanofiltration membranes (AlSawaftah et al., 2021). The next experiment tested the membrane with solutions containing iron and manganese, which were chosen because they are common contaminants in Navajo Nation groundwater and can be significant sources of fouling (Credo et al., 2019; Mariën et al., 2004). The solutions contained iron and manganese concentrations at 261 mg/L Mn^{2+} and 142 mg/L Fe^{2+} or 54 mg/L Fe^{3+}, which are orders of magnitude greater than natural sources, to expedite fouling in a shorter time frame than the typical lifetime of a nanofiltration membrane, which can be years (Credo et al., 2019; Li et al., 2019). The first feed solution contained ferric sulfate and manganese sulfate and was tested for one week and resulted in limited fouling. The second feed solution contained ferrous sulfate and manganese sulfate was tested for two days and resulted in rapid flux decline and system failure. This flux decline was accompanied by lower sulfate rejection. After the observed system failure, the membrane was cleaned with a 0.1% by weight NaOH solution, a 1mM SDS solution at pH 12, a 1mM EDTA solution at pH 12, and a

0.01% by weight citric acid solution (Li and Elimelech, 2004; Melliti et al., 20i18). These cleaning procedures were able to recover water flux to about 75% of the original levels when operated with the $MgSO_4$ and $CaCl_2$ solution. This kind of irreversible fouling can have a significant effect on the lifetime cost of the system if it occurs to such an extent that membrane replacement is necessary.

An autopsy of the fouled NF-270 membrane was conducted to understand the composition of the foulant and mechanisms of fouling, which can be valuable information for developing more effective operation and maintenance instructions of an off-grid system. The specific analyses chosen for the membrane autopsy were selected based on the anticipated composition of the foulant. While the elemental composition of the solution that caused the fouling is known to contain iron, manganese, and sulfate, the distribution of foulants and the specific complexes and species formed are not. XRD can provide some insight into those specifics, as was done in a study that found structural differences between the iron precipitates in the 5-micron cartridge filter and iron precipitates on an reverse osmosis (RO) membrane (Melliti et al., 2018). Similarly, XRD will be used in this study to identify the iron and/or manganese precipitates on the fouled 10-micron filter, 5-micron filter, and NF-270 membrane. SEM-EDX will be used to examine the membrane surface and filter surfaces and determine the elemental composition of the foulant of each surface. It was anticipated that XRD will identify iron complexes containing ferric iron on the NF-270 foulant and SEM-EDX will identify iron as the predominant foulant on the NF-270 membrane.

Iron oxyhydroxides and oxides may be present in the fouling layer because their low solubility could cause precipitation on the membrane surface. Because ferric salts are coagulants,

it is also possible that iron formed colloids with the humic acid present in the solution, which would form a cake layer on the membrane surface (Ning, 2009). Zeta potential and contact angle measurements of the fouled NF-270 membrane and virgin NF-270 membrane may also provide insight into the cause of the flux reduction and nature of the foulant. Comparing the zeta potential and contact angle between virgin NF-270 and the fouled membrane may also provide insight into the cause of the flux reduction and nature of the foulant. It is expected that the fouled membrane will have a more neutral or even zeta potential, as this could explain the decreased rejection of sulfate seen in previous experiments. The SEM/SEM-EDX showed an even layer of iron on the membrane surface as well as clumps that may have precipitated onto the membrane surface. The presence of iron at all stages (5-micron, 10-micron, and nanofiltration) indicates that iron was present in particles of varying sizes. The XRD results demonstrated that both manganese and iron foulants were mostly amorphous, although some magnetite may be present.

4.2. Materials and Methods

4.2.1. Nanofiltration Unit

A spiral-wound nanofiltration membrane (NF270-2540, Dupont) was used in a pilot-scale system operated with solutions containing contaminants relevant to Navajo Nation water sources. The NF-270 membrane consists of a bottom layer of polyester support, a middle layer of polysulfone, and a thin top layer of polyamide (Dupont, 2022). The system used a polypropylene 10-micron cartridge filter and a polypropylene 5-micron filter as pretreatment of the feed water

prior to entering the membrane. The system was operated at a pressure of 50 psi for five hours a day, five days a week to simulate realistic operation in the field to meet household water needs.

4.2.2. Water Composition

The composition of the solution tested, the amount of time the system was operated with that solution, and relevant operating conditions are summarized in chronological order in Table 10. During operation with the solution containing $Fe_2(SO_4)_3$ the membrane experienced significant flux decline (see Chapter 3 for more details). The membrane was cleaned with solutions containing 0.1% NaOH, 1mM SDS, 1mM EDTA, and 0.01% citric acid. Because the water flux could only be restored to about 75% of the pre-fouling flux, a new NF-270 was installed in the system and the fouled membrane was stored for analysis.

Table 10 Solution Composition and Operating Conditions.

Time period of operation	**Solution composition**	**Relevant operating conditions**
8 days (40 hrs)	1000 mg/L MSO_4	Rinsed with DI water between operation
5 days (25 hrs)	1000 mg/L $MgSO_4$	No rinsing between operation
5 days (25 hrs)	750 mg/L $MgSO_4$, 600 mg/L $CaCl_2$	Rinsed with DI water between operation
40 days (200 hrs)	750 mg/L $MgSO_4$, 600 mg/L $CaCl_2$	No rinsing between operation
5 days (25 hrs)	387.1 mg/L $FeSO_4$, 718.4 mg/L $MnSO_4$, 20 mg/L humic acid, 875 mg/L $MgSO_4$	Rinsed with DI water between operation
3 days (14 hrs)	387.1 mg/L $Fe_2(SO_4)_3$, 718.4 mg/L $MnSO_4$, 20 mg/L humic acid, 875 mg/L $MgSO_4$	Rinsed with DI water between operation

4.2.3. Nanofiltration Membrane Autopsy Procedure

The fouled NF-270 membrane was stored at 4°C in sealed bag before the autopsy was conducted. The autopsy was conducted in a clean environment on a surface cleaned and disinfected before use. The membrane housing was cut open, the membrane module was unwound, and clamped onto the benchtop on four sides. Each component was visually inspected for any defects, visible damage, or other notable features. The module consisted of four sheets of membrane surface that were joined in pairs to enclose two areas of permeate flow as shown in Figure 4.2.1. In general, the samples were taken from the sheets labeled Inner Membrane 1 and Outer Membrane 1 since the foulant layers were less disturbed by the unrolling process than the sheets labeled Inner Membrane 2 and Outer Membrane 2. Photos were taken of each component and each membrane surface. The effective area was calculated for each membrane area. Coupons of about 1 cm^2 each were cut for SEM-EDX, zeta potential calculations, and contact angle measurements from the influent end of the module (in triplicate), the effluent end of the module (in triplicate), and the middle. 1 cm^2 coupons of pristine NF-270 were collected and soaked in Milli-Q water to hydrate the membrane and to remove any materials on the surface (Chon and Cho, 2016). The pristine NF-270 was subjected to SEM-EDX, zeta potential measurements, and contact angle measurements to compare to the fouled membrane surface.

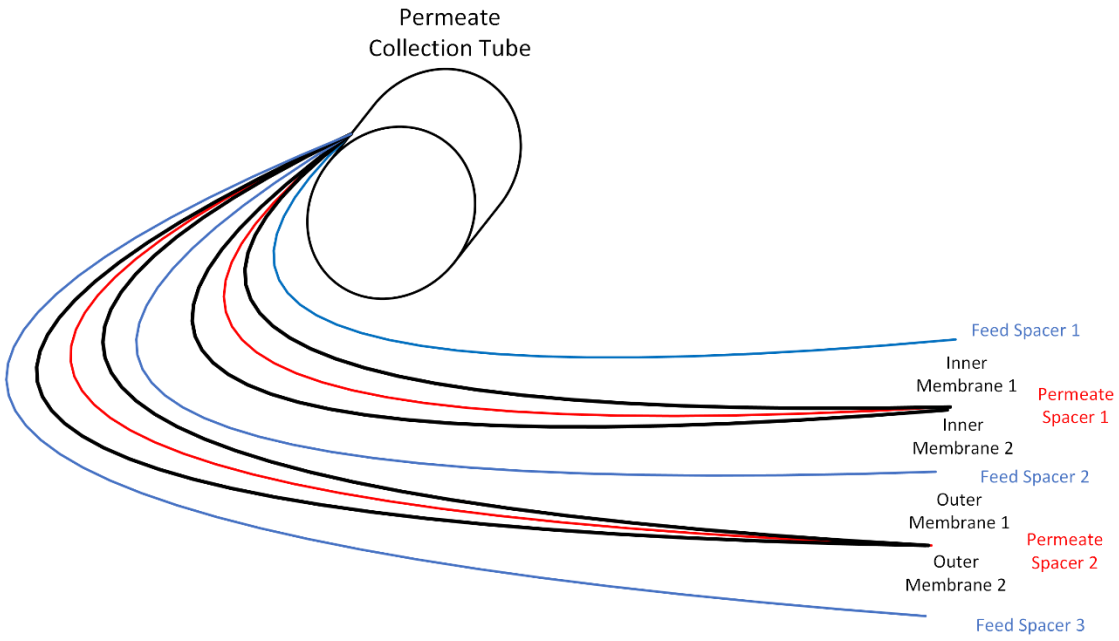

Figure 4.2.1 Layers of Spiral Wound NF-270 Membrane leading to the central permeate collection channel.

The fouling load on the membrane surface was calculated by gently scraping a surface area of 100 cm^2 to collect the foulants. The surface deposits were dried in a desiccator for about 24 hours to remove water and then the dry mass measured (Zhao et al., 2019). The weighed quantities were then placed in a muffle furnace at 550°C for 6 hours. This process ignites any organic matter and the deposit loses mass in the form of carbon dioxide, which may provide an indication of the organic matter present in the fouling layer (Heiri et al., 2001). However, a decrease in mass can also be explained by the release of water that is strongly bonded to iron oxyhydroxides and is released at a temperature range between 260 and 425°C (Strezov et al., 2010). After combustion at 550°C, the loss on ignition (LOI) is calculated using the following equation (Heiri et al., 2001):

Ὺ Ὺ̈Ϙ٣ ٣ سٍي ʾOὠ ٍ ت خ ٍ طي ʾOὠ ٣ ٣ / ʾOὠ ٍ ت خ ذ ي z ρ π π

The results of other analyses will be needed to determine whether the LOI is due to the decomposition of organics or iron oxyhydroxides.

4.2.4. Cartridge Filter Autopsy Procedure

Surface deposits were collected from the fouled 5-micron cartridge filter for XRD analysis with a plastic spatula. The foulant had infiltrated more deeply into the 5-micron filter and could not be collected in useful amounts. Coupons about 1 cm^2 in size were cut from the 10-micron and 5-micron filters for SEM-EDX analysis.

4.2.5. SEM and SEM-EDX

SEM provides images of the NF-270 membrane surface and cartridge filter surfaces to understand the morphology of the foulants. SEM-EDX provides elemental composition of the membrane surface, cartridges filter surfaces, and NF-270 cross-section. Coupons for SEM from the NF-270 and cartridge filters were placed in aluminum trays and vacuum oven dried for about 24 hours at a temperature of 105°C (Balcik, 2021). The samples were kept in a desiccator until analysis. The samples were sputter-coated with a thin layer of gold before analysis with scanning electron microscopy (FEI Inspec-S SEM) coupled with energy-dispersive X-ray spectroscopy by Thermo Noran System Six X-ray microanalysis system (EDS). SEM images were taken at 1,000x and 10,000x magnification.

4.2.6. X-Ray Diffraction

Powder x-ray diffraction is used to characterize the structure of the inorganic precipitants by looking at the angle at which the X-rays are diffracted. This characterization technique can help identify which iron or manganese precipitants formed (Melliti et al., 2018). After coupons were collected from the NF-270 surface, the membrane surface was scraped with a plastic spatula to collect as much surface deposit as possible for XRD analysis. Foulant was also collected from the 5-micron cartridge filter with a plastic spatula. The foulants were then dried in a vacuum oven at 105°C for ~24 hours (Balcik, 2021). Once dried, any remnants of membrane surface were removed and the scrapings were ground into a fine powder. XRD measurements were performed using Philips X'PERT MPD X-ray diffractometer, in the 2θ range of 5°-90° with a 0.017° step size, using Cu Kα to determine the crystallographic structure of the foulant material.

4.2.7. Contact Angle

Measurement of the contact angle of a drop of water on a surface can indicate the hydrophobicity or hydrophilicity of the surface (Al-Amoudi et al., 2008). The coupons of fouled NF-270 membrane were air-dried for ~24 hours before analysis with the sessile drop technique with a Krüss Drop Shape Analyzer with deionized water. The pristine membrane and the citric acid-soaked membrane were also analyzed for comparison.

4.2.8. Zeta-Potential

The zeta potential is defined as the electrostatic potential at the slip plane between the layer of counterions adhered to membrane surface and the diffuse layer of counterions further from the

membrane surface. Streaming potential measures the zeta potential by flowing a electrolyte solution between membranes mounted onto plates (Elimelech et al., 1994). Zeta potential is sensitive to changes in solution pH, solution composition, and membrane surface charge. Changes in zeta potential between the pristine membrane, the fouled membrane, and the citric-acid soaked membrane were measured to understand changes to the membrane surface due to fouling. The coupons of fouled membrane were air-dried for ~24 hours before the zeta potential was measured at a pH of 6.8 with the SupPASS 3 electrokinetic analyzer for solid surface analysis from Anton Parr.

4.3. Results and Discussion

4.3.1. Nanofiltration Membrane Visual Inspection

Inspection of the membrane elements clearly showed a significant orange-red fouling layer on the NF-270 surface evenly distributed over the membrane surface as shown in Figure 4.3.1. The orange color indicates that the foulant layer contains iron, which was expected based on the solutions that were used to operate the SNF system when fouling occurred. Apart from the orange colored foulant, there were no defects visible to the naked eye on the membrane surface or any of the membrane components.

Figure 4.3.1 Fouled NF-270 Membrane Surface.

The calculation of mass of foulant normalized by area and LOI are presented in Table 11. The low %LOI indicates that if organic fouling is present, it accounts for a very small portion of the foulant. Iron hydroxides can also be thermally dehydrated at temperatures from 140-500°C, which may account for some or all of the loss on ignition (Cornell and Schwertmann, 2003).

Table 11 Mass of NF-270 foulant per area (mg/m^2) and Loss on Ignition.

Sample Name	Fouling load after drying (mg/m^2)	Fouling load after ignition (mg/m^2)	Mass after ignition (g)	%LOI
Inlet (outer membrane)	1000	900	0.009	10%
Outlet (outer membrane)	900	800	0.008	11%

4.3.2. Cartridge Filter Visual Inspection

On the 5-micron cartridge filter a black foulant layer was apparent that did not penetrate deeply into the filter, while the 10-micron cartridge filter exhibited a deeper penetration of an orange red foulant, as seen in Figure 4.3.2. The foulant on the 5-micron filter also had a foul smell. The black-brown color of the fouled 5-micron filter is characteristic of manganese oxides (Post, 1999). The different colors of each cartridge filter indicates that different size precipitates formed from iron and manganese, with the manganese forming smaller precipitates.

Figure 4.3.2 Fouled 5-micron filter (left) and fouled 10-micron cartridge filter (right).

4.3.3. SEM and SEM-EDX

Representative SEM images of the pristine NF-270 membrane, fouled NF-270 membrane, 5-micron, cartridge filter, and 10-micron cartridge filter, respectively, are presented in Figure 4.3.3. The images of the fouled NF membrane surface show large deposits of precipitated foulant, as well as a thinner layer present over the entire membrane surface, which may indicate multiple mechanism of fouling. The larger deposits may be caused by precipitation at the membrane surface, whereas the evenness and lack of visible scales indicate that the thin layer may be caused by colloidal fouling. There is little evidence for biofouling, which is consistent with initial visual observations and would indicate that LOI was caused by the release of water that was strongly bonded to iron oxyhydroxides.

The 5-micron cartridge filter shows a distinct foulant layer that is characterized by a cracked texture. The black color (as seen in Figure 4.3.2) and the lack of visible crystallization indicates that this layer consists of deposited colloidal manganese oxides. The foulant on the 10-micron cartridge filter, however, is present as a thinner layer that is not as easily distinguished from the polypropylene surface of the filter.

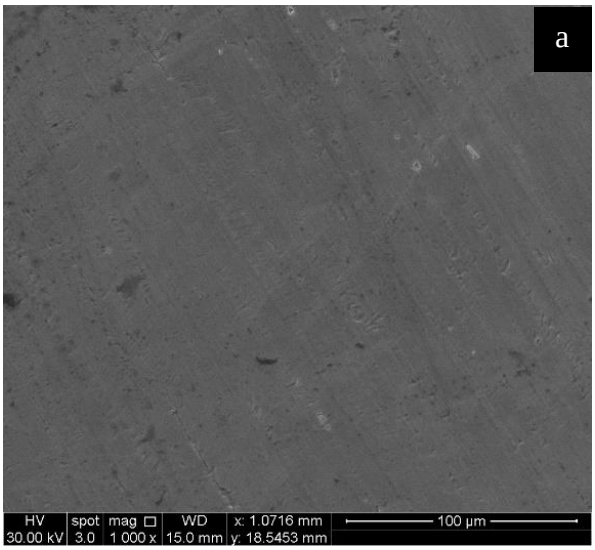
a
HV
30.00 kV
spot
3.0
mag
1 000 x
WD
15.0 mm
x: 1.0716 mm
y: 18.5453 mm
100 µm

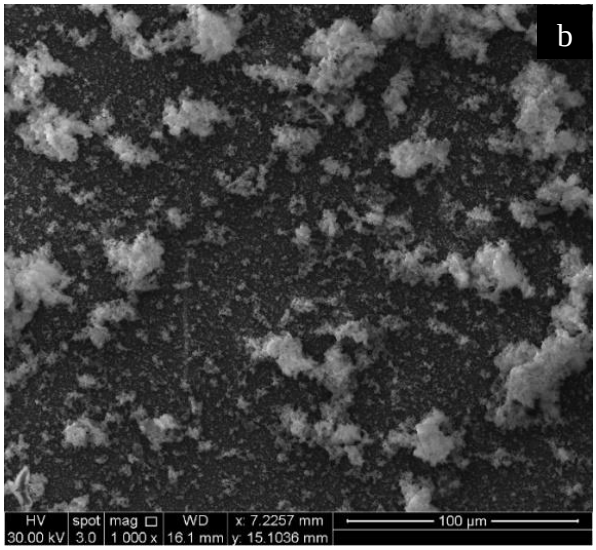
b
HV
30.00 kV
spot
3.0
mag
1 000 x
WD
16.1 mm
x: 7.2257 mm
y: 15.1036 mm
100 µm

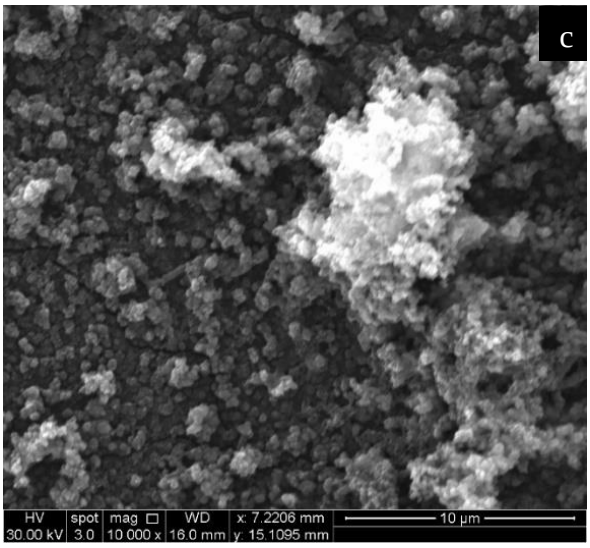
c
HV
30.00 kV
spot
3.0
mag
10 000 x
WD
16.0 mm
x: 7.2206 mm
y: 15.1095 mm
10 µm

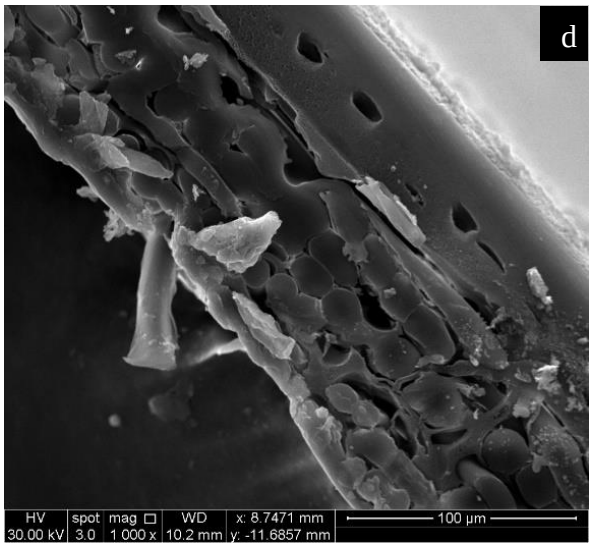
d
HV
30.00 kV
spot
3.0
mag
1 000 x
WD
10.2 mm
x: 8.7471 mm
y: -11.6857 mm
100 µm

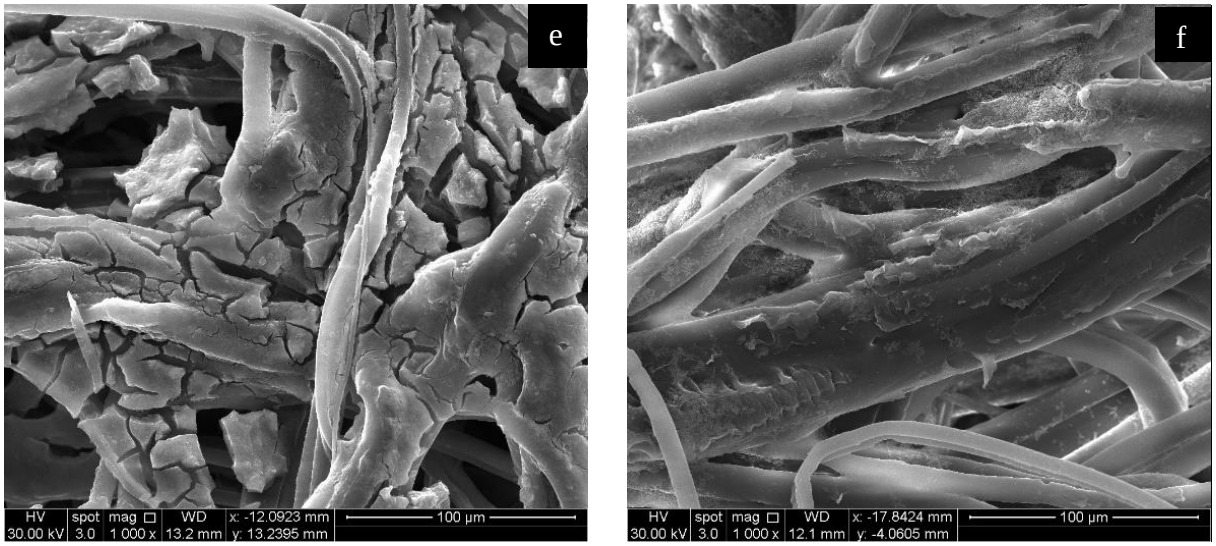

Figure 4.3.3 SEM images of the (a) pristine NF-270 membrane surface at 1,000X, (b) fouled NF-270 membrane surface at 1,000X and (c) at 10,000X, (d) cross-section of the fouled NF-270 membrane at 1,000X, (e) fouled 5-micron cartridge filter at 1,000X, and (f) fouled 10-micron cartridge filter at 1,000X.

Figure 4.3.4 shows the SEM-EDX spectra of the pristine NF-270 surface, fouled NF-270 surface, the 5-micron cartridge filter, and the 10-micron cartridge filter. A comparison of the pristine NF-270 (Figure 4.3.4.a) and the fouled NF-270 (Figure 4.3.4.b) shows the presence of iron and manganese on the fouled membrane, as well as an increase in oxygen and decrease in carbon and sulfur. This is consistent with observations that the membrane surface is almost entirely coated by the foulant, which obscures the carbon and sulfur present on the membrane surface. The increase in manganese was not expected because the red color of the NF-270 membrane fouling is characteristic of iron. The spectra of the fouled NF-270 membrane (Figure 4.3.4.b) also demonstrates that relatively little of the cleaning agents, specifically SDS, was deposited on the membrane surface, whereas other membrane autopsies conducted after cleaning procedures have

been found deposition of cleaning agent (Al-Amoudi et al., 2007). The increase in the oxygen peak indicates that the iron and manganese are in the form of hydroxides or oxides.

A comparison of the spectra of the fouled NF-270 surface, 5-micron filter, and 10-micron filter demonstrates the differences in foulant composition and can provide information about the water composition at each stage of the filtration system. The 10-micron SEM-EDX spectrum (Figure 4.3.4.c) shows the presence of iron but not manganese, which is consistent with the red color of the foulant observed on the 10-micron filter. This indicates that manganese formed precipitates with diameters smaller than 10-micron.

The 5-micron SEM-EDX (Figure 4.3.4.d) spectrum has peaks corresponding to iron as well as manganese and calcium. The peaks corresponding to iron are small in the 10-micron spectra compared to the peaks corresponding to iron in the 5-micron spectra. This may indicate that this is more iron present on the 5-micron filter than the 10-micron filter. However, the SEM-EDX can only identify elements present on the surface of a sample, thus any foulants that have penetrated into the filters will not be identified.

The solution that caused irreversible fouling contained iron but did not contain any calcium, indicating that some fouling was present from previous experiments that used solutions containing Ca^{2+}. This is interesting because there is relatively little calcium present on the fouled nanofiltration membrane, which would be expected if concentration polarization were the mechanism by which calcium precipitated in the system. Further research would be needed to understand why more calcium is present on the 5-micron filter than the nanofiltration membrane.

Iron fouling was present in each stage of the SNF system (10-micron filtration, 5-micron filtration, and nanofiltration), which indicates that iron formed particles in a range of sizes. The presence of manganese fouling on the 5-micron filter and the nanofiltration membrane indicates that it formed smaller particles.

(a) 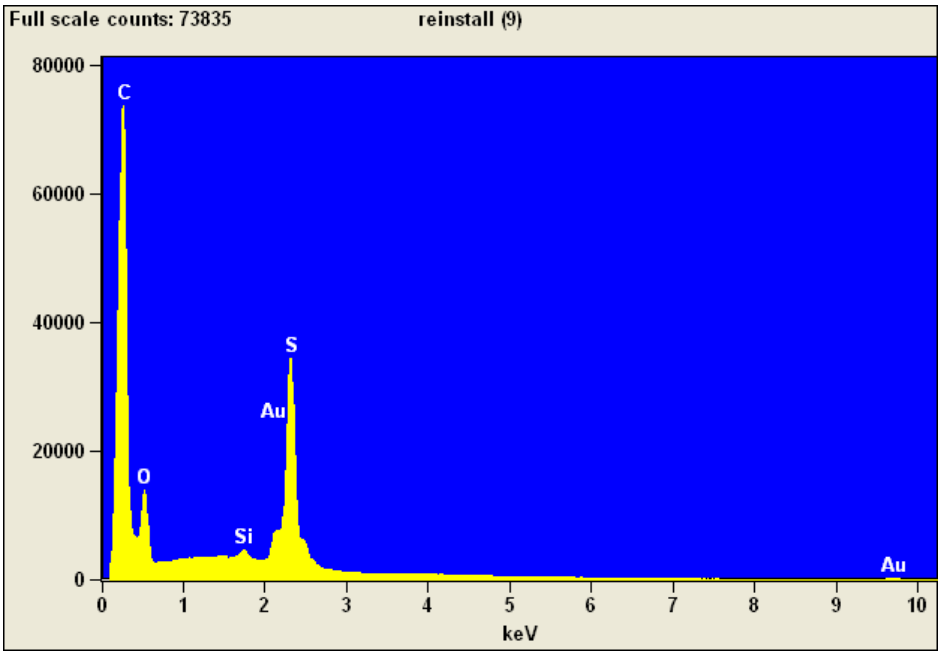

(b)

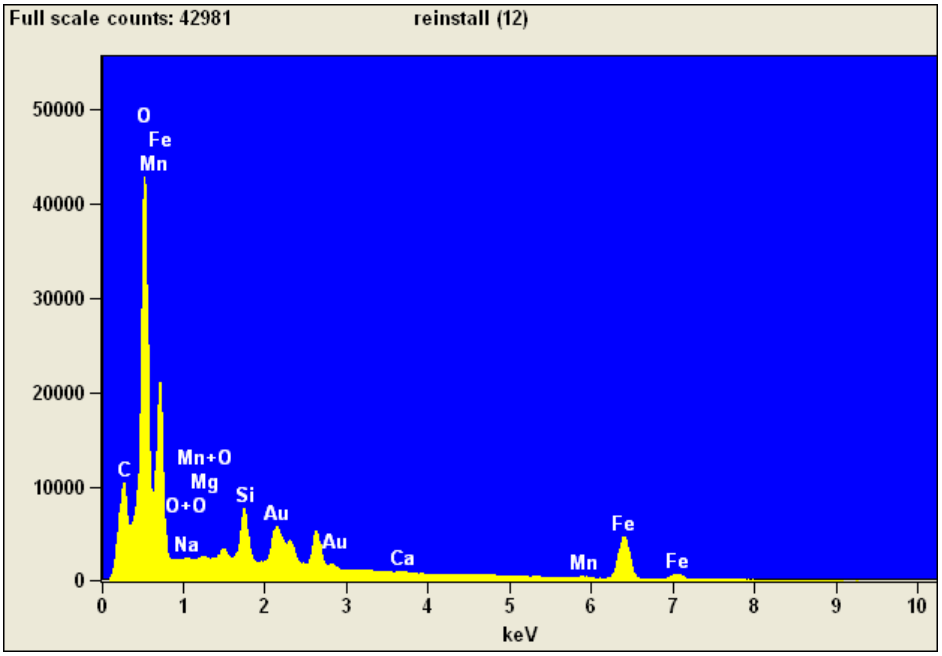
Full scale counts: 42981
reinstall (12)
50000
40000
30000
20000
10000
0
O
Fe
Mn
C
Mn+O
Mg
O+O
Na
Si
Au
Au
Ca
Mn
Fe
Fe
0
1
2
3
4
5
6
7
8
9
10
keV

(c)

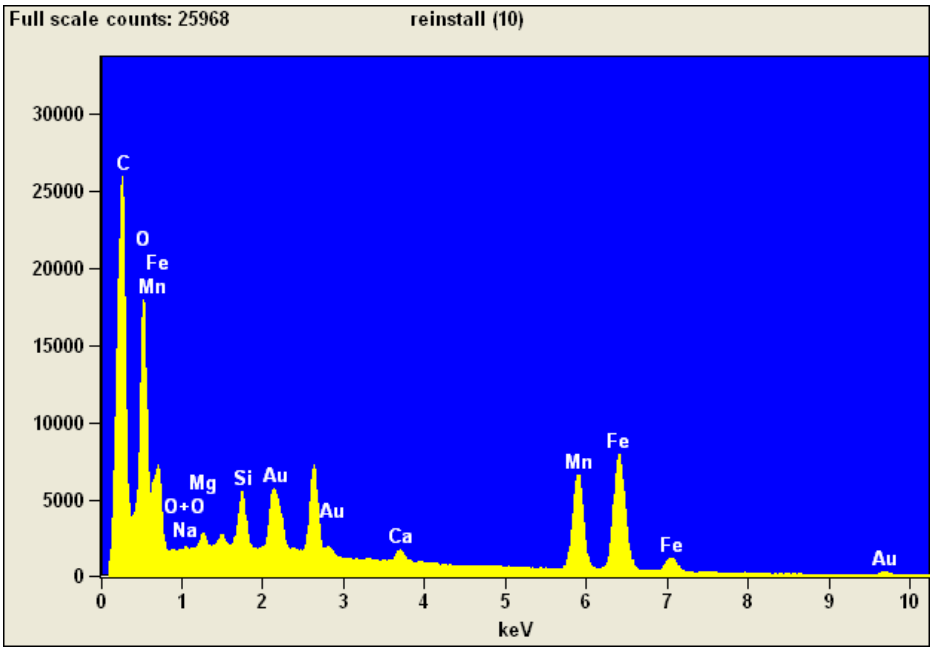
Full scale counts: 25968
reinstall (10)
30000
25000
20000
15000
10000
5000
0
C
O
Fe
Mn
Mg
O+O
Na
Si
Au
Au
Ca
Mn
Fe
Fe
Au
0
1
2
3
4
5
6
7
8
9
10
keV

(d) 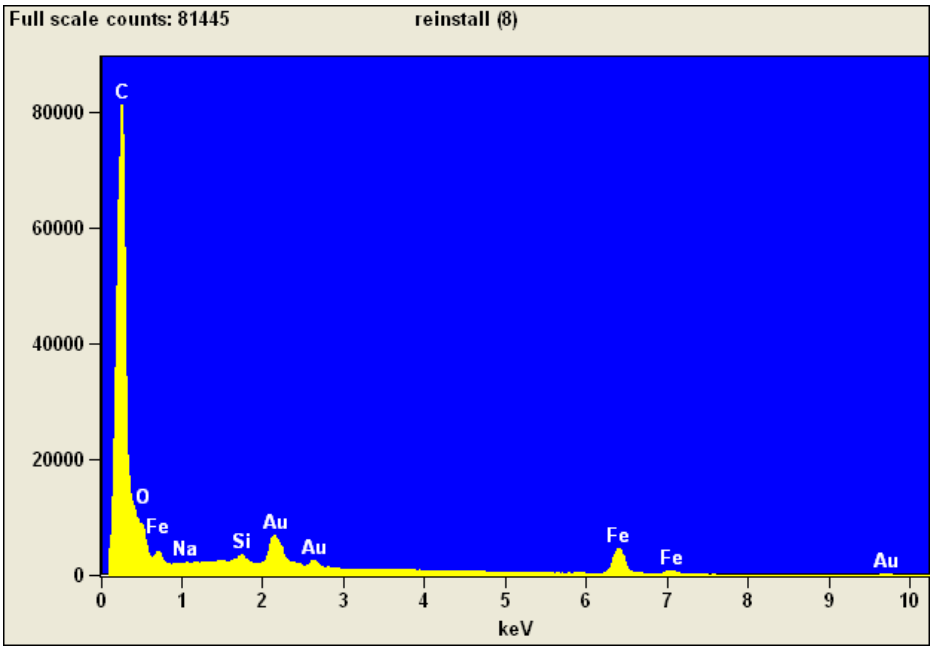

Figure 4.3.4 SEM-EDX spectra of the (a) pristine NF-270 surface, (b) fouled NF-270, (c) fouled 5-micron filter, (d) fouled 10-micron filter.

Spectral mapping as seen in Figure 4.3.5 further demonstrates the composition of the NF-270 foulant layer. In particular, the large deposits correspond to the presence of iron, and to a lesser extent, manganese. The polyamide layer on the membrane suface is more obscured where these large masses are present, as demonstrated in Figure 4.3.5.d by the areas with a weaker carbon signal which correspond to the areas in Figure 4.3.5.e with a stronger iron signal. Although manganese is present, the spectal mapping indicates that iron is a more signifcant foulant on the NF-270.

(a)

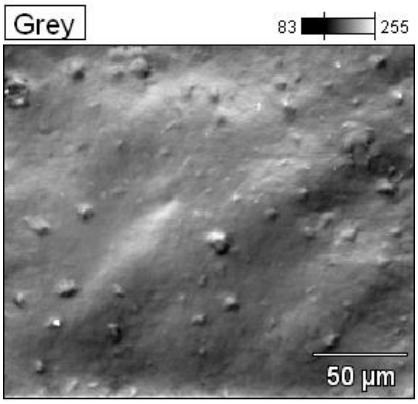
Grey
83
255
50 µm

(b)

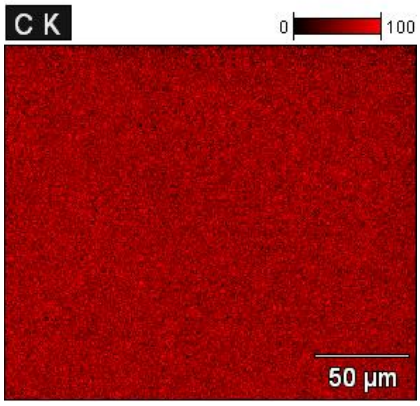
C K
0
100
50 µm

(c)

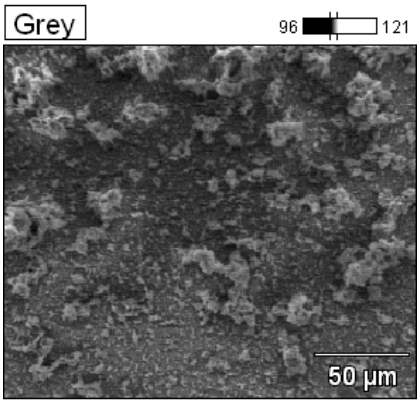
Grey
96
121
50 µm

(d)

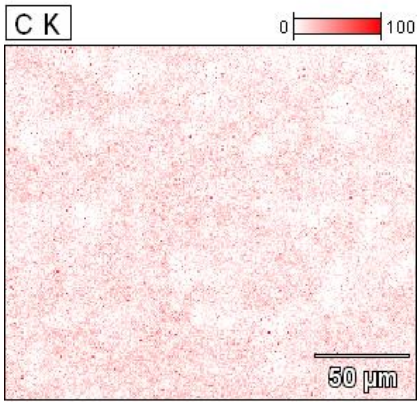
C K
0
100
50 µm

(e)

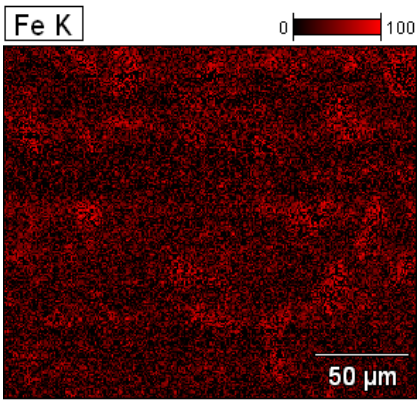
Fe K
0
100
50 µm

(f)

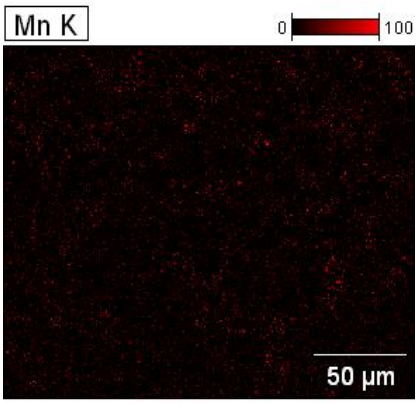
Mn K
0
100
50 µm

Figure 4.3.5 Spectral mapping of pristine NF-270 surface: (a) SEM image and (b) carbon. Spectral mapping of fouled NF-270 surface: (c) SEM image, (d) carbon, (e) iron, and (f) manganese.

Spectral mapping of the cartridge filters is presented in Figure 4.3.6. As noted in the visual inspection of the 10-micron filter, the iron foulant penetrated into the deeper areas of the 10-micron filter (Figure 4.3.6.c), whereas the iron foulant on the 5-micron filter is more uniformly present near the surface of the 5-micron filter (Figure 4.3.6.h). This may indicate that iron is present in particles that vary in size.

An interesting difference between the two filters is the distribution of oxygen seems to be inverted on the 5-micron filter versus the 10-micron filter. On the 10-micron filter the presence of oxygen (Figure 4.3.6.d) roughly corresponds to the presence of carbon (Figure 4.3.6.c), and where carbon is absent oxygen tends to be absent as well. However, this is not always true on the 5-micron filter as demonstrated in the overlay shown in Figure 4.3.6.f. In fact, the distribution of oxygen is more similar to that of manganese or iron, which indicates that it is present as part of metal oxides.

(a)

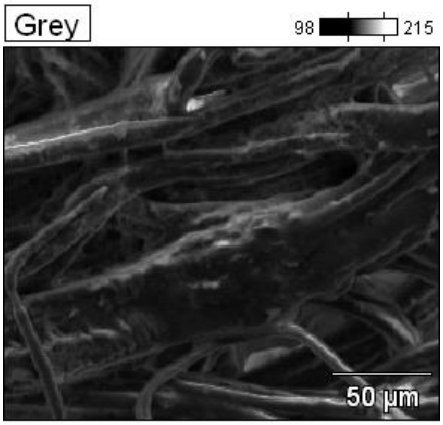

(b)

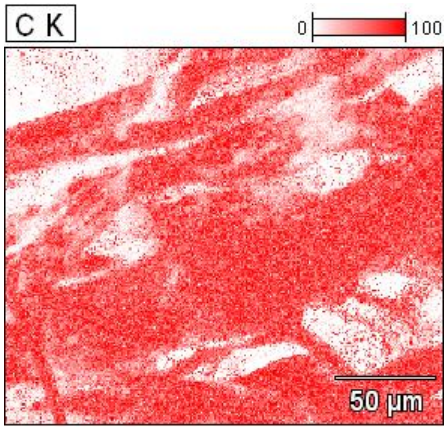

(c) 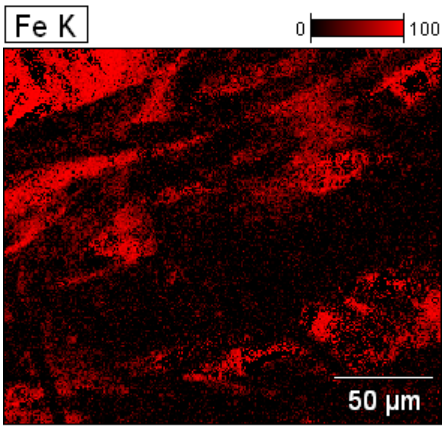
Fe K
0
100
50 µm

(d) 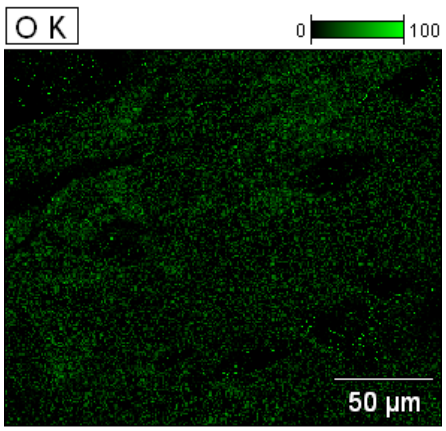
O K
0
100
50 µm

(e) 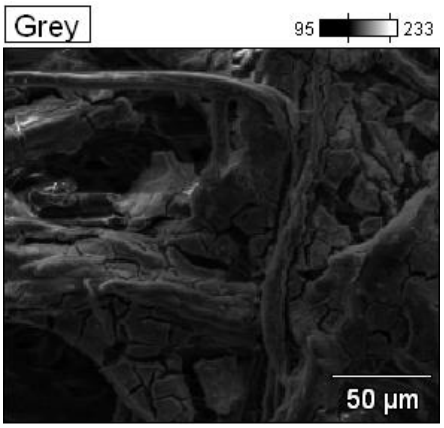
Grey
95
233
50 µm

(f) 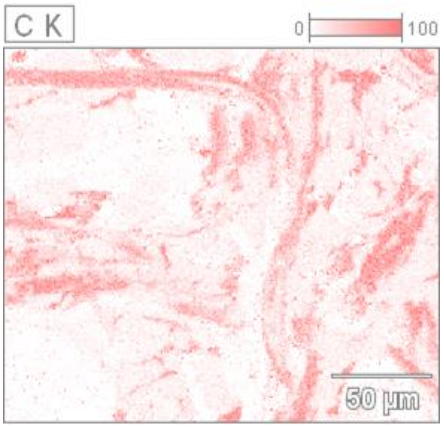
C K
0
100
50 µm

(g) 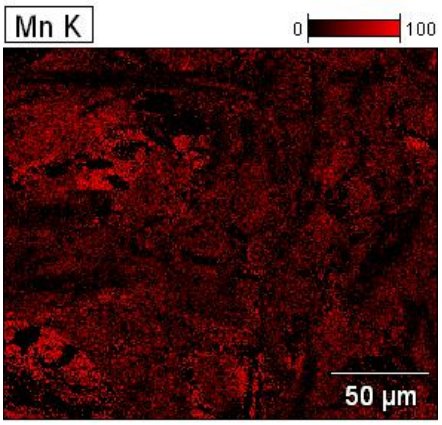
Mn K
0
100
50 µm

(h) 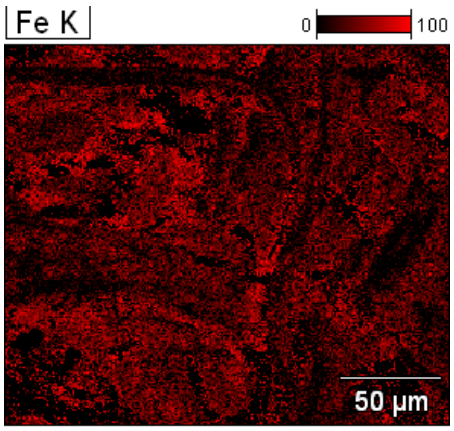
Fe K
0
100
50 µm

(i) 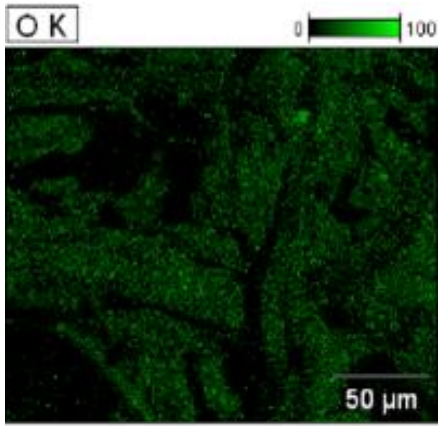

(f) 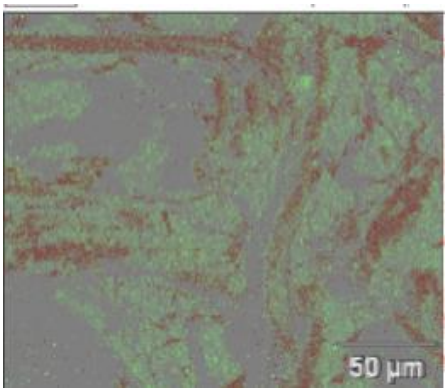

Figure 4.3.6 Spectral mapping: the 10-micron filter SEM image (a), 10-micron carbon (b), 10-micron iron(c), 10-micron oxygen (d), the 5-micron filter SEM image (e), 5-micron carbon (f), 5-micron manganese (g), 5-micron iron (h), 5-micron oxygen (i), and overlay of oxygen and carbon.

4.3.4. X-Ray Diffraction

The diffractogram shown in Figure 4.3.7 resulting from X-ray diffraction demonstrates that the foulants for both the NF-270 and the 5-micron filter are almost entirely composed of amorphous material. However, a larger peak at 36° and a smaller peak at 63° in the NF-270 foulant diffractogram can be explained by the presence of Fe_3O_4, also known as magnetite. The presence of magnetite would be interesting because magnetite contains both Fe(II) and Fe(III). While the rapid decline in flux occurred during the introduction of ferric iron, the presence of Fe(II) indicates the potential for fouling with ferrous iron as well. Of the many oxides and hydroxides of iron, ferrihydrite, also known as hydrous ferric oxide or amorphous ferric oxyhydroxide, is the most amorphous in structure. It can vary in structure and has the approximate formula of $Fe_5O_8H \cdot H_20$ (Cornell and Schwertmann, 2003). They form when the ferric ion is exposed to OH^- in acidic conditions, as was the case in the solution used (Misawa et al., n.d.). Ferric oxyhydroxides are

most likely the greatest constituent of the remaining foulant. They can form colloids that vary in size, which is consistent with the observations made in SEM-EDX analysis. A layer of ferric oxyhydroxides could account for the layer of fouling on the membrane surface observed in SEM images (Figure 4.3.3.c).

The 5-micron foulant was expected to contain greater amounts of manganese than the NF-270 foulant based on the SEM-EDX spectra results, so peaks for manganese containing compounds were compared to the 5-micron diffractogram. Mn_3O_4 was identified as one possible constituent of the 5-micron foulant, but it should be noted that the Fe_3O_4 could also explain the major peaks in the 5-micron diffractogram. Like the NF-270 foulant, the majority of the foulant was amorphous which may also be ferric oxyhydroxide or amorphous manganese oxide, which is a common form for manganese oxides (Post, 1999).

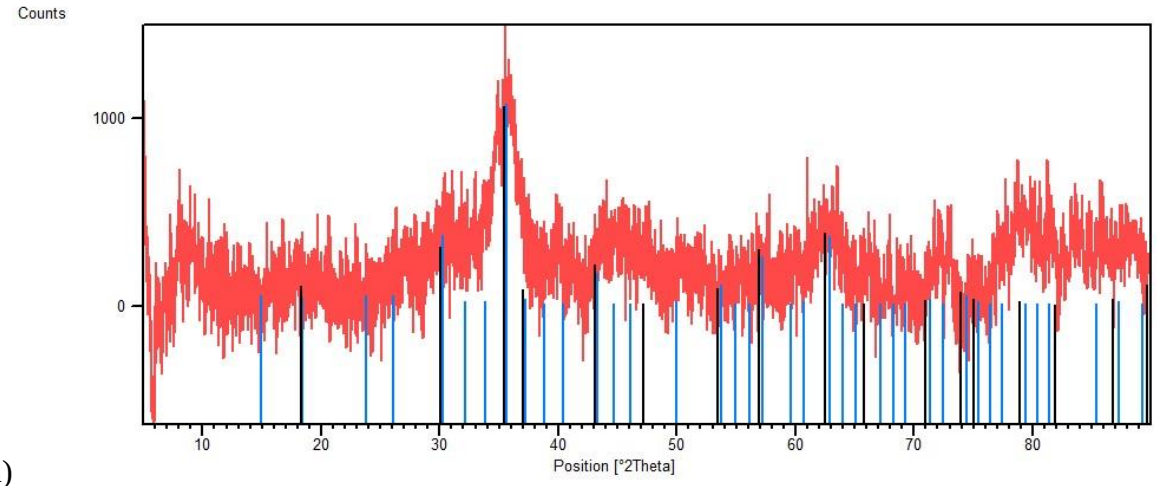

(a)

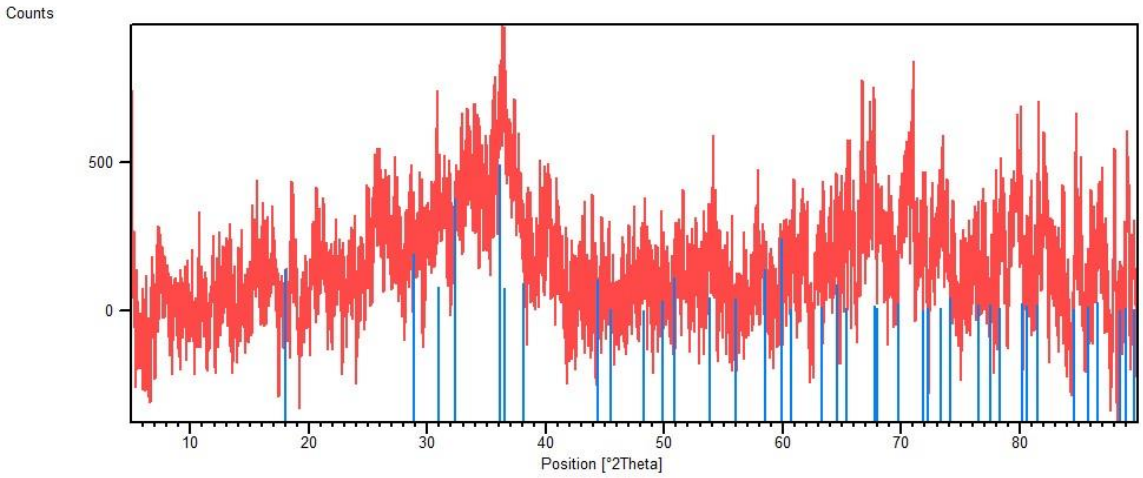

(b)

Figure 4.3.7 Diffractogram of (a) NF-270 foulant (red) compared to reference peaks for Fe3O4, magnetite (black), and Fe2O3, maghemite (blue), (b) diffractogram of 5-micron filter foulant (red) compared to reference peaks for Mn3O4 (blue).

4.3.5. Zeta Potential and Goniometer

The contact angles of the fouled NF-270 membrane, as presented in Table 12 show that the membrane is actually more hydrophilic after fouling than the pristine membrane. This was not expected because hydrophilicity has been associated with greater flux (Al-Amoudi et al., 2007). While that same study found that the application of SDS as a cleaning method resulted in increased hydrophilicity, the lack of sulfur on the fouled membrane surface suggests that this is not the case. However, studies have found that iron oxides, and especially iron oxyhydroxides, are hydrophilic (Iveson et al., 2004; Tang et al., 2017).

Table 12 Contact angles of pristine, fouled and cleaned NF-270 membranes.

	Contact Angle (°)
Pristine NF-270	25.1

Fouled NF-270	0
Fouled NF-270 cleaned with citric acid	0

The change in zeta potential, as demonstrated in Figure 4.3.8, was also not expected. Foulants are often cause a less charged membrane surface, especially when there is also evidence for a decrease in charge exclusion. However, studies on ferric salts used as coagulants have found that at dosages less than 1.5 g/L the zeta potential is negative (Liang et al., 2009).

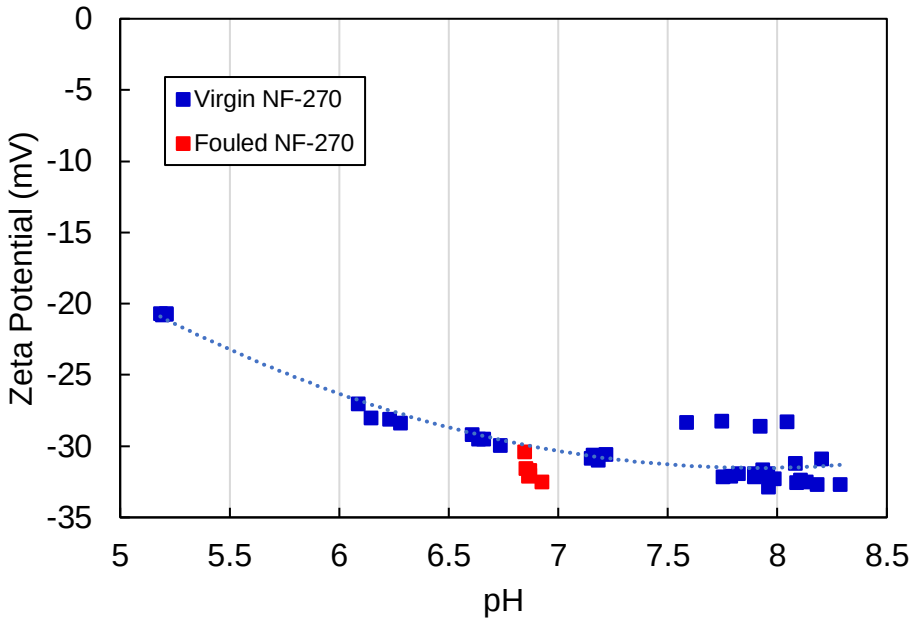

Figure 4.3.8 Zeta Potential of Pristine NF-270 membrane from pH 5 to 8 compared to Fouled NF-270 membrane at pH 6.9.

4.4. Conclusions and Further Research

The results of this membrane autopsy provide a greater understanding of the issues that iron fouling can cause for nanofiltration membranes. While the concentrations of iron used in this study are orders of magnitude larger than the values found in the groundwater tested on the Navajo

Nation, iron is still a concern for operation of the solar-powered nanofiltration units. Iron fouling must be controlled or prevented as much as possible to avoid performance decline.

The nature of the foulants investigated in this study are important for the operation and maintenance of solar-powered nanofiltration units on the Navajo Nation. The removal of much of the foulants by the cartridge filters alone, especially the 5-micron filter, indicates their importance when colloidal fouling is a possibility. The addition of a 1-micron cartridge may be worth investigating for that reason. Additionally, the fact that the vast majority of foulant was amorphous also has interesting implications for maintenance and operation. Antiscalants are commonplace in industrial applications (A.I. Schäfer et al.) but may not be feasible for realistic off-grid household applications because of the additional operational expertise and time needed for use. Results from this study may another reason antiscalants are not needed in this context.

Results of this study indicate the importance of water chemistry to the fate of colloids in membrane systems. Ferric salts are used as coagulants, which means the formation of colloids is expected but the effect of those colloids have can vary greatly. If conditions allow for the formation of larger flocs, flux can actually increase as seen in Schäfer et al., who used ferric chloride to prevent fouling of humic acid and calcium (A. I. Schäfer et al.). They found that at 100 mg/L ferric chloride the flux went down during the experiment due to the deposition of colloids on the membrane but was fully recoverable and some staining was observed. If the colloids remain small, they can instead cause irreversible fouling as was the case in the present study.

One limitation of this study is that the membrane surface had already been treated with cleaning solutions (EDTA, SDS, NaOH, and citric acid). The fouling layer may have been different

before the cleaning procedures, which may have provided different results. However, the results from this study are still relevant because the composition of the fouling layer that remains after cleaning procedures is most important to mitigating fouling. If another membrane is fouled, an autopsy could be completed before cleaning procedures to understand the impact of cleaning. Other topics for future research include operation of the SNF unit with natural waters that are high in iron and/or organic matter. Another area of inquiry would be the role of water storage in prevention of iron fouling. Feed water is collected in tanks before it is used to operate the SNF unit. It is possible that iron will precipitate during storage, which may mitigate iron fouling. Further research is needed to understand the role that iron and organic matter may play in the performance of these systems.

Chapter 5: Conclusion

The aims of this study were to better understand Navajo Nation groundwater, especially those aspects that may impact the suitability or performance of the SNF unit such as presence of uranium or arsenic, concentration of TDS, and presence of compounds that can cause fouling such as iron and manganese. The study identified five water sources which exceeded the MCLs for arsenic and/or uranium and the community was notified that these sources were unsafe. TDS was exceeded at 12 of the water sources. The SNF may be able to provide safer and more palatable water at the locations that exceeded uranium, arsenic, or TDS guidelines, although further research is needed to make recommendations.

In this study we were also able to observe consistent performance of the SNF unit with a variety of water quality conditions and operating conditions, including the presence of divalent ions, the presence of iron and manganese, the presence of humic acid, rinsing after operation, and no rinsing after operation. The only experiment in which water flux was noticeably affected was when a solution with a very high concentration of ferric iron was used to operate the system. This provides valuable information on the types of foulants that may cause a decline in performance.

Finally, a membrane autopsy was conducted which provided better understanding of the composition of the ferric iron fouling and the mechanisms by which it decreased water flux. The varying size of iron particles provides a challenge for pretreatment and further research is needed to understand how to mitigate fouling due to iron.

Appendix A: Water Sampling Results

Sample Name	**Conductivity (µS/cm)**	**TOC (mg/L)**	**pH**	**K^+ (mg/L)**	**Na^- (mg/L)**	**Mg^{2+} (mg/L)**	**Ca^{2+} (mg/L)**	**Fl^- (mg/L)**	**Cl^- (mg/L)**
Sand Spring 1	570.30	0.58		8.16	33.41	25.01	110.99		31.62
Sand Spring 2	570.30	0.51		7.27	34.16	24.55	109.41		30.39
Cameron	1737.00	3.71		16.62	290.99	21.76	45.56	1.32	245.42
Black Falls Drinking	1354.00	2.50		15.15	197.82	14.13	64.56	1.17	168.25
Oljato Feed	841.40	2.22		7.56	17.05	19.93	25.62	0.74	12.98
Oljato Permeate	313.00	2.54		12.09	52.51	21.74	34.36	1.02	35.31
Oljato Brine	1340.00	5.15		15.04	73.65	32.55	48.21	1.03	27.62
San Juan	812.60	2.60		7.31	30.38	16.62	356.63	0.93	12.66
Lupton Rain	98.24	5.09		6.58	1.99	0.59	3.57	0.34	2.29
Lupton Feed	297.20	Not collected		10.12	15.02	3.58	39.73	0.61	1.25
Lupton Treated Water	262.00	0.79							
Lupton Well	297.60	Not collected		13.47	14.27	3.56	39.61	0.51	11.84
Lupton Well Pump		Not collected			18.73	3.71	122.97	1.26	14.22
Landing Strip	1802.00	Not collected		7.72	357.12	7.43	10.47	3.08	62.06
Black Falls Drinking	1313.00	Not collected	7.63	4.50	180.41	12.61	62.53	0.71	170.19
Black Falls Farming	1540.00	Not collected	7.75	5.87	235.92	15.03	55.92	0.66	212.68
Chandler Spring	568.10	Not collected		1.15	144.77	12.59	32.25	0.40	141.83
Coyote Creek	1600.00	Not collected		1.32	63.64	10.21	16.34	3.34	202.17

Sample Name	**Conductivity (µS/cm)**	**TOC (mg/L)**	**pH**	**K^+ (mg/L)**	**Na^- (mg/L)**	**Mg^{2+} (mg/L)**	**Ca^{2+} (mg/L)**	**Fl^- (mg/L)**	**Cl^- (mg/L)**
Dilkon Chapter House	757.00	Not collected		4.03	64.49	19.05	49.89	1.07	68.77
Shonto	466.00	Not collected		4.97	84.03	4.73	9.81	0.17	8.61
Lewis Spring	1028.00	Not collected		0.83	189.28	4.34	10.96	1.50	101.33
Salt Spring North	2464.00	Not collected		1.61	736.44	7.55	7.35	3.48	585.10
Salt Spring South	12830.00	Not collected		2.07	405.52	9.72	18.75	1.14	161.40
Todo	683.10	Not collected		3.43	144.84	0.63	1.56	0.81	10.70
Mar Lupton Rain	76.00	4.513	6.79	1.23		0.80	15.06	0.04	1.78
Mar Lupton Well	313.20	0.688	7.14	2.84		3.37	37.84	0.12	9.42
Mar Lupton Treated Water	96.80	4.184	6.35	1.27		0.56	12.68	0.03	1.04

Sample Name	NO_2^- (mg/L)	SO_4^{2-} (mg/L)	Br^- (mg/L)	NO_3^- (mg/L)	PO_4^{3-} (mg/L)	Li (µg/L)	Be (µg/L)	Na (µg/L)	Mg (µg/L)
Sand Spring 1	570.30	0.58		8.16	33.41	25.01	110.99		31.62
Sand Spring 2	570.30	0.51		7.27	34.16	24.55	109.41		30.39
Cameron	1737.00	3.71		16.62	290.99	21.76	45.56	1.32	245.42
Black Falls Drinking	1354.00	2.50		15.15	197.82	14.13	64.56	1.17	168.25
Oljato Feed	841.40	2.22		7.56	17.05	19.93	25.62	0.74	12.98
Oljato Permeate	313.00	2.54		12.09	52.51	21.74	34.36	1.02	35.31
Oljato Brine	1340.00	5.15		15.04	73.65	32.55	48.21	1.03	27.62
San Juan	812.60	2.60		7.31	30.38	16.62	356.63	0.93	12.66
Lupton Rain	98.24	5.09		6.58	1.99	0.59	3.57	0.34	2.29
Lupton Feed	297.20	Not collected		10.12	15.02	3.58	39.73	0.61	1.25
Lupton Treated Water	262.00	0.79							
Lupton Well	297.60	Not collected		13.47	14.27	3.56	39.61	0.51	11.84
Lupton Well Pump		Not collected			18.73	3.71	122.97	1.26	14.22
Landing Strip	1802.00	Not collected		7.72	357.12	7.43	10.47	3.08	62.06
Black Falls Drinking	1313.00	Not collected	7.63	4.50	180.41	12.61	62.53	0.71	170.19
Black Falls Farming	1540.00	Not collected	7.75	5.87	235.92	15.03	55.92	0.66	212.68
Chandler Spring	568.10	Not collected		1.15	144.77	12.59	32.25	0.40	141.83
Coyote Creek	1600.00	Not collected		1.32	63.64	10.21	16.34	3.34	202.17
Dilkon Chapter House	757.00	Not collected		4.03	64.49	19.05	49.89	1.07	68.77

Sample Name	NO_2^- (mg/L)	SO_4^{2-} (mg/L)	Br^- (mg/L)	NO_3^- (mg/L)	PO_4^{3-} (mg/L)	Li (µg/L)	Be (µg/L)	Na (µg/L)	Mg (µg/L)
Shonto	466.00	Not collected		4.97	84.03	4.73	9.81	0.17	8.61
Lewis Spring	1028.00	Not collected		0.83	189.28	4.34	10.96	1.50	101.33
Salt Spring North	2464.00	Not collected		1.61	736.44	7.55	7.35	3.48	585.10
Salt Spring South	12830.00	Not collected		2.07	405.52	9.72	18.75	1.14	161.40
Todo	683.10	Not collected		3.43	144.84	0.63	1.56	0.81	10.70
Mar Lupton Rain	76.00	4.513	6.79	1.23		0.80	15.06	0.04	1.78
Mar Lupton Well	313.20	0.688	7.14	2.84		3.37	37.84	0.12	9.42
Mar Lupton Treated Water	96.80	4.184	6.35	1.27		0.56	12.68	0.03	1.04

Sample Name	Al (µg/L)	K (µg/L)	Ca (µg/)	V (µg/L)	Cr (µg/L)	Mn (µg/L)	Fe (µg/L)	Co (µg/L(	Ni (µg/L)
Sand Spring 1	1.68	2188.46		8.30	1.01	0.03	0.89	<0.000	0.01
Sand Spring 2									
Cameron	3.94	3596.80	47672.02	1.70	0.87	146.65	316.79	0.59	3.07
Black Falls Drinking	27.02	4035.78	69572.47	8.77	0.56	46.55	266.46	0.41	3.84
Oljato Feed	44.82	2519.16	27305.04	5.98	1.52	0.25	69.25	0.10	1.24
Oljato Permeate	45.88	2069.85	21120.15	1.47	0.19	11.69	82.51	0.11	4.52
Oljato Brine	56.29	4574.59	53589.67	8.02	1.21	20.50	146.24	0.30	5.76
San Juan	42.83	1663.52	132827.17	2.19	0.36	88.54	198.01	0.94	5.00
Lupton Rain	191.04	1268.71	14746.09	2.15	0.24	8.95	782.65	0.14	1.15
Lupton Feed									
Lupton Treated Water	54.55	2893.94	36857.23	2.40	0.34	1.88	0.12	0.18	1.59
Lupton Well	54.20	3300.48	42750.46	7.85	2.92	4.50	1049.95	0.24	2.96
Lupton Well Pump	1124.79	3716.62	44993.82	22.14	23.99	121.65	18459.06	1.51	16.45
Landing Strip	22.80	7587.42		0.09	0.08	3.66	291.20	0.03	
Black Falls Drinking	96.60	3243.05		8.02	0.12	51.09	85.57	0.04	1.46
Black Falls Farming	84.64	5614.18		12.83	0.21	0.50	7.84	#DIV/0!	0.11
Chandler Spring	105.72	380.93		35.69	5.38	1.85	21.62	0.02	1.07
Coyote Creek	106.19	656.04		134.89	1.31	3.25	219.29	0.04	1.34
Dilkon Chapter House	6.62	3593.45		0.11	0.02	29.88	126.94	0.01	

Sample Name	Al (µg/L)	K (µg/L)	Ca (µg/)	V (µg/L)	Cr (µg/L)	Mn (µg/L)	Fe (µg/L)	Co (µg/L(	Ni (µg/L)
Shonto	106.54	4541.91		14.93	1.05	0.62	15.46	0.02	1.59
Lewis Spring	100.78	652.36		76.20	1.80	0.37	11.24	0.01	0.91
Salt Spring North	145.42	271.49		235.18	14.99	8.26	498.02	0.12	8.35
Salt Spring South	96.10	1388.38		43.29	0.21	1.01	71.86	0.01	0.29
Todo	132.58	3102.56		85.57	0.48	0.57	25.60	0.01	1.11
Mar Lupton Rain	98.79	848.33		1.90	0.17	1.83	13.88	0.02	0.02
Mar Lupton Well	82.99	2847.29		4.45	1.49	8.44	543.936	0.06	0.26
Mar Lupton Treated Water	89.75	1545.47		1.94	0.11	1.58	9.53	0.02	0.34

Sample Name	Cu (µg/L)	Zn (µg/L)	Ga (µg/L)	As (µg/L)	Se (µg/L)	Rb (µg/L)	Sr (µg/L)	Mo (µg/L)	Ag (µg/L)
Sand Spring 1	0.45	<0.000		2.05	19.22		341.75	1.45	<0.000
Sand Spring 2									
Cameron	682.87	73.40	1.50	5.95	2.39	1.13	1694.81	7.54	0.02
Black Falls Drinking	3.78	707.07	1.50	2.27	3.23	4.58	1231.79	19.27	0.01
Oljato Feed	2.75	6.14	6.10	0.93	6.32	0.77	294.86	0.85	0.00
Oljato Permeate	3.50	13.43	3.73	0.69	2.28	1.00	209.55	0.34	0.00
Oljato Brine	3.51	108.51	11.18	1.61	8.49	1.90	552.74	1.59	0.00
San Juan	2.06	3.02	1.92	1.34	1.85	0.58	1061.97	2.07	0.00
Lupton Rain	4.78	124.19	1.05	0.47	4.45	0.69	52.08	0.12	0.00
Lupton Feed									
Lupton Treated Water	5.32	97.07	4.68	0.87	3.91	3.49	227.98	0.28	0.10
Lupton Well	18.85	236.46	0.77	2.55	0.00	0.79	259.21	0.37	0.00
Lupton Well Pump	85.36	725.69	1.93	4.16	0.34	1.35	268.72	1.75	0.04
Landing Strip	5.79	44.29		6.79	0.00		2411.11	156.49	
Black Falls Drinking	22.59	2522.74		1.75	0.34		1230.43	24.16	0.01
Black Falls Farming	22.98	175.20		2.42	1.97		848.10	10.31	0.01
Chandler Spring	22.73	87.51		8.19	9.34		970.98	16.19	
Coyote Creek	52.04	117.53		39.87	7.25		704.38	29.01	0.00
Dilkon Chapter House	2.87	22.00		2.29	1.30		1288.02	8.54	

Sample Name	Cu (µg/L)	Zn (µg/L)	Ga (µg/L)	As (µg/L)	Se (µg/L)	Rb (µg/L)	Sr (µg/L)	Mo (µg/L)	Ag (µg/L)
Shonto	24.26	276.33		2.80	4.57		126.44	2.73	
Lewis Spring	26.08	59.21		32.62	4.79		429.17	20.11	
Salt Spring North	409.37	995.69		95.74	29.35		397.79	12.97	0.06
Salt Spring South	24.98	80.38		21.49	14.24		834.65	6.32	0.01
Todo	24.92	59.59		54.42	28.06		57.38	44.42	
Mar Lupton Rain	191.17	243.95		0.46	0.69		41.03	0.16	NA
Mar Lupton Well	29.58	305.96		1.63	1.00		267.52	0.66	NA
Mar Lupton Treated Water	24.50	331.21		0.67	0.67		129.98	0.47	0.02

Sample Name	Cd (µg/L)	In (µg/L)	Sn (µg/L)	Sb (µg/L)	Cs (µg/L)	Ba (µg/L)	Tl (µg/L)	Pb (µg/L)	Bi (µg/L)	U (µg/L)
Sand Spring 1	0.45	<0.000		2.05	19.22		341.75	1.45	<0.000	4.02
Sand Spring 2										
Cameron	682.87	73.40	1.50	5.95	2.39	1.13	1694.81	7.54	0.02	3.64
Black Falls Drinking	3.78	707.07	1.50	2.27	3.23	4.58	1231.79	19.27	0.01	10.75
Oljato Feed	2.75	6.14	6.10	0.93	6.32	0.77	294.86	0.85	0.00	2.61
Oljato Permeate	3.50	13.43	3.73	0.69	2.28	1.00	209.55	0.34	0.00	0.03
Oljato Brine	3.51	108.51	11.18	1.61	8.49	1.90	552.74	1.59	0.00	4.42
San Juan	2.06	3.02	1.92	1.34	1.85	0.58	1061.97	2.07	0.00	3.00
Lupton Rain	4.78	124.19	1.05	0.47	4.45	0.69	52.08	0.12	0.00	0.05
Lupton Feed										
Lupton Treated Water	5.32	97.07	4.68	0.87	3.91	3.49	227.98	0.28	0.10	0.52
Lupton Well	18.85	236.46	0.77	2.55	0.00	0.79	259.21	0.37	0.00	0.99
Lupton Well Pump	85.36	725.69	1.93	4.16	0.34	1.35	268.72	1.75	0.04	1.02
Landing Strip	5.79	44.29		6.79	0.00		2411.11	156.49		0.45
Black Falls Drinking	22.59	2522.74		1.75	0.34		1230.43	24.16	0.01	10.96
Black Falls Farming	22.98	175.20		2.42	1.97		848.10	10.31	0.01	12.08
Chandler Spring	22.73	87.51		8.19	9.34		970.98	16.19		4.19

Sample Name	Cd (µg/L)	In (µg/L)	Sn (µg/L)	Sb (µg/L)	Cs (µg/L)	Ba (µg/L)	Tl (µg/L)	Pb (µg/L)	Bi (µg/L)	U (µg/L)
Coyote Creek	52.04	117.53		39.87	7.25		704.38	29.01	0.00	31.79
Dilkon Chapter House	2.87	22.00		2.29	1.30		1288.02	8.54		0.06
Shonto	24.26	276.33		2.80	4.57		126.44	2.73		2.84
Lewis Spring	26.08	59.21		32.62	4.79		429.17	20.11		8.62
Salt Spring North	409.37	995.69		95.74	29.35		397.79	12.97	0.06	131.99
Salt Spring South	24.98	80.38		21.49	14.24		834.65	6.32	0.01	56.83
Todo	24.92	59.59		54.42	28.06		57.38	44.42		7.77
Mar Lupton Rain	191.17	243.95		0.46	0.69		41.03	0.16		0.00
Mar Lupton Well	29.58	305.96		1.63	1.00		267.52	0.66		0.70
Mar Lupton Treated Water	24.50	331.21		0.67	0.67		129.98	0.47	0.02	0.11

Appendix B: Water Sampling Instruction

For ICP-MS (inorganic) sampling:

Inorganic sample vial: 15 mL polypropylene conical tubes

Acid to use: **Nitric Acid, 70%** (always keep the foil around the storage vial and do not leave the container in the sun)

ACID PPE: Goggles/safety glasses and gloves.

How many drops: about 4 drops in 10 mL of sample water, shake then store

Collect samples to send a field blank (DI H2O poured into sample container) at the site. Be sure to acidify this also and treat it like a sample. We should be acidifying them (as soon as possible after collection) to pH ~2 and then they can be stored at 4C.

For TOC sampling: Hydrochloric Acid

TOC sample vial: Amber glass vial 40 mL

Acid to use: **Hydrochloric Acid, 1M**

ACID PPE: Goggles/safety glasses and gloves.

TOC SAMPLE COLLECTION - The typical sample volume collected may vary from 40 mL to 1 L of sample. It is recommended that the sample collector coordinate the size of collection volume with the needs of the analytical laboratory. If the TOC sample is collected in a 40-mL injection vial, it is acidified to pH 2 by adding 4 drops of concentrated acid per 10 mL of sample. Amber bottles should be filled to the top with no headspace and they need about 15 drops of HCl. If the TOC sample is collected in a 1-L bottle, 1 mL of concentrated acid is added or the sample is drop wise adjusted to a pH < 2 (Sect. 8.3). TOC samples must be acidified at the time of collection. Cap the bottle or injection vial and invert several times to mix the acid. The sample is delivered as soon as possible to the laboratory and should arrive packed in ice or frozen gel packs. If there is no visible ice or the gel packs are completely thawed, the laboratory should report the conditions to the data user. Samples that are improperly preserved or shipped, cannot be used for compliance monitoring under the SDWA. The sample is stored at < 6 °C, until analysis. Stored and preserved samples must be analyzed within 28 days from time of collection.

**TOC BLANK: Collect samples to send a field blank (DI H2O poured into sample container) at the site. Be sure to acidify this also and treat it like a sample. We should be acidifying them (as soon as possible after collection) to pH ~2 and then they can be stored at 4C.

For Solar Nanofiltration System Testing:

Materials needed: six polypropylene 15 mL polypropylene conical vials, three amber glass vials, 25 liters of feed solution (a little more than half of a 10-gallon bucket).

Prepare at least 25 liters of feed water (preferably more). Collect feed water in two 15 mL polypropylene vials for IC and ICP-MS analysis. Follow the above ICP-MS sampling instructions for one vial and leave the other one at natural pH. Follow the above TOC sampling instructions to collect feed water sample for TOC analysis.

Turn on the system according to instructions provided with the system and set brine pressure to 50 psi. Allow at least 25 liters of feed water to flow through the system, which flushes out water that was previously in the system and ensures brine and permeate streams come from the feed water. Make sure that flow rates are constant. Record brine flow rate and permeate flow rate. Record after prefilter pressure and after prefilter pressure. Collect samples for IC, ICP-MS, and TOC analysis according to the instructions above from the permeate stream and the brine stream.

Notes:

For the TOC one sample per water source is fine

For all water sources we need one vial with just source water so we can measure pH and anions in the lab.

Please note down how many drops of acid you used for both the inorganic and organic analysis.

References

Abdelkareem MA, El Haj Assad M, Sayed ET, et al. Recent Progress in the Use of Renewable Energy Sources to Power Water Desalination Plants. Desalination 2018;435:97–113; doi: 10.1016/j.desal.2017.11.018.

Al-Amoudi A, Williams P, Al-Hobaib AS, et al. Cleaning Results of New and Fouled Nanofiltration Membrane Characterized by Contact Angle, Updated DSPM, Flux and Salts Rejection. Applied Surface Science 2008;254(13):3983–3992; doi: 10.1016/j.apsusc.2007.12.052.

Al-Amoudi A, Williams P, Mandale S, et al. Cleaning Results of New and Fouled Nanofiltration Membrane Characterized by Zeta Potential and Permeability. Separation and Purification Technology 2007;54(2):234–240; doi: 10.1016/j.seppur.2006.09.014.

AlSawaftah N, Abuwatfa W, Darwish N, et al. A Comprehensive Review on Membrane Fouling: Mathematical Modelling, Prediction, Diagnosis, and Mitigation. Water 2021;13(9):1327; doi: 10.3390/w13091327.

Amirbahman A and Olson TM. Deposition Kinetics of Humic Matter-Coated Hematite in Porous Media in the Presence of Ca2+. Colloids and Surfaces A: Physicochemical and Engineering Aspects 1995;99(1):1–10; doi: 10.1016/0927-7757(95)03134-Y.

Balcik C. Understanding the Operational Problems and Fouling Characterization of RO Membrane Used for Brackish Water Treatment via Membrane Autopsy. Water Science and Technology 2021;84(12):3653–3662; doi: 10.2166/wst.2021.456.

Begay SK. Navajo Residential Solar Energy Access as a Global Model. The Electricity Journal 2018;31(6):9–15; doi: 10.1016/j.tej.2018.07.003.

Bouhadjar SI, Kopp H, Britsch P, et al. Solar Powered Nanofiltration for Drinking Water Production from Fluoride-Containing Groundwater – A Pilot Study towards Developing a Sustainable and Low-Cost Treatment Plant. Journal of Environmental Management 2019;231:1263–1269; doi: 10.1016/j.jenvman.2018.07.067.

Boussouga Y-A, Frey H and Schäfer AI. Removal of Arsenic(V) by Nanofiltration: Impact of Water Salinity, PH and Organic Matter. Journal of Membrane Science 2021a;618:118631; doi: 10.1016/j.memsci.2020.118631.

Boussouga Y-A, Richards BS and Schäfer AI. Renewable Energy Powered Membrane Technology: System Resilience under Solar Irradiance Fluctuations during the Treatment of Fluoride-Rich Natural Waters by Different Nanofiltration/Reverse Osmosis Membranes. Journal of Membrane Science 2021b;617:118452; doi: 10.1016/j.memsci.2020.118452.

Brugge D and Goble R. The History of Uranium Mining and the Navajo People. Am J Public Health 2002;92(9):1410–1419.

Cai Y-H, Li S, Schäfer AI, et al. Renewable Energy Powered Membrane Technology: A Review of the Reliability of Photovoltaic-Powered Membrane System Components for Brackish Water Desalination. Applied Energy 2019;253; doi: 10.1016/j.apenergy.2019.113524.

Chenoweth WL and Malan RC. The Uranium Deposits of Northeastern Arizona. New Mexico Geological Society 24th Annual Fall Field Conference Guidebook 1973;13.

Chon K and Cho J. Fouling Behavior of Dissolved Organic Matter in Nanofiltration Membranes from a Pilot-Scale Drinking Water Treatment Plant: An Autopsy Study. Chemical Engineering Journal 2016;295:268–277; doi: 10.1016/j.cej.2016.03.057.

Chuang C-J, Wu C-Y and Wu C-C. Combination of Crossflow and Electric Field for Microfiltration of Protein/Microbial Cell Suspensions. Desalination 2008;233(1):295–302; doi: 10.1016/j.desal.2007.09.054.

Cornell RM and Schwertmann U. The Iron Oxides: Structures, Properties, Reactions, and Occurences, and Uses. 2nd ed. John Wiley & Sons, Ltd; 2003.; doi: 10.1002/3527602097.

Cozzetto K, Chief K, Dittmer K, et al. Climate Change Impacts on the Water Resources of American Indians and Alaska Natives in the U.S. Climatic Change 2013;120(3):569–584; doi: 10.1007/s10584-013-0852-y.

Credo J, Torkelson J, Rock T, et al. Quantification of Elemental Contaminants in Unregulated Water across Western Navajo Nation. Int J Environ Res Public Health 2019;16(15):2727; doi: 10.3390/ijerph16152727.

Dupont. FilmTec^{TM} Reverse Osmosis Membranes Technical Manual. 2022.

El-ghzizel S, Jalté H, Zeggar H, et al. Autopsy of Nanofiltration Membrane of a Decentralized Demineralization Plant. 1 2019;10(4):277–286.

Elimelech M, Chen WH and Waypa JJ. Measuring the Zeta (Electrokinetic) Potential of Reverse Osmosis Membranes by a Streaming Potential Analyzer. Desalination 1994;95(3):269–286; doi: 10.1016/0011-9164(94)00064-6.

Environmental Protection Agency. Drinking Water Standard for Arsenic. Environmental Protection Agency; 2001a.

Environmental Protection Agency. Radionuclides Rule: A Quick Reference Guide. 2001b.

Environmental Protection Agency. Regional Screening Level (RSL) Resident Tapwater Table (TR=1E-06, HQ=1) November 2021. Environmental Protection Agency; 2021.

Freire-Gormaly M and Bilton AM. Experimental Quantification of the Effect of Intermittent Operation on Membrane Performance of Solar Powered Reverse Osmosis Desalination Systems. Desalination 2018;435:188–197; doi: 10.1016/j.desal.2017.09.013.

Freire-Gormaly M and Bilton AM. Design of Photovoltaic Powered Reverse Osmosis Desalination Systems Considering Membrane Fouling Caused by Intermittent Operation. Renewable Energy 2019a;135:108–121; doi: 10.1016/j.renene.2018.11.065.

Freire-Gormaly M and Bilton AM. Impact of Intermittent Operation on Reverse Osmosis Membrane Fouling for Brackish Groundwater Desalination Systems. Journal of Membrane Science 2019b;583:220–230; doi: 10.1016/j.memsci.2019.04.010.

García-Vaquero N, Lee E, Jiménez Castañeda R, et al. Comparison of Drinking Water Pollutant Removal Using a Nanofiltration Pilot Plant Powered by Renewable Energy and a Conventional Treatment Facility. Desalination 2014;347:94–102; doi: 10.1016/j.desal.2014.05.036.

Guo W, Ngo H-H and Li J. A Mini-Review on Membrane Fouling. Bioresource Technology 2012;122:27–34; doi: 10.1016/j.biortech.2012.04.089.

Gwon E, Yu M, Oh H, et al. Fouling Characteristics of NF and RO Operated for Removal of Dissolved Matter from Groundwater. Water Research 2003;37(12):2989–2997; doi: 10.1016/S0043-1354(02)00563-8.

Heiri O, Lotter AF and Lemcke G. Loss on Ignition as a Method for Estimating Organic and Carbonate Content in Sediments: Reproducibility and Comparability of Results. Journal of Paleolimnology 2001;25(1):101–110; doi: http://dx.doi.org/10.1023/A:1008119611481.

Hong S and Elimelech M. Chemical and Physical Aspects of Natural Organic Matter (NOM) Fouling of Nanofiltration Membranes. Journal of Membrane Science 1997;132(2):159–181; doi: 10.1016/S0376-7388(97)00060-4.

Hoover J, Gonzales M, Shuey C, et al. Elevated Arsenic and Uranium Concentrations in Unregulated Water Sources on the Navajo Nation, USA. Expo Health 2017;9(2):113–124; doi: 10.1007/s12403-016-0226-6.

Hussain A, Janson A, Matar JM, et al. Membrane Distillation: Recent Technological Developments and Advancements in Membrane Materials. emergent mater 2022;5(2):347–367; doi: 10.1007/s42247-020-00152-8.

Iavorivska L, Boyer EW and DeWalle DR. Atmospheric Deposition of Organic Carbon via Precipitation. Atmospheric Environment 2016;146:153–163; doi: 10.1016/j.atmosenv.2016.06.006.

Iveson SM, Holt S and Biggs S. Advancing Contact Angle of Iron Ores as a Function of Their Hematite and Goethite Content: Implications for Pelletising and Sintering. International Journal of Mineral Processing 2004;1–4(74):281–287; doi: 10.1016/j.minpro.2004.01.007.

Jones L, Credo J, Parnell R, et al. Dissolved Uranium and Arsenic in Unregulated Groundwater Sources – Western Navajo Nation. Journal of Contemporary Water Research & Education 2020;169(1):27–43; doi: 10.1111/j.1936-704X.2020.03330.x.

Jones LM. Temporal and Spatial Variability of Dissolved Uranium and Arsenic in Unregulated Groundwater Sources - Western Navajo Nation. M.S. Northern Arizona University: United States -- Arizona; 2019.

Kipton H, Powell J and Town RM. Solubility and Fractionation of Humic Acid; Effect of PH and Ionic Medium. Analytica Chimica Acta 1992;267(1):47–54; doi: 10.1016/0003-2670(92)85005-Q.

Lewis J, Hoover J and MacKenzie D. Mining and Environmental Health Disparities in Native American Communities. Curr Environ Health Rep 2017;4(2):130–141; doi: 10.1007/s40572-017-0140-5.

Li Q and Elimelech M. Organic Fouling and Chemical Cleaning of Nanofiltration Membranes: Measurements and Mechanisms. Environ Sci Technol 2004;38(17):4683–4693; doi: 10.1021/es0354162.

Li S, Cai Y-H, Schäfer AI, et al. Renewable Energy Powered Membrane Technology: A Review of the Reliability of Photovoltaic-Powered Membrane System Components for Brackish Water Desalination. Applied Energy 2019;253:113524; doi: 10.1016/j.apenergy.2019.113524.

Liang Z, Wang Y, Zhou Y, et al. Hydrolysis and Coagulation Behavior of Polyferric Sulfate and Ferric Sulfate. Water Science and Technology 2009;59.6; doi: 10.2166/wst.2009.096.

Macy JP and Unema JA. Groundwater, Surface-Water, and Water-Chemistry Data, Black Mesa Area, Northeastern Arizona: 2011-2012. Open-File Report. Open-File Report. U.S. Geological Survey: Reston, VA; 2014.

Mänttäri M, Puro L, Nuortila-Jokinen J, et al. Fouling Effects of Polysaccharides and Humic Acid in Nanofiltration. Journal of Membrane Science 2000;165(1):1–17; doi: 10.1016/S0376-7388(99)00215-X.

Mariën H, Verbeke R and Vankelecom IFJ. Nanofiltration Membrane Materials and Preparation. In: Nanofiltration: Principles and Applications. Chapter 2 Elsevier; 2004; pp. 169–239.

Martin C, Doyle J, LaFrance J, et al. Change Rippling through Our Waters and Culture. Journal of Contemporary Water Research & Education 2020;169(1):61–78; doi: 10.1111/j.1936-704X.2020.03332.x.

Meehan M, Stokka G and Mostrom M. Livestock Water Quality. 2021.

Melliti E, Touati K, Abidi H, et al. Iron Fouling Prevention and Membrane Cleaning during Reverse Osmosis Process. International Journal of Environmental Science and Technology 2018;16; doi: 10.1007/s13762-018-1899-0.

Mello MM and Wolf LE. The Havasupai Indian Tribe Case — Lessons for Research Involving Stored Biologic Samples. New England Journal of Medicine 2010;363(3):204–207; doi: 10.1056/NEJMp1005203.

Misawa T, Hashimoto K and Shimodaira S. The Mechanism of Formation of Iron Oxide and Oxyhydroxides in Aqueous Solutions at Room Temperature. n.d.; doi: 10.1016/S0010-938X(74)80051-X.

Necefer L, Wong-Parodi G, Jaramillo P, et al. Energy Development and Native Americans: Values and Beliefs about Energy from the Navajo Nation. Energy Research & Social Science 2015;7:1–11; doi: 10.1016/j.erss.2015.02.007.

Ning RY. Colloidal Iron and Manganese in Water Affecting RO Operation. Desalination and Water Treatment 2009;12(1–3):162–168; doi: 10.5004/dwt.2009.918.

Nozadi SS, Li L, Luo L, et al. Prenatal Metal Exposures and Infants' Developmental Outcomes in a Navajo Population. International Journal of Environmental Research and Public Health 2022;19(1):425; doi: 10.3390/ijerph19010425.

Office of Water Environmental Protection Agency. 2018 Edition of the Drinking Water Standards and Health Advisories Tables. Environmental Protection Agency; 2018.

Pontié M, Rapenne S, Thekkedath A, et al. Tools for Membrane Autopsies and Antifouling Strategies in Seawater Feeds: A Review. Desalination 2005;181(1):75–90; doi: 10.1016/j.desal.2005.01.013.

Post JE. Manganese Oxide Minerals: Crystal Structures and Economic and Environmental Significance. Proceedings of the National Academy of Sciences 1999;96(7):3447–3454; doi: 10.1073/pnas.96.7.3447.

Racar M, Dolar D, Špehar A, et al. Optimization of Coagulation with Ferric Chloride as a Pretreatment for Fouling Reduction during Nanofiltration of Rendering Plant Secondary Effluent. Chemosphere 2017;181:485–491; doi: 10.1016/j.chemosphere.2017.04.108.

Rahman MM, Al-Sulaimi S and Farooque AM. Characterization of New and Fouled SWRO Membranes by ATR/FTIR Spectroscopy. Appl Water Sci 2018;8(6):183; doi: 10.1007/s13201-018-0806-7.

Richards LA, Richards BS and Schäfer AI. Renewable Energy Powered Membrane Technology: Salt and Inorganic Contaminant Removal by Nanofiltration/Reverse Osmosis. Journal of Membrane Science 2011;369(1):188–195; doi: 10.1016/j.memsci.2010.11.069.

Sari MA and Chellam S. Relative Contributions of Organic and Inorganic Fouling during Nanofiltration of Inland Brackish Surface Water. Journal of Membrane Science 2017;523:68–76; doi: 10.1016/j.memsci.2016.10.005.

Sarker NR and Bilton AM. Real-Time Computational Imaging of Reverse Osmosis Membrane Scaling under Intermittent Operation. Journal of Membrane Science 2021;636:119556; doi: 10.1016/j.memsci.2021.119556.

Schäfer AI, Andritsos N, Karabelas AJ, et al. Fouling in Nanofiltration. In: Nanofiltration: Principles and Applications. Chapter 20 Elsevier; 2004; pp. 169–239.

Schäfer AI, Fane AG and Waite TD. Direct Coagulation Pretreatment in Nanofiltration of Waters Rich in Organic Matter and Calcium. Water Science & Technology: Water Supply 2001;1(4):25–33.

Schulte-Herbrüggen HMA, Semião AJC, Chaurand P, et al. Effect of PH and Pressure on Uranium Removal from Drinking Water Using NF/RO Membranes. Environ Sci Technol 2016;50(11):5817–5824; doi: 10.1021/acs.est.5b05930.

Shon HK, Phuntsho S, Vigneswaran S, et al. Physical, Chemical, and Biological Characterization of Membrane Fouling. 2013;457–503; doi: 10.1061/9780784412275.ch16.

Simpson GB and Jewitt GPW. The Development of the Water-Energy-Food Nexus as a Framework for Achieving Resource Security: A Review. Frontiers in Environmental Science 2019;7.

Sneezer S. An Assessment of the Potential for Utility-Scale Solar Energy Development on the Navajo Nation. Sandia National Lab. (SNL-NM), Albuquerque, NM (United States); 2020.; doi: 10.2172/1599701.

Strezov V, Ziolkowski A, Evans TJ, et al. Assessment of Evolution of Loss on Ignition Matter during Heating of Iron Ores. J Therm Anal Calorim 2010;100(3):901–907; doi: 10.1007/s10973-009-0398-4.

Tang K, Xuan S, Lv W, et al. Contact Angle of Iron Ore Particles with Water: Measurements and Influencing Factors. In: Characterization of Minerals, Metals, and Materials 2017. (Ikhmayies S, Li B, Carpenter JS, et al. eds). The Minerals, Metals & Materials Series Springer International Publishing: Cham; 2017; pp. 321–328; doi: 10.1007/978-3-319-51382-9_35.

Tanne N, Xu R, Zhou M, et al. Influence of Pore Size and Membrane Surface Properties on Arsenic Removal by Nanofiltration Membranes. Frontiers of Environmental Science and Engineering 2019;13(2); doi: 10.1007/s11783-019-1105-8.

U.S. Census Bureau. 2020 Census State Redistricting Data (Public Law 94-171) Summary File—Navajo Nation. 2021. Available from: https://data.census.gov/cedsci/table?g=2520000US2430R [Last accessed: 4/18/2022].

US EPA O. Data Summary of The Third Unregulated Contaminant Monitoring Rule. Data and Tools. 2015a. Available from: https://www.epa.gov/dwucmr/data-summary-third-unregulated-contaminant-monitoring-rule [Last accessed: 4/30/2022].

US EPA O. Secondary Drinking Water Standards: Guidance for Nuisance Chemicals. Overviews and Factsheets. 2015b. Available from: https://www.epa.gov/sdwa/secondary-drinking-water-standards-guidance-nuisance-chemicals [Last accessed: 4/29/2022].

US EPA R 09. Providing Safe Drinking Water in Areas with Abandoned Uranium Mines. Overviews and Factsheets. 2022. Available from: https://www.epa.gov/navajo-nation-uranium-cleanup/providing-safe-drinking-water-areas-abandoned-uranium-mines [Last accessed: 4/18/2022].

Zhao D, Su C, Liu G, et al. Performance and Autopsy of Nanofiltration Membranes at an Oil-Field Wastewater Desalination Plant. Environ Sci Pollut Res 2019;26(3):2681–2690; doi: 10.1007/s11356-018-3797-x.